


Cite this: *Biomater. Sci.*, 2022, **10**, 10

# Influence of nanoparticles on the haemostatic balance: between thrombosis and haemorrhage

Huong D. N. Tran,<sup>a,b</sup> Shehzahdi Shebbrin Moonshi,<sup>a</sup> Zhi Ping Xu<sup>b</sup> and Hang Thu Ta <sup>\*a,b,c</sup>

Maintenance of a delicate haemostatic balance or a balance between clotting and bleeding is critical to human health. Irrespective of administration route, nanoparticles can reach the bloodstream and might interrupt the haemostatic balance by interfering with one or more components of the coagulation, anticoagulation, and fibrinolytic systems, which potentially lead to thrombosis or haemorrhage. However, inadequate understanding of their effects on the haemostatic balance, along with the fact that most studies mainly focus on the functionality of nanoparticles while forgetting or leaving behind their risk to the body's haemostatic balance, is a major concern. Hence, our review aims to provide a comprehensive depiction of nanoparticle-haemostatic balance interactions, which has not yet been covered. The synergistic roles of cells and plasma factors participating in haemostatic balance are presented. Possible interactions and interference of each type of nanoparticle with the haemostatic balance are comprehensively discussed, particularly focusing on the underlying mechanisms. Interactions of nanoparticles with innate immunity potentially linked to haemostasis are mentioned. Various physicochemical characteristics that influence the nanoparticle-haemostatic balance are detailed. Challenges and future directions are also proposed. This insight would be valuable for the establishment of nanoparticles that can either avoid unintended interference with the haemostatic balance or purposely downregulate/upregulate its key components in a controlled manner.

Received 26th August 2021,  
Accepted 14th October 2021

DOI: 10.1039/d1bm01351c

rsc.li/biomaterials-science

## 1. Introduction

Nanoparticles are a fundamental building block of nanotechnology, referring to particles with three dimensions at the nanoscale (approximately 1–1000 nm).<sup>1</sup> Nanoparticles possess unique physicochemical properties owing to the large surface to volume ratio. They can be potentially employed in diverse fields including biosensors, biotechnology, the food industry, agriculture, waste management, energy, cosmetics, and especially biomedicine.<sup>2–8</sup> The pivotal role of nanoparticles in biomedicine has been affirmed with the continuously increasing number of their applications in molecular imaging, image-guided therapy and therapeutic treatment of various diseases.<sup>7,9–23</sup> However, very few can successfully progress to clinical translation and commercialization in spite of positive preclinical data that has been reported. One of the remaining challenges is the lack of a full assessment of their health risks

as there are always cell–nanoparticle or blood–nanoparticle interactions when they enter the body *via* any route.<sup>2,24</sup>

Maintenance of the haemostatic balance is critical to human body health.<sup>25</sup> The term “haemostasis” is defined as a natural response process of the body to stop bleeding from damaged blood vessels.<sup>26</sup> In 1958, the prevalent notion “haemostatic balance” was first elaborated by Astrup, describing the balance between the tendency of blood to clot and for such clots to lyse.<sup>27</sup> This is the delicate equilibrium between procoagulant and anticoagulant factors that interact with each other to ensure effective haemostasis at the sites of vascular injury. The notion has now been broadened to the concept that blood has a strong tendency to clot when tissue is injured, and the intact vasculature requires major anticoagulant systems to prevent clots adhering to and stabilising in the vasculature.<sup>28</sup> As a result, the delicate thrombo-haemorrhagic balance, in other words the balance between clotting and bleeding, is always maintained under normal physiological conditions. Any interruption in the haemostatic balance might lead to either excess bleeding (haemorrhage) or abnormal clot formation in the absence of bleeding (thrombosis).<sup>2,25,29,30</sup>

Regardless of the administration route and the intended target, nanoparticles can reach the circulatory system due to their ability to permeate epithelium after dermal penetration,

<sup>a</sup>Queensland Micro- and Nanotechnology, Griffith University, Nathan, Queensland 4111, Australia. E-mail: h.ta@griffith.edu.au

<sup>b</sup>Australian Institute for Bioengineering and Nanotechnology, University of Queensland, St Lucia, Queensland 4072, Australia

<sup>c</sup>School of Environment and Science, Griffith University, Nathan, Queensland 4111, Australia

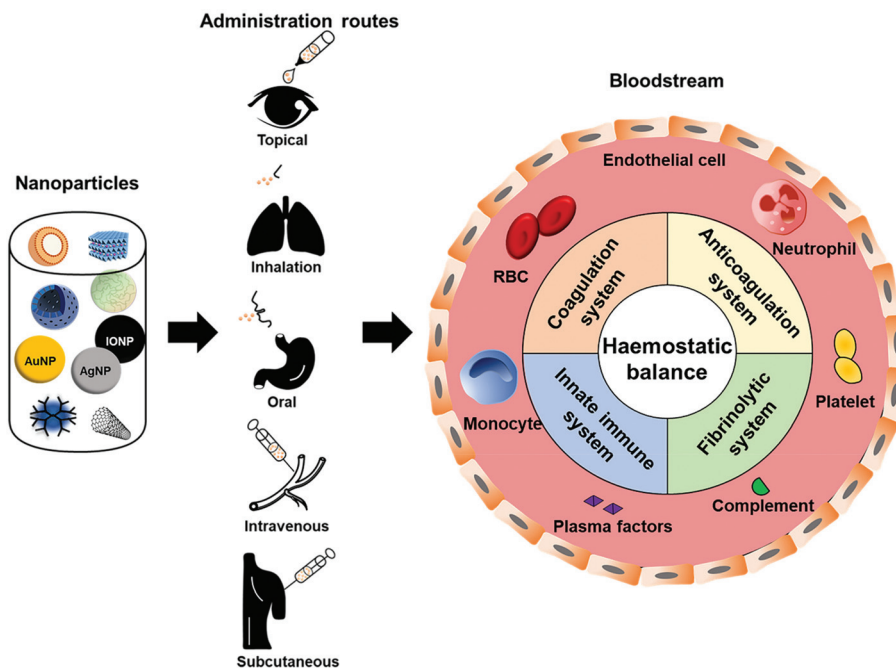


**Fig. 1** Nanoparticles encounter the haemostatic balance. Owing to their ability to permeate through epithelium, nanoparticles can reach the circulatory system regardless of the administration routes. Once inside the blood stream, nanoparticles encounter and interact with one or more components of the coagulation, anticoagulation, and fibrinolytic systems, and innate immune system, thus possibly interfering with the delicate haemostatic balance in the body.

oral ingestion, or inhalation.<sup>2,25,31</sup> Once inside the blood stream, they can potentially interfere with the haemostatic balance in unintended ways<sup>29,32,33</sup> (Fig. 1), causing haemorrhage or lethal coagulation disorders (*i.e.* disseminated intravascular coagulation and deep vein thrombosis), and thus raising concerns regarding the safety of these

nanoparticles.<sup>31,33</sup> To date, thrombosis and related complications are the greatest hurdles involved in the clinical translation of many nanoparticles.<sup>30</sup> Different types of nanoparticles will affect the haemostatic balance in a different manner. Changes in one or more physicochemical characteristics of a specific type of nanoparticle (*i.e.* size, shape, surface



**Huong D. N. Tran**

*Ms Huong D. N. Tran obtained her BSc. (Honours) in 1<sup>st</sup> rank in Biotechnology from the International University – Vietnam National University. She received a full-ride scholarship and is currently a PhD candidate at the Australian Institute for Bioengineering and Nanotechnology, The University of Queensland, and a visiting scholar at the Queensland Micro- and Nanotechnology Centre, Griffith University. She is under the supervision of Assoc. Prof. Hang T. Ta and Prof. Zhi Ping Xu. Her current research direction is the development of hemostatic materials for emergency treatment of bleeding.*



**Shehzahdi Shebbrin Moonshi**

*Dr Shehzahdi Moonshi is a Research Fellow at the Queensland Micro- and Nanotechnology Centre, in Associate Professor Hang Ta's group at Griffith University. Her projects are focused on the development of targeted theranostic nanomaterials for cardiovascular and cancerous diseases. She was awarded a New Researcher Grant at Griffith University for her research project. She completed her PhD at the University of Queensland, Australia. Her research interest is in the design and application of molecular imaging agents and drug delivery systems based on metal oxide and biocompatible polymers accompanied with the utilisation of multimodal imaging systems such as MRI and Photoacoustic imaging.*

charge, stabilizing/coating material) could significantly alter its effect on haemostatic balance. However, inadequate understanding of nanoparticles' effects on the haemostatic balance, which is the root of their toxicity in the blood system, is a major concern. Most studies usually focus on the functionality of the nanoparticle systems while forgetting or leaving behind their risks to the body's haemostatic balance. Therefore, cautious design of nanoparticles based on in-depth knowledge of their behaviours toward the blood haemostasis would be beneficial in tackling the complications accompanied with their use, thereby improving their haemocompatibility and speeding up their translation to the clinic and market.

All previous reviews with similar topics mainly focused on the nanomaterials with coagulation effects and left out those with anticoagulant or thrombolytic effects. Moreover, the underlying mechanisms were often not discussed. With that consideration in mind, this review aims to provide a complete depiction of the interactions between nanoparticles and the haemostatic balance (thrombosis/haemorrhage), which has yet to be thoroughly discussed to date. The roles of cells and plasma factors participating in coagulation and anticoagulation systems along with fibrinolytic systems to maintain the thrombo-haemorrhagic balance will be presented. Importantly, nanoparticle interactions with each component of the haemostatic balance are discussed comprehensively with a focus on the underlying mechanisms. The interaction of nanoparticles with innate immunity, which could potentially interfere with the haemostatic balance concerning the intrinsic link between the innate immune system and haemostasis, will be discussed. Moreover, various physicochemical characteristics of nanoparticles that influence the nanoparticle-haemostatic balance will be detailed. Challenges and future directions will also be proposed.

In comparison with previous reviews with similar topics, our paper (1) is the first review discussing the influence of nanoparticles on the whole haemostatic balance through their interaction with the haemostasis components and the innate immune system, which is potentially linked to haemostasis, (2) categorises and discusses all possible effects, along with the underlying mechanisms of each type of nanoparticle on each component of the haemostatic balance, (3) provides a comprehensive conclusion for the effects of each type of nanoparticle (along with its specified physicochemical characteristics) on the haemostatic balance, which would be beneficial for the design of nanoparticles.

## 2. The role of blood coagulation, anticoagulation, and fibrinolytic systems in haemostatic balance

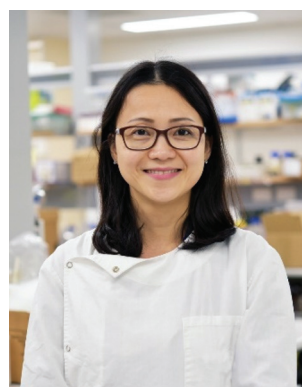
A haemostatic balance under normal physiological conditions is achieved through the clotting and anticlotting effects, in equilibrium with each other, controlled by blood coagulation, anticoagulation, and fibrinolytic systems.<sup>34,35</sup> The blood coagulation system mediates haemostasis at the vascular injury sites.<sup>36</sup> Upon injury, damaged endothelial cells expose sub-endothelial collagens for the initiation of primary haemostasis, where platelets aggregate and form a temporary platelet plug. Subsequently, secondary haemostasis is initiated with the involvement of a coagulation cascade, which results in a fibrin mesh that entraps the platelet plug and red blood cells (RBCs) to form a blood clot and stops the bleeding.<sup>37,38</sup> In contrast, the anticoagulation system prevents clots from forming (prevents primary and/or secondary haemostasis) while the



**Zhi Ping Xu**

*Professor Zhi Ping Xu is a senior group leader at the Australian Institute for Bioengineering and Nanotechnology, the University of Queensland. His research focuses on control preparation of anionic clay, i.e. layered double hydroxide nanomaterials, calcium phosphate nanoparticles, chemosensors and nanosensors, and their biomedical applications for diagnosis, therapy and prevention of*

*cancers and cardiovascular diseases, as well as crop prevention. Prof. Xu has been awarded over \$25 million grants from various organizations and industry partners to support his group research in nanobiomedicine and nano-agro-biotechnology. He has published over 310 journal papers with over 16 000 citations and H index of 67.*



**Hang Thu Ta**

*Hang Ta is an Associate Professor at the School of Environment and Science and Queensland Micro- and Nanotechnology Centre, Griffith University. She currently leads a team of 12 students and post-docs working on nanomaterials for diagnosis and treatment of life-threatening diseases including inflammatory and cardiovascular diseases, cancers, and bleeding disorders. She has a unique skill set combining chemistry and biology skills.*

*She got a PhD in biomaterials for drug delivery from the University of Melbourne and then worked at the Baker Heart and Diabetes Institute and the University of Queensland before moving to Griffith University in 2020. Prof. Ta has been awarded a number of prizes, grants and prestigious fellowships.*

fibrinolytic system breaks down clots that have already been formed.<sup>39</sup> As a result, clot formation is restricted to the injury site, thus preventing haemostasis at the wrong place, which inadvertently results in thrombosis. Nevertheless, induced anticoagulation and fibrinolysis could lead to prolonged bleeding or haemorrhage.

Vascular endothelial cells, platelets, red blood cells, along with plasma coagulation factors, anticoagulation factors, and fibrinolytic enzymes and activators are components of blood coagulation, anticoagulation, and fibrinolytic systems. The roles of each component and their association with others in order to maintain the haemostatic balance will be discussed in the following subsections.

### 2.1 Vascular endothelium

Vascular endothelial cells play an important role in the regulation of platelet adhesion, thrombosis, and fibrinolysis.<sup>31</sup> Healthy endothelial cells are protected by a glycocalyx layer consisting of heparan sulfate that has an affinity for anticoagulant proteins such as antithrombin III (AT III or AT) and tissue factor pathway inhibitor (TFPI) (Fig. 2A). These proteins (AT and TFPI) and anticoagulant mediators (heparin cofactor II, endothelial protein C receptor (EPCR), and thrombomodulin (TM)) expressed on the endothelium surface, together with platelet adhesion and aggregation inhibitors (nitric oxide (NO), prostacyclin (PGI<sub>2</sub>), and CD39/NTPDase1), are secreted by the endothelium to maintain the thrombo-resistant or anticoagulant nature of intact vascular endothelial cells.<sup>40–43</sup> In addition, AT also further stimulates PGI<sub>2</sub> production which results in the inhibition of platelet aggregation and vasodilation.<sup>39</sup>

Interaction with nanoparticles can cause endothelium dysfunction. Damage to endothelial cells not only leads to the exposure of tissue factors (TFs) (CD142 or FIII), which activates the extrinsic pathway of haemostasis, but also exposes sub-endothelial collagens that bind FXII to initiate the intrinsic pathway. Moreover, von Willebrand factor (vWF), thromboxane A2 (TXA<sub>2</sub>), P-selectin (CD62P/GMP-140/PADGEM), and platelet-activating factors (PAFs) released by injured endothelial cells along with the exposed collagens are associated with platelet recruitment, adhesion, and activation<sup>31,36</sup> (Fig. 2B).

### 2.2 Platelets

Platelets (thrombocytes) are a crucial cellular component that is involved in the regulation of haemostatic balance.<sup>3</sup> They originate from megakaryocytes and are anucleate, discoid in shape, and around 2–4 μm in diameter. Around 33% of all platelets are stored in the spleen, while the rest circulate in the circulatory system (~150 000–450 000 platelets per mm<sup>3</sup>) without adhering to the intact vascular endothelium.<sup>31</sup> Upon injury, damaged endothelium exposes TF, collagen, and other thrombogenic factors such as vWF, TXA<sub>2</sub>, and PAFs for the initiation of primary haemostasis. Platelets become activated once they come in contact with vWF and sub-endothelial collagens and adhere to the injured endothelium and vessel wall.<sup>37,44–46</sup> The platelet activation process is characterised by a

drastic increase in cytosolic Ca<sup>2+</sup>, which elicits the reorganisation of the platelet cytoskeleton, resulting in a change in shape (from disc to sphere shape), pseudopodia formation, aggregation, and exocytosis of contents stored inside the platelet's granules<sup>47</sup> (Table 1). Adhesive glycoproteins (vWF, fibrinogen, P-selectin, thrombospondin, and vitronectin), coagulation factors (plasminogen, kininogen, factor V, XI, XIII), plasminogen activator inhibitor-1 (PAI-1), TXA<sub>2</sub>, PAFs, adenosine diphosphate (ADP), and serotonin secreted by activated platelets mediate vasoconstriction and platelet aggregation, activate more platelets and attract them to come to form a weak platelet plug that temporarily seals the injured area.<sup>37,41,47,48</sup> There is a certain number of glycoprotein IIb/IIIa (GpIIb/IIIa) receptors presented on the surface of resting platelets (approximately 50 000 per platelet).<sup>49</sup> Upon activation, GpIIb/IIIa stored in the internal pool of platelets will move to their surface, thereby increasing the number of expressed GpIIb/IIIa. These receptors, both the newly expressed and the previously presented ones, undergo a conformation change process, which is related to extracellular ionised calcium and the expression of ligand-induced binding sites to develop a high-affinity for fibrinogen.<sup>49–51</sup> Fibrin forms the bridge between platelets and entraps the platelet plug and other surrounding blood cells to form a stable clot.<sup>37,41,47,48</sup>

Generally, the interactions of nanoparticles with platelets can affect platelet functions. Different types of nanoparticles with varied size, charge, coating materials, and composition may lead to different outcomes, including activating effect, inhibitory effect, or no effect on platelets (Fig. 3). Excess activation effects on platelets without the presence of injury would lead to a hypercoagulable state (thrombophilia) and increase the risk of thrombosis. Meanwhile, excessive inhibitory effects of platelets would lead to prolonged and uncontrolled bleeding when the injury occurs.

### 2.3 Red blood cells (RBCs)

RBCs (erythrocytes) are a cellular component that also takes part in haemostatic balance control and has been underestimated in the past. Detailed mechanisms on how RBCs perform their roles in haemostasis have been reviewed in-depth previously.<sup>52</sup> Briefly, RBCs attribute to haemostatic balance through hemorheological properties owing to their abundance and large size.<sup>53</sup> The influence of hemorheology, which can be defined as the flow property of blood, and its elements on haemostasis and thrombosis are dependent on the blood shear rates and viscosity where RBCs are a main contributor.<sup>54,55</sup> The blood viscosity affects platelet distribution within vessels based on the axial margination phenomenon in which RBCs tend to move to the centre of vessels and push platelets towards the periphery, facilitating their collision with the vasculature for haemostatic events.<sup>56</sup>

Interactions of nanoparticles with RBCs can cause RBC aggregation<sup>57</sup> (Fig. 4A). Aggregation of RBCs, especially in small vessels, normally increases the blood viscosity in the centre of vessels and platelet margination, resulting in induced endothelium activation and platelet aggregation.<sup>54</sup>

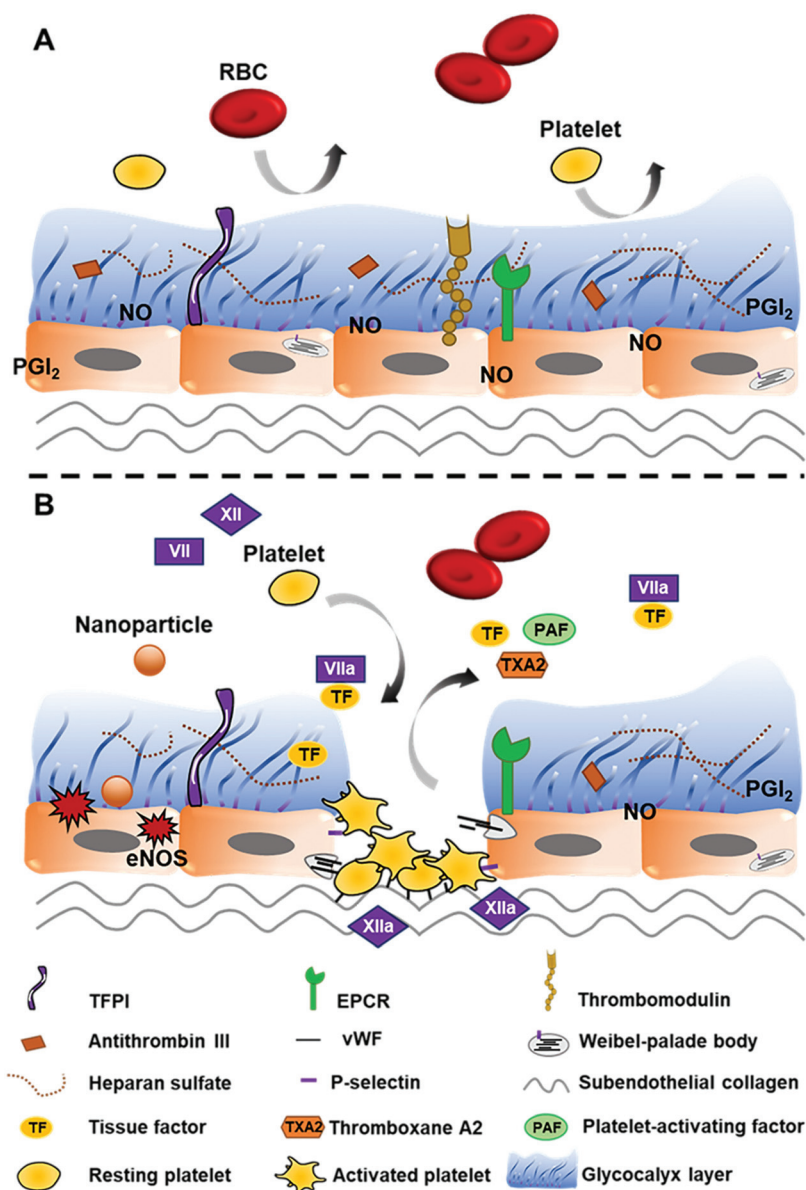


**Fig. 2** Possible effects of nanoparticles on vascular endothelial cells. (A) Healthy endothelium is protected by an intact glycocalyx layer containing inhibitory mediators, thus exhibiting anticoagulant properties and preventing thrombotic events. (B) Interaction with nanoparticles can cause endothelium dysfunction, leading to the exposure of subendothelial collagen, imbalance of endothelial NO synthase (eNOS), and the release of procoagulant factors. Subendothelial collagen comes in contact with FXII and converts it to the active form (FXII → FXIIa) to trigger the intrinsic pathway of the coagulation cascade. vWF and P-selectin stored inside Weibel-palade bodies together with TXA2 and PAF are released from damaged endothelial cells, promoting platelet recruitment, adhesion, and activation.

Furthermore, nanoparticle interactions with RBCs can also alter the deformability of RBCs, which is the ability of RBCs to change their shape in response to applied stress without resulting in haemolysis<sup>58</sup> (Fig. 4B). A decrease in RBC deformability is related to higher risk of thrombosis since rigid RBCs can block small vessels easily, alter the blood flow, and provoke platelet activation.<sup>59</sup> In addition to hemorheology, RBC-nanoparticle interactions can lead to the exposure of phosphatidylserine (PS) on the RBCs surface, contributing to blood coagulation<sup>60</sup> (Fig. 4C). PS is a key phospholipid localised within the plasma membrane. Upon the high shear

stress, oxidative stress, or complement attack, damaged RBCs expose PS on the membrane surface, providing a procoagulant surface for the accumulation of coagulation complexes such as prothrombinase and intrinsic tenase that facilitate thrombus formation.<sup>53</sup>

#### 2.4 Plasma factors

Besides cellular components, the haemostatic balance is mediated by plasma factors which function as components of blood coagulation, anticoagulation, and fibrinolytic systems. The majority of circulating plasma coagulation factors are

**Table 1** Platelet storage granules and their contents (reproduced with permission ref. 2)

Granules	Content class	Factors released
Alpha granules	Adhesive glycoproteins	vWF, thrombospondin, P-selectin, fibrinogen, fibronectin, vitronectin
	Coagulation factors	Plasminogen, kininogens, protein S, factor V, factor XI, factor XIII
	Growth factors	IGF, EGF, PDGF, TGF- $\beta$
	Angiogenic factors	PF4 inhibitor, VEGF
	Protease inhibitors	C1-inhibitor, PAI-1, TFPI, $\alpha$ 2-antiplasmin, $\alpha$ 2-antitripsin, $\alpha$ 2-macroglobulin
	Immunoglobulins-chemokines	IL8, IL1 $\beta$ , CD40, CXCL4 (platelet basic protein/NAP-2), CXCL (PF4), CXCL1, CXCL5, CCL5 (RANTES), CCL (MIP-1 $\alpha$ )
Dense granules (or delta granules)	Proteases	MMP2, MMP9
	Amines	Serotonin, histamine
	Bivalent cations	Ca <sup>2+</sup> , Mg <sup>2+</sup>
Lysosome granules	Polyphosphates	ADP, ATP, GDP, GTP
	Enzymes	Acid proteases, glycohydrolases
Other soluble mediators	NO, TXA2, defensins, PAF	

vWF, von Willebrand factor; IGF, insulin-like growth factor; EGF, epidermal growth factor; PDGF, platelet-derived growth factor; TGF- $\beta$ , transforming growth factor  $\beta$ ; PF4, platelet factor 4; VEGF, vascular endothelial growth factor; PAI-1, plasminogen activator inhibitor-1; TFPI, tissue factor pathway inhibitor; MMP, matrix metalloproteinase; ADP, adenosine diphosphate; ATP, adenosine triphosphate; GDP, guanosine diphosphate; GTP, guanosine triphosphate; NO, nitric oxide; TXA2, thromboxane A2; PAF, platelet-activating factor.

zymogens, precursors of enzymes, which will be converted into the active form once the coagulation cascade is initiated. The other plasma coagulation factors are non-enzymatic and act as either a cofactor (*e.g.*, TF (or factor III or FIII), FV and FVIII, high-molecular-weight kininogen (HMWK or HK)) or substrate (*e.g.*, fibrinogen). These factors form a coagulation cascade in secondary haemostasis, which can be divided into extrinsic and intrinsic pathways (Fig. 5). Both pathways lead to thrombin generation and ultimately fibrin formation to create a stable blood clot at the injury site. The extrinsic pathway is activated by TFs exposed on damaged endothelial cells or tissues, initiating the coagulation cascade. TFs then form a TF-FVIIa complex through the direct capture of TFs with free FVIIa circulated in plasma and/or the binding of TFs with VII, followed by the proteolytic conversion of FVII to FVIIa due to the exposed TFs.<sup>61</sup> In a parallel manner, the intrinsic pathway begins with FXII, prekallikrein (PK), and HMWK.<sup>44</sup> FXII can be activated *via* the contact with negatively charged molecules and nanoparticle surfaces such as dextran sulfate, glass, kaolin, Celite, and silica.<sup>62–65</sup> It can also be auto-activated by the membrane of activated platelets,<sup>66</sup> resulting in the activation of the kallikrein-kinin system and FXI, as well as other downstream zymogens in the intrinsic pathway.<sup>33</sup> It is important to note that, apart from activated FXII (FXIIa), a small amount of thrombin generated by the extrinsic pathway can in turn activate FXI and thus facilitate the activation of the intrinsic pathway and amplification of thrombin generation.

In different circumstances, plasma factors of the anticoagulation system and fibrinolytic system function in the opposite manner to the coagulation system to downregulate and balance the haemostasis. The anticoagulation system regulates the haemostatic balance by preventing clot formation *via* four pathways, including the AT glycosaminoglycan pathway, protein C pathway, TFPI pathway, and protein Z dependent inhibitor pathway.<sup>39</sup> AT is a small protein in the bloodstream that has anticoagulant activity. It binds to heparan sulfate

expressed on vascular endothelial cell surfaces and then exerts inhibitory effects on thrombin, FXa, FIXa, FXIa, and FXIIa.<sup>39,67</sup> In addition, it also inhibits platelet aggregation by triggering the production of PGI<sub>2</sub>.<sup>39</sup> Protein C and protein S are the main elements of the protein C pathway. Protein C is presented to a TM-thrombin complex by EPCR on endothelial cells for the conversion to its activated form, activated protein C (APC). APC degrades two coagulation factors, FVa and FVIIIa, with assistance from protein S as a cofactor. Moreover, protein S can independently and reversibly inhibit prothrombinase complex (FXa-FVa) in the intrinsic pathway of the coagulation cascade. TFPI is another anticoagulant factor which targets the extrinsic pathway. TFPI binds to FXa to form TFPI-FXa complex and inactivates FXa. TFPI can also form a quaternary complex of TFPI-FXa-TF-FVIIa to inhibit both FXa and FVIIa. Lastly, another group of anticoagulant plasma factors are protein Z-dependent protease inhibitor (ZPI) and protein Z (PZ) as a cofactor of ZPI. ZPI not only independently inhibits FXIa but also inactivates FXa in the presence of PZ.<sup>39</sup>

In addition to the anticoagulation system, the haemostatic balance is also regulated by the fibrinolytic system to break down clots that have been formed.<sup>39</sup> Plasmin is a key enzyme of the fibrinolytic system, which is converted from clot-bound plasminogen by two distinct plasminogen activators named t-PA (tissue-type plasminogen activator) and u-PA (urokinase-type plasminogen activator) synthesised by endothelial cells.<sup>39</sup> As a proteolytic enzyme, plasmin can cleave cross-linked fibrin of the clot to soluble fibrin degradation products which will be cleared away by flowing blood, thus dissolving blood clots.<sup>68</sup> Furthermore, plasmin can also upregulate the production of itself by making more active forms of u-PA and t-PA.<sup>39</sup>

Since nanoparticle surfaces can activate coagulation factor XII to initiate the intrinsic pathway of coagulation or possibly affect plasminogen activation, it is reasonable to anticipate that nanoparticles might unintentionally interfere with the coagulation cascade, fibrinolytic system, and overall haemostasis.

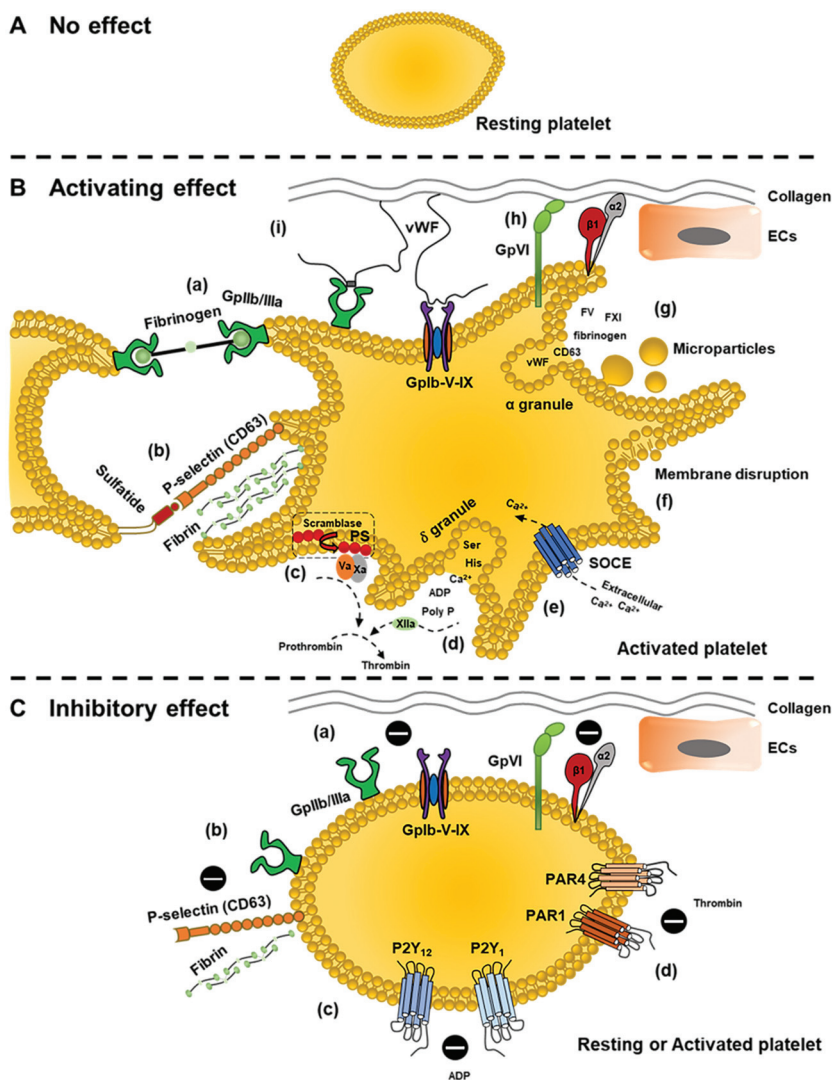


**Fig. 3** Possible effects of nanoparticles on platelets. (A) No effect. (B) Activating effect: (a) upregulation and activation of GpIb/IIIa receptor on the surface of platelets to form GpIb/IIIa-fibrinogen bridge for platelet aggregation; (b) expression of P-selectin on the platelet surface. P-selectin interacts with adjacent platelet sulfatide to facilitate platelet-platelet interaction, stabilising the initial platelet aggregation formed by GpIb/IIIa-fibrinogen. Also, P-selectin stimulates fibrin deposition; (c) increased expression of phosphatidylserine (PS) on platelet membrane *via* scramblase activity provides the requisite surface for the generation of thrombin; (d) rupture of dense ( $\delta$ ) granules. Released polyphosphate (poly P) activates FXII, which also contributes to thrombin generation; (e) store-operated  $\text{Ca}^{2+}$  entry (SOCE) activation as a result of intracellular  $\text{Ca}^{2+}$  depletion caused by  $\delta$ -granules rupture; (f) membrane interruption that stimulates platelet activation; (g) release of  $\alpha$ -granules and platelet microparticles; and induced platelet adhesion (or increased number of adhered platelets to the exposed collagen) due to (h) direct binding *via* GpVI and integrin  $\alpha_2\beta_1$  or (i) indirect binding through vWF utilizing GpIb-V-IX receptor complex. (C) Inhibitory effect: (a) impedes integrin-mediated platelet responses (GpVI, integrin  $\alpha_2\beta_1$ , and GpIb-V-IX receptor complex) for platelet adhesion and aggregation; (b) impedes GpIb/IIIa response for platelet adhesion to immobilized fibrinogen or reduced expression of GpIb/IIIa and P-selectin; nanoparticles can also inhibit platelet aggregation induced by (c) ADP or (d) thrombin by respectively inhibiting responses of P2Y<sub>1</sub> and P2Y<sub>12</sub> or PAR-1 (protease-activated receptor-1) and PAR-4 (protease-activated receptor-1).

### 3. Effects of nanoparticles on haemostatic balance – the underlying mechanisms

Upon reaching the bloodstream, nanoparticles encounter many blood components and biological systems, including the blood coagulation, anticoagulation, and fibrinolytic systems. Unintended interactions of nanoparticles with these systems can result in a dysregulation of the haemostatic balance.<sup>2,29</sup> The

possible effects of various types of nanoparticles on haemostatic balance, along with the underlying molecular mechanisms, will be discussed in the following subsections (Fig. 2–5).

Nanoparticles can be purposefully engineered to interact with these systems, thus intentionally affecting the haemostatic balance by either inducing or preventing coagulation in order to avoid bleeding or prevent thrombosis, respectively. They can be synthesised from the haemostasis-induced naturally-derived materials or can be engineered (*i.e.* be loaded with drugs and/or decorated with peptides, antibodies, recombinant factors, or





Table 2 A summary of the effects of common inorganic nanoparticles on haemostatic balance *in vitro* and *in vivo*

Nanoparticle	Shape	Size	Charge	Coating/stabiliser	Concentration tested	Main finding	Ref.
Carbon nanotube	Tube	SWCNTs: 1–2 nm in outer diameter, 5–30 $\mu\text{m}$ in length (TEM) MWCNTs: 60–100 nm or $30 \pm 15$ nm in outer diameter, 1–5 $\mu\text{m}$ in length (TEM)	Not specified	None	100 and 200 $\mu\text{g mL}^{-1}$ <i>in vitro</i>	Induced platelet activation and aggregation <i>in vitro</i>	71 and 72
Carbon nanotube	Tube	60 nm (TEM)	Neutral	None	100 $\mu\text{g mL}^{-1}$	Caused vascular thrombosis <i>in vivo</i>	73
Carbon nano-diamond	Tetragonal	4–10 nm (TEM)	Negative	None	1 $\mu\text{g mL}^{-1}$ <i>in vitro</i>	Evoked platelet activation <i>in vitro</i>	78
Nano-diamond	Not specified	100 nm (SEM)	Negative	Carboxylate groups	250 $\mu\text{g kg}^{-1}$ of mice (IV route) 0.1 $\text{mg mL}^{-1}$	Caused pulmonary thromboembolism <i>in vivo</i> Caused abnormal RBC aggregates	79
Carbon nanotube (pristine, amine- and carboxyl-modified)	Tube	Diameter: 26–31 nm; length: 490–580 nm (TEM)	Not specified	DSPE-PEG or pluronic F127	100 $\mu\text{g mL}^{-1}$ <i>in vitro</i>	Except for pluronic-coated pristine carbon nanotubes exhibiting no effect, all nanotubes triggered intrinsic cascade <i>via</i> interaction with FIXa and promote its enzyme activity <i>in vitro</i> Functionalization mitigated procoagulant effect <i>in vivo</i>	74
Carbon nanotube	Tube	Diameter: 4–5 nm; length: 500–1000 nm (TEM)	Not specified	Albumin	250 $\mu\text{g}$ per mice (~100 $\mu\text{g mL}^{-1}$ as <i>in vitro</i> ) (IV route) 30–150 $\mu\text{g mL}^{-1}$	Pre-treatment with albumin lessens thrombogenic effect of carbon nanotubes <i>in vitro</i>	84
Carbon nanotube	Tube	Diameter: 6–20 nm; length: 700–4000 nm (TEM)	Not specified	None	Cumulative dose: 32 or 128 $\mu\text{g}$ per mice (oropharyngeal aspiration)	Induced fibrinogen and factor VII levels, reduced TT, showed procoagulant activity <i>in vitro</i>	75
Carbon nanotube (long and short carboxyl-modified; long and short amine-modified)	Tube	Length: 926 and 223 nm (long and short carboxyl-modified nanotube, respectively) 945 and 266 nm (long and short amine-modified nanotube, respectively)	Negative and positive	None	0.005–0.16 $\text{mg mL}^{-1}$	Induced platelet activation and RBC damage by altering the cell's integrity	254
Carbon dots synthesized from <i>Cirsium setosum</i> Carbonisata extract	Nearly spherical	$2.6 \pm 0.7$ nm (TEM)	Not specified	None	High dose: 8.33 $\text{mg kg}^{-1}$ ; medium dose: 3.33 $\text{mg kg}^{-1}$ ; low dose: 1.67 $\text{mg kg}^{-1}$ of mice (intraperitoneal injection)	Reduced bleeding time <i>in vivo</i> by activating fibrinogen and triggering the extrinsic pathway	76

Table 2 (Contd.)

Nanoparticle	Shape	Size	Charge	Coating/stabiliser	Concentration tested	Main finding	Ref.
Carbon dots	Round	3 nm (TEM)	Not specified	None	25–120 $\mu\text{M}$ <i>in vitro</i> 1 mg $\text{kg}^{-1}$ of mice <i>in vivo</i> (IV route)	Inhibited platelet activation and aggregation <i>in vitro</i> Decreased death rate of pulmonary thromboembolism-induced mice <i>in vivo</i>	77
Fullerenol $\text{C}_{60}(\text{OH})_{24}$	Spherical	$4.3 \pm 0.2$ (DLS)	Not specified	None	100 $\mu\text{g mL}^{-1}$	Triggered TF expression on HUVECs <i>in vitro</i>	80
Fullerenol $\text{C}_{60}(\text{OH})_{24}$	Spherical	$\sim 1.3$ nm in outer diameter (TEM)	Not specified	None	100 $\mu\text{g mL}^{-1}$	No effect on platelets <i>in vitro</i>	72
Fullerenol	Not specified	$1.13 \pm 0.32$ nm (AFM)	Negative	None	0.1, 0.5 and 1.0 mM <i>in vitro</i> and <i>in vivo</i> in rat (IV route)	Affected both extrinsic and intrinsic pathway, inhibited Xa and thrombin activity <i>in vitro</i> Prolonged bleeding time and inhibited thrombosis <i>in vivo</i>	81
Silver	Spherical	$\sim 20$ nm (TEM, DLS)	Not specified	Citrate	2 and 4 mg $\text{L}^{-1}$	HUVECs increased permeability which is a main factor leading to endothelial dysfunction <i>in vitro</i>	85
Silver	Spherical	$\sim 20$ nm (TEM, DLS)	Not specified	PEG	125–625 $\mu\text{M}$	Reduced platelet adhesion and inhibited platelet aggregation <i>in vitro</i>	90
Silver	Spherical	10–100 nm	Not specified	None	10–250 $\mu\text{g mL}^{-1}$ <i>in vitro</i> 0.05–0.1 mg $\text{kg}^{-1}$ (IV route) or 5–10 mg $\text{kg}^{-1}$ of rat (intratracheal instillation route)	Induced platelet activation and aggregation <i>in vitro</i> Enhanced venous thrombus formation, platelet aggregation, and PS externalization <i>in vivo</i>	88
Silver	Spherical	10–15 nm (TEM) 12 (DLS)	Not specified	Sodium polyacrylate	30 mg $\text{L}^{-1}$	Triggered platelet activation, induced kallikrein-like, FXIIIa-like, and thrombin-antithrombin III complex <i>in vitro</i>	89
Silver	Spheroid	16 (DLS)	Not specified	Polyvinyl pyrrolidone (PVP)	50 $\mu\text{g mL}^{-1}$	Promoted platelet adhesion and procoagulant effect <i>in vitro</i>	91
Silver	Spherical	$\sim 20$ nm (TEM)	Negative	PVP or citrate	$\sim 500$ $\mu\text{g mL}^{-1}$	No effect of platelet aggregation and coagulation <i>in vitro</i>	92
Silver	Spherical	AgNP-PVP: $58.6 \pm 2.4$ nm (DLS) AgNP-citrate: $26.6 \pm 1.89$ nm (DLS) $\sim 10$ – $15$ nm (TEM, SEM)	Not specified	Lignin	0–60 $\mu\text{g mL}^{-1}$	At 530 $\mu\text{g mL}^{-1}$ , citrate-AgNPs showed prolonged coagulation time Reduced platelet aggregation of PRP at 15 $\mu\text{g}$ per 0.25 mL reaction <i>in vitro</i>	93

Table 2 (Contd.)

Nanoparticle	Shape	Size	Charge	Coating/stabiliser	Concentration tested	Main finding	Ref.
Silver	Spherical or nanowire	Spherical nanoparticles: 30 or 100 nm	Nanoparticles: negative	PVP	50 and 150 $\mu\text{g mL}^{-1}$	Reduced RBC deformability by all AgNPs and silver nanowires. 30 nm-NPs reduced RBC deformability the most compared with 100 nm-NPs and nanowires <i>in vitro</i>	94
Silver	Spherical	Nanowires: diameter of 40 nm; length of 1–2 $\mu\text{m}$	Nanowires: not specified	Citrate	0.5–50 $\mu\text{M}$ <i>in vitro</i> 2–8 $\text{mg kg}^{-1}$ of mice (IV route) 0.05–5 $\mu\text{M}$	All silver nanomaterials reduced RBC aggregation at 150 $\mu\text{g mL}^{-1}$ . At 50 $\mu\text{g mL}^{-1}$ , 30 nm-NPs did not <i>in vitro</i> Antiplatelet property <i>in vitro</i> and <i>in vivo</i>	87
Silver	Spherical	13–45 nm	Not specified	D-Glucose		Prevented platelet adhesion and integrin-mediated platelet responses <i>in vitro</i>	95
Silver	Spherical	2–3.7 nm (TEM)	Not specified	Reduced glutathione (GSH), polyethylene glycol (PEG) and lipoic acid (LA)	12.5–100 $\mu\text{g mL}^{-1}$	Decreased the level of P-selectin, GPIIb/IIIa, TXB <sub>2</sub> , and the release of MMP-1, MMP-2 by AgNPs-LA at 100 $\mu\text{g mL}^{-1}$ and AgNPs-GSH and AgNPs-PEG at 50 and 100 $\mu\text{g mL}^{-1}$ <i>in vitro</i> No effect on endothelial cells and platelet viability <i>in vitro</i> Caused dispersion of RBCs of the clot Exerted anticoagulant and thrombolysis activities <i>in vitro</i>	97
Silver synthesized from leaf and seed extracts of <i>Synsepalum dulcificum</i>	Fairly spherical	5–26 nm (TEM)	Not specified	None	Use 0.5 mL of 150 $\mu\text{g mL}^{-1}$ nanoparticles in 5 mL of blood		107
Silver synthesized from nest extract of paper wasp ( <i>Polistes sp.</i> )	Sphere, hexagon, rod, and rhombus	12.5–95.55 nm (TEM)	Not specified	None	Use 0.5 mL of 150 $\mu\text{g mL}^{-1}$ nanoparticles in 5 mL of blood	Exerted anticoagulant activities <i>in vitro</i>	106
Silver synthesized from extract of spider cobweb (CB), pod (KP), seed (KS) and seed shell (KSS) of kolanut ( <i>Cola nitida</i> )	Nearly spherical	3–80 nm (SAED)	Not specified	None	100 $\mu\text{g mL}^{-1}$	Exerted anticoagulant activity <i>in vitro</i>	105
Silver synthesized from leaf extract of <i>Petiveria alliacea</i> (PA)	Nearly spherical	16.70–33.74 nm (TEM)	Not specified	None	~167 $\mu\text{g mL}^{-1}$	Exhibited anticoagulant property similar to EDTA <i>in vitro</i> Preserved RBC structure <i>in vitro</i> Showed thrombolytic activity <i>in vitro</i>	104
Silver synthesized from <i>Euphorbia acruensis</i>	Closely spherical	10–40 nm (TEM)	Not specified	None	50 $\mu\text{g mL}^{-1}$		103

Table 2 (Contd.)

Nanoparticle	Shape	Size	Charge	Coating/stabiliser	Concentration tested	Main finding	Ref.
Silver synthesized from <i>Pseudomonas aeruginosa</i>	Spherical	80 nm (DLS)	Not specified	None	0.5% (v/v)	Displayed excellent anticoagulant activity <i>in vitro</i>	102
Silver synthesized from <i>Glucobacter roseus</i>	Irregular shape	10 nm (TEM) 68 nm (DLS)	Negative	None	0.9–3.5 nM	Reduced platelet aggregation and showed anticoagulant effect <i>in vitro</i>	101
Silver	Spherical	6–16 nm (TEM)	Negative	Low-molecular-weight sulfoethyl chitosan	0.1 mg mL <sup>-1</sup>	Inhibited the activity of Xa <i>in vitro</i>	100
Silver	Triangular, truncated triangular, hexagon/elongated hexagon and spherical	148 ± 9 nm to 610 ± 112 nm (DLS)	Negative	Heparin	10 µM	Delayed coagulation time with the longest time caused by hexagonal nanoparticles <i>in vitro</i>	109
Silver and gold	Not specified	AgNPs: 10 nm AuNPs: 12.8 nm (TEM)	Not specified	Citrate	Low dose: 10 µg kg <sup>-1</sup> day <sup>-1</sup> ; high dose: 100 µg kg <sup>-1</sup> day <sup>-1</sup> of rat <i>in vivo</i> (IV route)	No effect on APTT and PT compared with blood only control	96
Gold	Spherical	~20–70 nm (TEM)	Not specified	Citrate	0–50 µM	68 nm-nanoparticles were inert to platelets while ~20 nm-nanoparticles exerted platelet activation <i>in vitro</i>	111
Gold	Nearly spherical	~30 nm (TEM)	Positive and negative	Citrate, 11-mercaptopundecanoic acid, or 11-mercaptopundecylamine	50 µg mL <sup>-1</sup>	No effect on platelets <i>in vitro</i>	112
Gold	Spherical	20–50 nm (DLS)	Not specified	PEI or PVP	1–10%	Induced platelet aggregation <i>in vitro</i>	118
Gold	Spherical, oval	12–85 nm (TEM)	Negative	Citrate, PEG-thiol, protein corona (HFib), clopidogrel, or RGD	1.2–5 nM	Nanoparticles with RGD coating exhibited procoagulant effect while those with PEG-thiol, clopidogrel, and HFib affected platelet adhesion, fibrin build-up, and finally prevented clot formation <i>in vitro</i>	116
Gold	Spherical	~18 nm (DLS) 16.5 ± 2 nm (TEM)	Negative	Citrate	5 µg mL <sup>-1</sup>	Citrate-AuNPs had no effect at 1.2 nM while demonstrating pro-thrombogenic effect at 5 nM <i>in vitro</i>	120

Table 2 (Contd.)

Nanoparticle	Shape	Size	Charge	Coating/stabiliser	Concentration tested	Main finding	Ref.
Gold	Spherical	5–60 nm	Not specified	Citrate	5–40 $\mu\text{M}$	No effect of platelet aggregation with nanoparticles <30 nm while inhibited platelet aggregation with nanoparticles >60 nm <i>in vitro</i>	119
Gold synthesized from earthworm extract	Spherical	$6.13 \pm 2.13$ nm (TEM)	Not specified	None	Involve 0.03% extract and 60 $\mu\text{M}$ $\text{HAuCl}_4 \cdot 3\text{H}_2\text{O}$	Reinforced the anticoagulant activity when combining with heparin (0.02 U $\text{mL}^{-1}$ ) <i>in vitro</i>	268
Gold	Spherical, rodlike, hollow, core/shell silica/gold	$\sim 25$ –51 nm (not specified for rodlike) (DLS)	Negative	Monocarboxy (1-mercaptopoundec-11-yl) hexaethylene glycol (OEG)	0.8–3.3 nM	No significant effect on HUVECs	117
Iron carbide	Not specified	$\sim 30$ nm (TEM)	Not specified	Carbon and/or PEG with different end groups including $-\text{CH}_3$ , $-\text{NH}_2$ , $-\text{COOH}$ , $-\text{IgG}$ , and $-\text{ProteinA}$ -protected-IgG	0.5–2 mg $\text{mL}^{-1}$	Platelet activation and reduced blood clotting time <i>in vitro</i>	121
Iron oxide	Not specified	Not specified	Not specified	PAA	1–62 $\mu\text{g mL}^{-1}$	PEGylation attenuated the observed effect on coagulation	124
Iron oxide	Spheroid-like	$72.6 \pm 0.57$ nm (TEM)	Not specified	None	25–200 $\mu\text{g mL}^{-1}$ <i>in vitro</i>	No effect on platelet activation and aggregation <i>in vitro</i>	122
Iron oxide	Spheroid-like	88.78 nm (DLS)	Negative or positive	Hyaluronic acid, chitosan, or PAA	12 mg Fe per kg of rat (IV route) 4–1000 $\mu\text{g mL}^{-1}$	Induced RBC aggregation and altered RBC rigidity by PS externalisation <i>in vitro</i>	130
Iron oxide	Spherical	60–70 nm (DLS)	Negative	Amorphous silica	0.025–0.1 mg $\text{mL}^{-1}$	Caused RBC apoptosis <i>in vivo</i>	123
Iron oxide	Irregular	$9.08 \pm 1.48$ nm (TEM) $25.3 \pm 0.97$ nm (DLS)	Negative	Dextran	0.008–1 mg $\text{mL}^{-1}$	Iron oxide nanoparticles with chitosan and hyaluronic coating showed least effect on platelets, RBCs, and coagulation <i>in vitro</i>	129
Iron oxide	Not specified	Starch-iron oxide NP: 45 nm (DLS) Citrate-iron oxide NP: 35 nm (DLS)	Not specified	Starch or citrate	64–256 $\mu\text{M}$	Induced platelet aggregation at dose >0.05 mg $\text{mL}^{-1}$ <i>in vitro</i>	125
Iron oxide	Not specified	$68 \pm 22$ nm to $88 \pm 30$ nm (DLS)	Positive, negative, neutral	PVA (12 or 31 kDa)	50–500 $\mu\text{g mL}^{-1}$	No effect on platelets <i>in vitro</i>	126
Iron oxide	Spherical	57–62 nm (DLS)	Negative	Citrate	75, 150, and 300 $\mu\text{M}$	Starch-iron oxide nanoparticles had no effect on platelets while those coated with citrate had antiplatelet effect <i>in vitro</i>	127

Table 2 (Contd.)

Nanoparticle	Shape	Size	Charge	Coating/stabiliser	Concentration tested	Main finding	Ref.
Iron oxide	Irregular shape	150 nm (DLS)	Negative	Sodium alginate sulfate (SAS)	0.01–10 mg mL <sup>-1</sup>	Reduced PF4 concentration, and platelet activation, fibrinogen solidification. Prolonged coagulation time <i>in vitro</i>	128
Silica	Spherical	58 nm (TEM) 106.33 ± 1.23 nm (DLS)	Negative	None	50 and 100 µg mL <sup>-1</sup>	NO imbalance, HUVECs dysfunction <i>in vitro</i>	137
Silica	Near spherical	58.11 ± 7.30 nm (TEM)	Negative	None	1.8–16.2 mg kg <sup>-1</sup> of rat (tracheal instillation route)	Increased CD31 expression, NO imbalance, increased coagulant factors (TF, vWF, FXa) and decreased anticoagulant factors (TFPI, antithrombin, t-PA) <i>in vitro</i>	134
Silica	Not specified	16–310 nm	Not specified	None	1000–30 000 nanoparticles per cell	Exhibited procoagulatory effect on HUVECs <i>in vitro</i>	252
Silica	Not specified	10–40 nm	Not specified	None	0.001, 0.01, 0.2, 0.4 mg mL <sup>-1</sup>	Enhanced FX activation and shortened coagulation time <i>in vitro</i>	269
Organically (organosilane derivatives) modified silica	Not specified	Non-PEGylated: 51 nm (DLS)	Negative	None or PEG	50–350 µg mL <sup>-1</sup>	Significant procoagulant effect <i>in vitro</i> except for highly PEGylated nanoparticles with poor procoagulant effect <i>in vitro</i>	142
Synthetic amorphous silica		PEGylated: 45 nm (DLS)		None			
Amorphous silica	Spherical	35 nm (DLS) 10–500 nm (TEM)	Negative	None	10–200 µg mL <sup>-1</sup>	Induced platelet activation and aggregation <i>in vitro</i>	139
Silica	Nearly spherical	58.11 ± 7.30 nm (DLS)	Negative	None	1.8–16.2 mg per kg bw of rat (intratracheal instillation route)	Increased endothelial dysfunction and pre-thrombotic state <i>in vivo</i>	134
Dye-labelled core/shell silica	Spherical	245 ± 10.82 nm (TEM)	Negative	None	10–250 µg mL <sup>-1</sup>	Promoted platelet adhesion to endothelial cells <i>in vitro</i>	140
Silica	Spherical	47.9 ± 7.1 nm (TEM)	Not specified	PEG	20–1000 µg mL <sup>-1</sup>	Slightly reduced platelet adhesion to endothelial cells and no effect to platelet aggregation at low dose (20–200 µg mL <sup>-1</sup> ) <i>in vitro</i>	141
		66.8 ± 0.3 nm (DLS)				Significantly induced platelet adhesion and aggregation at high dose (1000 µg mL <sup>-1</sup> ) <i>in vitro</i>	
Silica	Spherical	50 and 500 nm (TEM and DLS)	Negative	None	0.2–5 µg mL <sup>-1</sup> <i>in vitro</i>	Induced platelet aggregation <i>in vitro</i>	253
					0.5 mg kg <sup>-1</sup> of mice (intraperitoneal route)	Caused systemic coagulation events <i>in vivo</i>	

Table 2 (Contd.)

Nanoparticle	Shape	Size	Charge	Coating/stabiliser	Concentration tested	Main finding	Ref.
Silica	Spherical	70–1000 nm (DLS)	Not specified	None	0.02 mg mL <sup>-1</sup> <i>in vitro</i>	70 nm-NPs activated intrinsic pathway <i>via</i> the interaction with FXII <i>in vitro</i> 70 nm-NPs caused consumptive coagulopathy <i>in vivo</i>	48
Silica	Spherical	30–1000 nm (DLS)	Not specified	None	100 mg kg <sup>-1</sup> of mice (IV route)	30 and 70 nm-NPs promoted abnormal activation of intrinsic coagulation <i>in vivo</i> NPs with 12–85 nm in size inhibited coagulant effect <i>in vitro via</i> the FXII distortion	132
Silica	Spherical	4–85 nm	Negative	None	0.01–100 nM	Induced thrombin generation and triggered contact pathway of coagulation cascade <i>in vitro</i>	133
Silica	Spherical	53.79 ± 1.75 nm (DLS)	Negative	Polyphosphate (polyP)	0.05–0.5 mg mL <sup>-1</sup>	Initiated extrinsic pathway, induced TF level, and might cause endothelial cells dysfunction <i>in vivo</i>	135
Silica	Spherical or multi-faceted	20 nm (TEM, SEM)	Negative in 0.9% saline	None	20 mg kg <sup>-1</sup> of rat (IV route)	Caused prethrombotic and hypercoagulable state <i>via</i> induced platelet aggregation, platelet activation, hyperactivity of coagulation and resistance of fibrinolysis <i>in vivo</i>	136
Silica	Spherical	52.05 ± 8.38 nm (TEM)	Negative	None	20 mg kg <sup>-1</sup> of rat (IV route)	Prolonged coagulation time by PEG-MSN, R-MSN, P-MSN, and bare MSN at 1.0 mg mL <sup>-1</sup> <i>in vitro</i>	138
Silica	Spherical	~80 nm except RMSN with 62 ± 12 nm (TEM)	Negative charge except A-MSN with positive charge	Functionalized with PEG, aminopropyl (A-MSN), methylphosphonate propyl (P-MSN), methyl (M-MSN), phenyl (Ph-MSN), mercaptopropyl (T-MSN), and Rhodamine B-propyl (R-MSN)	0.1 and 1.0 mg mL <sup>-1</sup>	Triggered platelet aggregation <i>in vitro</i> and <i>in vivo</i>	143
Rutile titanium oxide	Rod	4–6 nm (TEM)	Not specified	None	0.4–10 µg mL <sup>-1</sup> <i>in vitro</i> 1 or 5 mg kg <sup>-1</sup> of rat (intratracheal instillation route)	No effect on platelets and hemodynamic parameters <i>in vivo</i>	144
Rutile titanium oxide	Not specified	67 nm (SEM) 309 ± 38 nm (DLS)	Not specified	None	1 mg kg <sup>-1</sup> of mice (arterial catheterization route)	No effect on platelets and did not exert prothrombotic effect <i>in vivo</i>	145
Rutile titanium oxide	Needle-like	10 × 40 nm (TEM)	Not specified	None	0.1 mg mL <sup>-1</sup> <i>in vitro</i> 1 mg kg <sup>-1</sup> of mice (arterial catheterization route)	Inhibited platelet aggregation and exhibited super antiplatelet and anticoagulant activities <i>in vitro</i>	146
Titanium oxide synthesized from <i>Alternaria solani</i>	Irregular shapes (SEM)	~15 nm crystallite size (XRD)	Not specified	None	50–100 µg mL <sup>-1</sup>	Prevented coagulation <i>in vitro</i>	148
Titanium oxide synthesized from extract of <i>Cola nitida</i>	Nearly spherical	25.00–191.41 nm (TEM)	Not specified	None	80 µg mL <sup>-1</sup>		147

Table 2 (Contd.)

Nanoparticle	Shape	Size	Charge	Coating/stabiliser	Concentration tested	Main finding	Ref.
Nickel	Spherical	62 nm (SEM)	Not specified	None	0.05 mg mL <sup>-1</sup>	Changed platelet shape <i>in vitro</i>	270
Zinc oxide	Rectangular	431 nm in 0.3 M glucose (DLS) Strong agglomeration and fast sedimentation in PBS-citrate	Negative	None	3 : 1 v/v ratio of platelet rich plasma	Promoted platelet activation <i>in vitro</i>	149
Zinc oxide	Spherical	20 and 100 nm (DLS)	Positive and negative	Bare, citrate, and L-serine	0.01–0.5 mg mL <sup>-1</sup>	Increased APTT and PT regardless of size or surface coating of the nanoparticles <i>in vitro</i>	150
Zinc oxide	Spherical	Diameter: 20–250/50–350 nm (TEM)	Not specified	None	Cumulative dose: 32 or 64 µg per mice (oropharyngeal aspiration)	Induced factor VIII level and showed procoagulant activity <i>in vitro</i>	75
Hydroxyapatite	Rod-like (HAp1) and needle-shape (HAp2)	Rod-like: width ~15–30 nm, length ~40–70 nm Needle-shape: 30–60 nm, length ~200–500 nm (TEM)	Not specified	None	10 µg mL <sup>-1</sup> –10 mg mL <sup>-1</sup>	No effect on platelet adhesion, aggregation, activation as well as both intrinsic and extrinsic pathway of coagulation system at 1–10 mg mL <sup>-1</sup> Exhibited slight thrombogenic activity at 10 mg mL <sup>-1</sup> by HAp2 Interfered with vWF and CD31 expression in endothelial cells by HAp2 at 10 and 50 µg mL <sup>-1</sup> <i>in vitro</i>	271
Tungsten	Mostly spherical	20 nm (TEM)	Not specified	None	10–100 µg mL <sup>-1</sup>	Prolonged clotting time at all concentration with the maximum effect at 40 µg mL <sup>-1</sup> <i>in vitro</i>	272
EMT-type zeolite	Cage-like	10–20 nm (DLS)	Negative	None	100 and 200 µg mL <sup>-1</sup>	Exhibited high selective affinity to fibrinogen and inhibited the interaction between fibrinogen and β-amyloid (Aβ), decreasing the delay in clot dissolution <i>in vitro</i> in the presence of Aβ	273
Calcium carbonate (CaCO <sub>3</sub> )	Nearly spherical	100 nm	Not specified	None	1 : 1 volume ratio between NPs and whole blood <i>in vitro</i> 500 mg and 1000 mg per mice every three days for up to 15 days <i>in vivo</i> (topical) 0–50 µg mL <sup>-1</sup>	Caused rapid coagulation at pH 5.0 but no thrombus at pH 7.4 <i>in vitro</i> Induced thrombus and fibrin clots <i>in vivo</i>	274
Cerium	Cubic crystallite structure	5 and 40 nm (TEM)	Not specified	None		No significant effect on platelet aggregation and coagulation	275



particles (MCN), single wall carbon nanotubes (SWCNT), and multiple wall carbon nanotubes (MWCNT) ( $0.2\text{--}300\ \mu\text{g ml}^{-1}$ ), was evaluated and compared with standard urban particulate matter (SRM1648,  $1.4\ \mu\text{m}$ ) in a study by Radomski *et al.*<sup>71</sup> Results showed that all tested materials induced platelet aggregation and increased the vascular thrombosis rate in rat carotid artery models in the order from highest to lowest:  $\text{MCN} \geq \text{SWCNT} > \text{MWCNT} > \text{SRM1648}$ . The platelet aggregation induced by these carbon nanoparticles correlated to the activation of the GpIIb/IIIa receptors, platelet degranulation, translocation of P-selectin to the platelet surface, and the tendency to mimic molecular bridges in platelet–platelet interactions. The prothrombotic effect of carbon nanotubes regarding platelet activation and aggregation was further explored in studies by Simak's group.<sup>72</sup> Their results were consistent with the previous study in which SWCNTs (outer diameter  $<2\ \text{nm}$ ,  $5\text{--}15\ \mu\text{m}$  in length for S1 SWCNT and  $1\text{--}2\ \text{nm}$  of outer diameter,  $5\text{--}30\ \mu\text{m}$  in length for S2 SWCNT) had higher platelet aggregation ( $34 \pm 5\%$  for S1 and  $32 \pm 6\%$  for S2) than MWCNTs (outer diameter was  $60\text{--}100\ \text{nm}$ ,  $1\text{--}2\ \mu\text{m}$  in length for M60 and  $30 \pm 15\ \text{nm}$  of outer diameter,  $1\text{--}5\ \mu\text{m}$  in length for M30) with platelet aggregation of  $27 \pm 3\%$  (M60) and  $38 \pm 9\%$  (M30). Amorphous carbon nanopowder (ACN) (outer diameter was  $\sim 30\ \text{nm}$ ) showed a weak effect on platelet aggregation ( $15 \pm 2\%$ ). It was reported that the effects of carbon nanotubes on platelet activation, degranulation, and aggregation were accompanied by elevated intracellular  $[\text{Ca}^{2+}]$  in platelets, which is the second key messenger-mediating platelet activation. Platelets raised intracellular  $[\text{Ca}^{2+}]$  by either releasing it from intracellular stores or the entering of extracellular  $\text{Ca}^{2+}$  through plasma membrane channels, including store-operated  $\text{Ca}^{2+}$  entry (SOCE), second messenger-operated  $\text{Ca}^{2+}$  entry (SMOC), and receptor-operated  $\text{Ca}^{2+}$  entry (ROC).<sup>72</sup> As the carbon nanotube-facilitated extracellular  $\text{Ca}^{2+}$  influx was sensitive to calcium entry blockers 2-APB and SKF 96365, SOCE was proved to be involved in platelet activation induced by carbon nanotubes.<sup>72,73</sup> It was proposed that MWCNTs ruptured the dense tubular system, a  $\text{Ca}^{2+}$  pool after penetrating the instantly resealed platelet membrane, leading to intracellular  $\text{Ca}^{2+}$  depletion and activating SOCE.<sup>73</sup>

Besides affecting platelets, carbon nanotubes and carbon dots also interfere with plasma factors of the coagulation system. By evaluating activated partial thromboplastin time (APTT) or partial thromboplastin time (PTT), Burke *et al.* concluded that, except for pluronic-coated pristine MWCNTs, all MWCNTs (pristine, carboxylated, or amidated; coated with pluronic F127 or distearoylphosphoethanolamine-(polyethylene glycol)-5000 (DSPE-PEG); range of diameter was  $26\text{--}31\ \text{nm}$ , median length was  $490\text{--}580\ \text{nm}$ ) at the concentration of  $100\ \mu\text{g mL}^{-1}$  triggered the intrinsic pathway by preferentially interacting with FIXa and acting as a platform to promote its enzyme activity.<sup>74</sup> It was revealed that the levels of fibrinogen and FVII were increased *in vivo* by carbon nanotubes (diameter was  $6\text{--}20\ \text{nm}$ ; length:  $700\text{--}4000\ \text{nm}$ ), demonstrating procoagulant activity.<sup>75</sup> As reported by Luo *et al.*, carbon dots synthesized from *Cirsium setosum* Carbonisata extract ( $\sim 2.6\ \text{nm}$ ) reduced

the bleeding time in mice by triggering the extrinsic pathway and activating fibrinogen.<sup>76</sup> However, there was a study presenting the anticoagulant activity of carbon dots synthesized from garlic (*Allium sativum*) extract through the reduced death rate of pulmonary thromboembolism-induced mice models.<sup>77</sup> This was due to the ability to inhibit platelet activation by decreasing the phospholipase C/PKC and mitogen activated protein kinase (MAPK) activation.

Carbon nano-diamonds (CNDs) with the size range of  $4\text{--}10\ \text{nm}$  can evoke platelet activation at low concentration ( $1\ \mu\text{g mL}^{-1}$ ).<sup>78</sup> Kumari *et al.* demonstrated that CNDs elevated the intracellular  $\text{Ca}^{2+}$  level in platelets and increased the expression of phosphatidylserine on the platelet membrane. CND-treated platelets showed reduced viability and altered morphology with developed lamellipodia or filopodia. *In vivo* results evidenced extensive pulmonary thromboembolism in mice after intravenous (IV) injection of CNDs.<sup>78</sup> Furthermore, nanodiamonds ( $100\ \text{nm}$ ) were found to greatly increase attraction forces between RBC membranes, leading to the formation of large and abnormal RBC aggregates<sup>79</sup> (Fig. 6).

Gelderman *et al.* reported that fullereneol  $\text{C}_{60}(\text{OH})_{24}$  nanoparticles ( $\sim 4.3\ \text{nm}$ ) at  $100\ \mu\text{g mL}^{-1}$  significantly triggered the expression of TF (CD142) on human umbilical vein endothelial cells (HUVECs) for the extrinsic coagulation pathway after 24 h of *in vitro* culture ( $4 \pm 2\%$  CD142<sup>+</sup> cells in control vs.  $54 \pm 20\%$  CD142<sup>+</sup> cells in treatment group).<sup>80</sup> In contrast, fullereneol nanoparticles ( $\sim 1.13 \pm 0.32\ \text{nm}$ ), at 0.5 and 1.0 mM, inhibited thrombin and FXa, thus delaying bleeding time in rats.<sup>81</sup> At 0.1 mM concentration, the fullereneol nanoparticles had no effect. In another study, fullereneol C60 ( $\sim 1.3\ \text{nm}$ ) and fullerene C60 ( $\sim 0.7\ \text{nm}$ ) had no effect on platelets at the concentration of  $100\ \mu\text{g mL}^{-1}$ .<sup>72</sup>

An *in vivo* study carried out by Singh *et al.* depicted an extreme thrombotic effect in mice after IV injection of atomically thin graphene oxide sheets (GO).<sup>82</sup> As explored in *in vitro* tests, GO sheets triggered platelet aggregation through the intracellular release of  $\text{Ca}^{2+}$  and the activation of Src kinases. At the concentration of  $2\ \mu\text{g mL}^{-1}$ , this effect of GO sheets was higher than that induced by  $1\ \text{U mL}^{-1}$  of thrombin. Continuing this study, Singh *et al.* discovered that amine-modified GO sheets (GO-NH<sub>2</sub>) ( $2$  and  $10\ \mu\text{g mL}^{-1}$ ) did not show any induced or inhibitory effect on platelets, without noticeable change in the ROS level.<sup>83</sup> There was no *in vivo* pulmonary thromboembolism after GO-NH<sub>2</sub> exposure.

In summary, most carbon-based nanoparticles discussed in this section (Table 2) had either negative charge or charge not specified. Regardless of size and shape, all of them exhibited thrombogenic effects except pristine carbon nanotubes coated with pluronic F127<sup>74</sup> or pre-treated with albumin,<sup>84</sup> carbon dots synthesized from garlic (*Allium sativum*) extract,<sup>77</sup> and most of the investigated fullereneol.<sup>72,81</sup> Coating the nanoparticles with pluronic or albumin meant they were able to prevent or lessen the thrombogenic effect of carbon-based nanoparticles.<sup>74,84</sup>

**Silver nanoparticles.** The interactions between silver nanoparticles (AgNPs) and endothelial cell membranes can increase

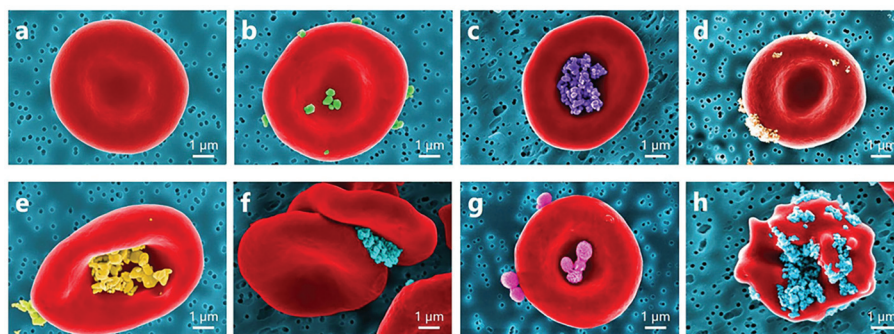


**Fig. 6** Coloured SEM images presenting a diversity of observed NP localizations on the RBC surface: (a) normal conditions; RBC incubated with (b) rutile-coated TiO<sub>2</sub> nanoparticles, (c) alumina-polyol-coated TiO<sub>2</sub> nanoparticles, (d) uncoated TiO<sub>2</sub> nanoparticles (15 nm), (e) uncoated ZnO nanoparticles, (f) carboxylate nanodiamonds (100 nm), and (g) polymeric nanoparticles; (h) echinocyte form of RBC due to adhesion of carboxylate nanodiamonds. Among the interactions with inorganic nanoparticles, RBC incubation with nanodiamonds results in stronger RBC aggregation forces and influences the shape of RBCs.<sup>79</sup>

the cells' permeability, which is a main factor leading to endothelium dysfunction.<sup>85</sup> Danielsen *et al.* reported that AgNPs (capped with polyoxylaurat Tween-20, <20 nm) induced cytotoxicity at a concentration of 64  $\mu\text{g mL}^{-1}$  after 24 h of incubation with HUVECs.<sup>86</sup>

Furthermore, various studies demonstrated the procoagulant and prothrombotic properties of AgNPs exhibited *via* the interaction with platelets. The accumulation of AgNPs within

platelets can interfere with intra-platelet activities regardless of surface coating<sup>87–90</sup> (Fig. 7). AgNPs, 10–100 nm in diameter, induced intracellular [Ca<sup>2+</sup>] (250  $\mu\text{g mL}^{-1}$  of AgNPs), which upregulated GpIIb/IIIa (100  $\mu\text{g mL}^{-1}$  of AgNPs) and P-selectin expression (100  $\mu\text{g mL}^{-1}$  of AgNPs), and serotonin secretion (250  $\mu\text{g mL}^{-1}$  of AgNPs).<sup>88</sup> Enhanced thrombin and phosphatidylserine generation (250  $\mu\text{g mL}^{-1}$  of AgNPs) were observed in fresh human platelets as evidence for platelet aggregation

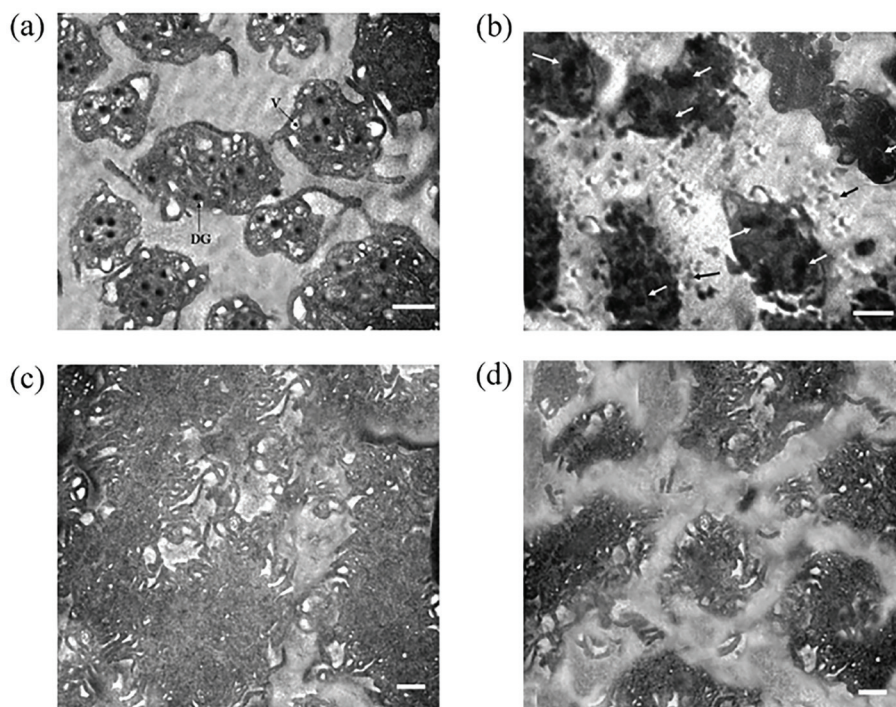


**Fig. 7** Electron micrographs through sections of activated and aggregated platelets with and without pre-treatment of AgNPs. (a) Intact platelets showing hyaloplasmic processes (pseudopods), dense granules with eccentric opacity, and vacuoles with limiting membrane. (b) Platelets pretreated with silver nanoparticles showed accumulation of AgNPs in vacuolar spaces (white arrow) with the absence of hyaloplasmic processes. Nanoparticle clusters (black arrow) are also seen in the surrounding microenvironment. (c) Electron micrograph demonstrating intimate adherence between the platelets during thrombus formation. Only occasional narrow spaces are visible between some cells. (d) AgNPs-pretreated platelets failed to aggregate and could only manage to form small, diffuse, and loosely packed clumps separated by wide distances.<sup>87</sup>

induced by AgNPs. Accumulated AgNPs (stabilized with sodium polyacrylate,  $30 \text{ mg L}^{-1}$ , 10–15 nm) triggered  $\alpha$ -granule secretion and induced kallikrein-like, FXIIa-like, and thrombin-antithrombin III complex.<sup>89</sup> Further exposure of AgNPs in rats ( $0.05\text{--}0.1 \text{ mg kg}^{-1}$  intravenous or  $5\text{--}10 \text{ mg kg}^{-1}$  intratracheal instillation) induced platelet aggregation, phosphatidylserine externalization, and vascular thrombus formation *ex vivo*.<sup>88,89</sup> In another study, AgNPs (16 nm, coated with polyvinylpyrrolidone (PVP)) only promoted platelet adhesion but not platelet aggregation at the concentration of  $50 \text{ }\mu\text{g mL}^{-1}$  as compared with the control<sup>91</sup> (Fig. 8). However, AgNPs (20 nm) with neither PVP coating nor citrate coating exerted any effect on platelet aggregation and coagulation at a concentration of up to  $\sim 500 \text{ }\mu\text{g mL}^{-1}$ .<sup>92</sup> The lignin capped AgNPs ( $\sim 10\text{--}15 \text{ nm}$ ) significantly reduced platelet aggregation of platelet rich plasma (PRP) at  $15 \text{ }\mu\text{g per } 0.25 \text{ mL}$ .<sup>93</sup> In addition to platelets, a study investigated the effect of AgNPs on RBCs and established that after 4 h of incubation, all silver nanomaterials functionalised with PVP (30 nm AgNPs, 100 nm AgNPs, and silver nanowires) exhibited a significant reduction in RBCs deformability at both 50 and  $150 \text{ }\mu\text{g mL}^{-1}$ .<sup>94</sup> AgNPs (30 nm) reduced RBC deformability the most compared with 100 nm AgNPs and silver nanowires. Unlike RBC deformability, all PVP coated silver nanomaterials decreased RBC aggregation at high concentration ( $150 \text{ }\mu\text{g mL}^{-1}$ ) whilst 30 nm AgNPs had no effect on RBC aggregation at low concentration ( $50 \text{ }\mu\text{g mL}^{-1}$ ).

By contrast, some other studies reported the antiplatelet properties of AgNPs (stabilised with either citrate or D-glucose).<sup>87,95,96</sup> Accumulative AgNPs within platelet granules impeded integrin-mediated platelet responses such as adhesion to immobilized fibrinogen and platelet conformation change, namely retraction of a fibrin clot, in a concentration-dependent manner *in vitro* and *in vivo*, regardless of agonists used.<sup>87,95</sup> AgNPs (stabilised with D-glucose) also inhibited platelet aggregation induced by either ADP, thrombin, or collagen *in vitro* and in mouse whole blood in a dose-dependent

manner.<sup>95</sup> AgNPs functionalized with lipoic acid, reduced glutathione (GSH) and polyethylene glycol (PEG) decreased aggregation of platelets by reducing the level of P-selectin, GPIIb/IIIa, TXB2, and the release of MMP-1, MMP-2.<sup>97</sup> It was stated that platelet aggregation can be promoted by MMP-1 and MMP-2. While the mechanism of action of MMP-2 remained unclear, MMP-1 activates PAR1 on platelets.<sup>98</sup> The MMP1-PAR1 obstruction can curtail thrombogenesis.<sup>98</sup>

Aside from platelets, plasma factors are also the target of AgNP interactions that leads to anticoagulant and antifibrinolytic effects. Several studies described the conformational change of fibrin through its interactions with AgNPs (either being coated with PEG or stabilised with citrate),<sup>87,90,99</sup> which leads to the inhibition of fibrin polymerization and thrombus formation *in vitro*.<sup>99</sup> Nevertheless, it is worth noting that this effect is less pronounced in plasma than in a purified system due to nonspecific interactions of AgNPs with other plasma proteins such as globulin and albumin. In another study, chitosan coated AgNPs showed inhibitory effects on FXa.<sup>100</sup> Interestingly, almost all biogenic or green AgNPs exerted thrombolysis activity<sup>101–107</sup> (Table 2). The proposed mechanisms are (1) green AgNPs may activate the conversion of plasminogen to plasmin which then dissolves the blood clot, or (2) directly targeting fibrin causes fibrin degradation as reported by Harish *et al.*<sup>108</sup>

To sum up, all reported biogenic AgNPs exhibited anticoagulant effects regardless of their physicochemical characteristics such as size, shape, and charge.<sup>101–107</sup> Coating or stabilizing the non-biogenic AgNPs with PEG,<sup>90,97</sup> citrate,<sup>87,92,96</sup> D-glucose,<sup>95</sup> lignin,<sup>93</sup> reduced glutathione (GSH),<sup>97</sup> lipoic acid (LA),<sup>97</sup> heparin,<sup>109</sup> and low molecular weight sulfoethyl chitosan<sup>100</sup> can prevent their procoagulant effects or even promote the anticoagulant activity (*i.e.* those with citrate coating). Coating of AgNPs with PVP exhibited inconsistent results. In some studies, PVP-AgNPs were shown to be compatible with the haemostatic balance with no effect on platelet aggregation

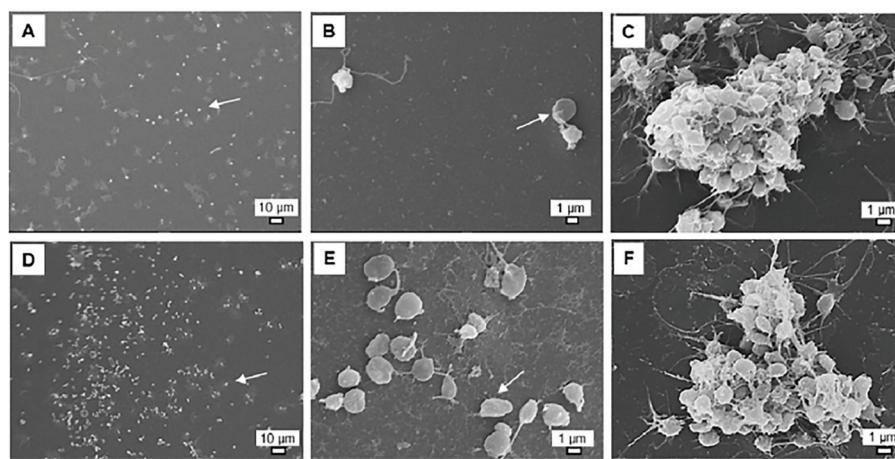


Fig. 8 SEM pictures of platelet adhesion without (A–C) or with PVP-AgNPs at a final concentration of  $50 \text{ }\mu\text{g mL}^{-1}$  (D–F). Platelet aggregation was induced by arachidonic acid (C, F). Arrows indicate adherent platelets.<sup>91</sup>

and coagulation<sup>92</sup> and decreased RBC aggregation.<sup>94</sup> In contrast, PVP-AgNPs in other studies exhibited procoagulant, promoted platelet adhesion<sup>91</sup> and reduced RBC deformability.<sup>94</sup> These inconsistencies were not related to PVP-AgNPs size, shape, and concentration. Pristine non-biogenic AgNPs<sup>88</sup> and AgNPs coated with sodium polyacrylate<sup>89</sup> interfered and shifted the haemostatic balance to the thrombogenic side. In contrast, AgNPs coated with heparin shifted the haemostatic balance to the anticoagulant side, regardless of their shape.<sup>109</sup>

**Gold nanoparticles.** The effect of gold nanoparticles (AuNPs) on platelets was first demonstrated in rats by Berry *et al.*<sup>110</sup> The presence of a high amount of AuNPs in platelets of alveolar capillaries affected platelet aggregation, leading to microthrombus and atheromatous plaques formation. Deb *et al.* demonstrated that the molecular mechanism of platelet aggregation induced by AuNPs (stabilized with citrate) is linked to degranulation and the increased expression level of P-selectin and tyrosine phosphorylation.<sup>111</sup> This study revealed that platelet response constantly decreased with the increment in AuNP size, where AuNPs greater than 60 nm (>40  $\mu\text{M}$ ) were inert to platelets compared with maximal platelet activation effects of smaller ones (~20 nm) at 40  $\mu\text{M}$ . This effect might be attributed to the higher accumulation of small AuNPs in platelets.<sup>111</sup> In contrast, Love *et al.* found that either AuNPs, Au(+) nanoparticles, or Au(-) nanoparticles (stabilized with either citrate, 11-mercaptoundecanoic acid, or 11-mercaptoundecylamine, respectively) of around 30 nm and up to 50  $\mu\text{g mL}^{-1}$  did not induce platelet aggregation after short-term exposure, probably because of protein corona formation on the surface of examined AuNPs.<sup>112</sup>

Fibrinogen can strongly bind to gold nanoparticles (stabilised with citrate) due to the presence of cysteine residues presented in alpha, beta, and gamma chains of fibrinogen, which allows Au-S bond formation and could induce blood clots.<sup>113</sup> However, another study reported that fibrinogen bound on the surface of gold nanoparticles which were stabilised with citrate only increased the nanoparticle size but did not cause blood coagulation as in the above study.<sup>114</sup> Deng *et al.* demonstrated that poly(acrylic acid) (PAA) conjugated on the surface of gold nanoparticles binds to fibrinogen and unfolds its conformation.<sup>115</sup> Unexpectedly, gold nanoparticles functionalized with human fibrinogen (HFib), PEG-thiol, or clopidogrel on the surface, prevented fibrin build-up as well as cross-linking with platelets, thus disrupting clot formation.<sup>116</sup>

All AuNPs reviewed in this paper are provided in Table 2. Taken together, AuNPs coated with 11-mercaptoundecanoic acid,<sup>112</sup> 11-mercaptoundecylamine,<sup>112</sup> PEG-thiol,<sup>116</sup> HFib,<sup>116</sup> clopidogrel,<sup>116</sup> and monocarboxy (1-mercaptoundec-11-yl) hexaethylene glycol (OEG)<sup>117</sup> had no effect on platelets,<sup>112,116</sup> HUVECs,<sup>117</sup> or coagulation,<sup>116</sup> while those with polyethylenimine (PEI) or polyvinylpyrrolidone (PVP) coating induced platelet aggregation.<sup>118</sup> Although there was a study reporting that citrate-coated gold nanoparticles could interact with fibrinogen and induce blood clot,<sup>113</sup> most citrate-coated AuNPs reviewed in this section had no thrombotic

effect,<sup>96,111,112,114,116,119</sup> except for 20 nm-citrate coated AuNPs<sup>111</sup> and 12 to 85 nm-citrate coated AuNPs at high dose (5 nM).<sup>116</sup> These results implied that the size and dose of nanoparticles influence the effect of AuNPs on the haemostatic balance in addition to surface functionalisation. Analysis methods also had impact as well. In Santos-Martinez *et al.*'s study, induced platelet aggregation by citrate coated AuNPs was detected by quartz crystal microbalance with dissipation (QCM-D), while no aggregation was observed by the light aggregometry method.<sup>120</sup> Indeed, most investigated AuNPs were spherical in shape. Hence, further investigations for the effect of other shapes of gold nanoparticles, such as rod, cage, star, triangle, hexagonal, were highly needed.

**Iron oxide nanoparticles.** The effect of iron oxide nanoparticles (IONPs) on haemostatic balance is somehow contradictory as they can have either induced,<sup>121–123</sup> inhibitory,<sup>124–128</sup> or neutral effects,<sup>121,125,129</sup> highly dependent on the stabilising agents coated on the nanoparticle surface. According to a study reported by Bircher *et al.*, iron carbide nanoparticles coated with carbon (~30 nm) increased the expression of GpIIb/IIIa and P-selectin by platelets, which led to a reduced blood clotting time by 25% at the concentration of 1 mg  $\text{mL}^{-1}$ .<sup>121</sup> Also, IONPs coated amorphous silica (~60–70 nm) triggered platelet aggregation.<sup>123</sup> Bare  $\text{Fe}_3\text{O}_4$  magnetic nanoparticles (~73 nm, 25–200  $\mu\text{g mL}^{-1}$ )<sup>122</sup> induced the aggregation of RBCs. Ran *et al.* reported that IONPs (72.6  $\pm$  0.57 nm, 25–200  $\mu\text{g mL}^{-1}$ ) dramatically altered RBC rigidity by externalising PS on the cell surface (the PS-expressed cells reached 40% after 48 h), which ultimately changed the thrombotic potential of blood.<sup>122</sup>

In contrast, PEGylation of iron carbide nanoparticles attenuated the influence of the nano-magnets on haemostatic components. No significant effect was observed at a concentration of 0.5 mg  $\text{mL}^{-1}$ .<sup>121</sup> In other comparable studies, starch-coated IONPs (45 nm, 128–256  $\mu\text{M}$ )<sup>125</sup> and dextran-stabilised IONPs (25.3  $\pm$  0.97 nm, 0.008–1 mg  $\text{mL}^{-1}$ )<sup>129</sup> did not exert any effect on platelet function.

However, Deb *et al.* indicated that citric acid-stabilised iron oxide nanoparticles (FeNP(C)) (35 nm, tested concentration range was 64, 128, 192, and 256  $\mu\text{M}$ ) had antiplatelet properties, which was higher than what citric acid has by itself, as reflected in various molecular events including ATP release of dense granules, the level of tyrosine phosphorylation, and the expression of GpIIb/IIIa and CD62P (P-selectin).<sup>125</sup> In another study, IONPs stabilized with citrate (~57–62 nm) also diminished platelet aggregation.<sup>127</sup> In addition, poly(acrylic acid)-coated IONPs presented no effect on platelet activation and aggregation, even up to 62  $\mu\text{g mL}^{-1}$  of the nanoparticles.<sup>124</sup> Polyvinyl alcohol (PVA) coated IONPs showed antiplatelet effects regardless of PVA charge and molecular weight.<sup>126</sup> It was demonstrated that PVA-IONPs affected and changed fibrinogen confirmation, which disrupts the bridging between fibrinogen and platelets. Moreover, sodium alginate sulfate (SAS) coated IONPs caused fibrinogen aggregation and solidification as well as reduced PF4 concentration, which was probably due to the excessive presence of sulfonic acid in SAS.

These effects led to diminished platelet activation and prolonged clotting time.<sup>128</sup>

To conclude, IONPs were mostly coated or stabilised with other materials. Coating IONPs with PEG,<sup>121</sup> hyaluronic acid,<sup>130</sup> chitosan,<sup>130</sup> dextran,<sup>129</sup> starch,<sup>125</sup> PVA,<sup>126</sup> and citrate<sup>127</sup> attenuated or prevented their effect on the haemostatic balance. PAA-coated IONPs showed stronger effect on platelets, RBCs, and coagulation compared with those with hyaluronic acid (HA) and chitosan, indicating that HA and chitosan were safer coating materials for IONPs.<sup>130</sup> In contrast, coating IONPs with SAS<sup>128</sup> or citrate<sup>125</sup> can lead to anticoagulant effects. Bare,<sup>122</sup> silica coated,<sup>123</sup> or carbon coated IONPs<sup>121</sup> exerted prothrombotic effects.

**Silica nanoparticles.** Silica nanoparticles can trigger procoagulant effects and dysregulate haemostatic balance through the interference with plasma factors of coagulation cascade, endothelial cells, and platelets. For example, Baker *et al.* reported that mesocellular silica foams (MCFs) with the window size >11 nm and the total pore volume at 0.0006 cm<sup>3</sup> facilitated clotting in FXII dependent mechanisms.<sup>131</sup> The authors stated that FXII, with a hydrodynamic size of 7.5 nm, can diffuse into and adhere to MCF cells, thus activating and initiating coagulation cascade. Silica nanoparticles (70 nm) at 0.02 mg mL<sup>-1</sup> were reported to activate the intrinsic pathway *via* their interaction with FXII *in vitro*.<sup>48</sup> Decreasing the silica particle size from micrometer to nanometer (30 and 70 nm), *i.e.* increasing the particle surface, resulted in a higher degree of FXII activation after intranasal exposure in mice for 7 days at 500 µg per mouse.<sup>132</sup> Kushida *et al.* explored that silica nanoparticles at varied concentrations of 0.01–100 nM with the size of 12–85 nm had significant coagulation activity, while those with very small sizes (4–7 nm) did not.<sup>133</sup> The reason may be that very small nanoparticles (4–7 nm) have a higher surface curvature, which do not distort the configuration of FXII after its adsorption on the surface of the nanoparticles and affects the activation of other factors such as kallikrein, leading to a coagulant “silent” surface. Besides, coagulant factors such as FXa and vWF were induced whilst anti-coagulant factors were reduced after 30 days of exposure to silica nanoparticles (58.11 ± 7.30 nm) in rats.<sup>134</sup> The tested concentration of the nanoparticles was 1.8–16.2 mg kg<sup>-1</sup>. In a study reported by Kudela *et al.*, silica nanoparticles (53.79 ± 1.75 nm) functionalized with polyphosphate triggered intrinsic pathways and induced thrombin generation.<sup>135</sup> Bare 20 nm silica nanoparticles can also induce TF levels that initiate extrinsic pathways and might cause endothelial cell dysfunction when being IV injected in rats at a dose of 20 mg kg<sup>-1</sup>.<sup>136</sup>

Silica nanoparticles, as demonstrated by Feng *et al.*, caused hypercoagulation through inducing vascular endothelial cells dysfunction.<sup>134</sup> The increased expression of TFs and platelet endothelial cell adhesion molecule-1 (PECAM-1 or CD31), as well as the imbalance of the NO/NOS (nitric oxide synthase) system, were detected after the exposure to silica nanoparticles (starting from 1.8 mg kg<sup>-1</sup> in rats). Correspondingly, silica nanoparticles (58 nm), especially at high concentrations of 50

and 100 µg mL<sup>-1</sup>, interrupted the NO balance, leading to HUVECs dysfunction.<sup>137</sup> In another study, silica nanoparticles (52.05 ± 8.38 nm, IV dose: 20 mg kg<sup>-1</sup>) induced platelet activation and aggregation, coagulation hyperactivity, and fibrinolysis resistance, causing prethrombotic and hypercoagulable state in rats.<sup>138</sup> Anionic amorphous silica nanoparticles (SiNPs) (10–500 nm) with concentrations varying from 10 to 200 µg mL<sup>-1</sup> were reported to induce platelet activation and aggregation, accompanied with GpIIb/IIIa and CD62P upregulation.<sup>139</sup> Since the thrombotic activity of SiNPs was hindered by inhibitors of ADP and the matrix metalloproteinase-2 (MMP2) pathway, the author discussed that the nanoparticles interacted with Ca<sup>2+</sup> ion channels and resulted in extracellular Ca<sup>2+</sup> influx into platelets cytoplasm, leading to the activation of endothelial NOS (eNOS) for NO generation. After the substrate (L-arginine) is used up, eNOS is uncoupled, and superoxide is produced to interact with NO to form ONOO<sup>-</sup> (peroxynitrite anion). Low ratio of NO/ONOO<sup>-</sup> is a marker of oxidative stress and diminished NO<sup>-</sup> availability, which promotes platelet activation. In other studies, silica nanoparticles (around 58 and 245 nm) were reported to enhance the expression of PECAM-1 (starting from 1.8 mg per kg bw of rat), resulting in NO/NOS system imbalance (>1.8 mg per kg bw of rat), and increase in platelet number on endothelial cells (both 10 µg mL<sup>-1</sup> and 250 µg mL<sup>-1</sup>), promoting platelet adhesion and prethrombotic state.<sup>134,140</sup> Such phenomena is in contrast with another study where PEGylated silica nanoparticles at 20–200 µg mL<sup>-1</sup> led to a decrease in adhered platelet number compared with the control and the treatment group at higher concentrations of the nanoparticles (~1000 µg mL<sup>-1</sup>).<sup>141</sup> The differences between the two studies might be attributed to the PEG coating, porosity, size (50 nm *vs.* 250 nm), and the fabrication method (Stöber *versus* mesoporous silica nanoparticles) of the particles.

As explored in a study by Tavano *et al.*, PEGylated organically modified silica nanoparticles (PEG-ORMOSIL) had poor procoagulant activity thanks to a thick superficial PEG coating (accounts for ~37% w/w of the nanoparticles).<sup>142</sup> By contrast, both synthetic amorphous silica nanoparticles (SAS-NPs) and bare ORMOSIL had appreciable procoagulant effect. In another study, not only PEG coated mesoporous silica nanoparticle (MSN), but also phenyl coated MSN, Rhodamine B coated MSN, and bare MSN led to delayed coagulation time *in vitro* at 1.0 mg mL<sup>-1</sup>.<sup>143</sup>

In conclusion, all investigated silica nanoparticles exerted profound prothrombotic effects on the haemostatic balance, except for those with PEG coating<sup>141–143</sup> and phenyl surface functionalisation.<sup>143</sup>

**Other inorganic nanoparticles.** Rutile titanium (TiO<sub>2</sub>) nanorods (0.4–10 µg mL<sup>-1</sup>, 4–6 nm) were reported to cause significant platelet aggregation in rat blood in a concentration-dependent manner.<sup>144</sup> After intratracheal instillation of TiO<sub>2</sub> nanorods in rats, the platelet count was significantly decreased, indicating platelet aggregation *in vivo*. The molecular mechanism for platelet response to TiO<sub>2</sub> nanorods is still ambiguous but could be associated with the shape and/or

surface feature of the material. However, rutile TiO<sub>2</sub> nanoparticles (67 nm in size, needle-like shape) showed no effect on murine platelets with an injection dose of 1 mg kg<sup>-1</sup> in other studies.<sup>145,146</sup> Spherical TiO<sub>2</sub> nanoparticles synthesized from extract of *Cola nitida*<sup>147</sup> and irregular shape TiO<sub>2</sub> nanoparticles synthesized from *Alternaria solani*<sup>148</sup> showed antiplatelet and anticoagulant effects *in vitro*.

As described in some studies, rectangular zinc oxide nanoparticles (ZnO NPs) caused procoagulant effects by either promoting platelet activation<sup>149</sup> or inducing FVIII in the coagulation cascade.<sup>75</sup> However, spherical ZnO NPs (bare, citrate, and L-serine coating) suppressed thrombin generation and absorbed coagulation clotting factors that led to prolonged coagulation time in another study.<sup>150</sup> Layered double hydroxide nanoparticles (MgAl-Cl-LDH) had no effect on HUVECs at concentrations up to 10 µg mL<sup>-1</sup>.<sup>151</sup> Fibre-like gadolinium oxide (Gd<sub>2</sub>O<sub>3</sub>) nanoparticles (diameter: 13.7 ± 6 nm, length: 54.8 ± 29 nm) were both apoptotic and necrotic to HUVECs after 48 h of exposure (IC<sub>50</sub> = 304 ± 17 µg mL<sup>-1</sup>).<sup>152</sup> The effects of other types of nanoparticles such as nickel, cerium, tungsten, and hydroxyapatite toward haemostatic balance are presented in Table 2.

### 3.2 Organic nanoparticles

Physicochemical characteristics of all nanomaterials discussed in this section are detailed in Table 3.

**Dendrimers.** As reported, dendrimer nanoparticles can interfere with haemostatic balance by affecting vascular endothelial cells or platelets. Cationic dendrimer nanoparticles interacted with HUVEC membranes, and poly(amidoamine) (PAMAM) dendrimer generation 4 and 7 (G4 and G7) (IV administration doses >10 mg kg<sup>-1</sup>) caused disseminated intravascular coagulation in mice.<sup>153</sup> Several studies have demonstrated that large, cationic poly(amidoamine) (PAMAM) dendrimers (above G4) induced platelet aggregation. Dobrovolskaia *et al.* revealed that only large and cationic PAMAM dendrimers (amine-G4, amine-G5, and amine-G6) induced platelet aggregation by evaluating 12 PAMAM dendrimers of different generations (G3 to G6) functionalized with succinamic acid (anionic), amidoethanol (neutral), and amine (cationic).<sup>154</sup> Moreover, the aggregation effect was proportional to the number of amine groups on the surface. The author stated that the observed platelet aggregation was neither accompanied by the release of platelet membrane microparticles nor sensitive to inhibitors interfering with platelet activation pathways. Hence, the proposed mechanism is supposed to involve the capability of cationic PAMAM to disrupt platelet membrane integrity and thus induce the aggregation. Computational simulations also supported this proposal.<sup>155</sup> In a study by Jones *et al.*, large and cationic PAMAM G7 dendrimer nanoparticles (100 µg mL<sup>-1</sup>) exerted their effect in altering platelet morphology, which substantially interfered with platelet function, and induced platelet adhesion and aggregation.<sup>156</sup> Greish *et al.* also reported that G4 and G7 PAMAM dendrimer nanoparticles caused DIC-like

manifestations in mice at a dose >10 mg kg<sup>-1</sup>.<sup>153</sup> As compared with PAMAM dendrimers, triazine dendrimers (0.01–1 µM) evoked less aggressive platelet aggregation due to differences in the assembly of supramolecular structure and/or cationic charge.<sup>157</sup>

In summary, the effect of dendrimer nanoparticles was highly dependent on their surface charge and generation. Large and cationic PAMAM (≥G4) and large generation of triazine dendrimer (G5 and G7) were prothrombotic. Moreover, PAMAM dendrimers exhibited more profound effects on the haemostatic balance than triazine dendrimers.

**Lipid-based nanoparticles.** It has been reported that anionic lipid-based (cetyl alcohol/polysorbate) nanoparticles (bare or PEG coating, 1–1000 µg mL<sup>-1</sup>)<sup>158</sup> and both anionic and cationic liposomes prepared from a photopolymerizable phosphatidylcholine derivative (100–360 µg per 0.5 mL platelet)<sup>159</sup> inhibited platelet activation and aggregation in a concentration-dependent manner. However, Reinish *et al.* reported a reduction in platelet number in the first 5 min after IV injection of anionic liposomes (dose level of 25 mg kg<sup>-1</sup>) in rats.<sup>160</sup> The platelet count was recovered after 60 min post-injection. Similarly, anionic liposomes (phosphatidylcholine : phosphatidic acid = 8 : 1), not cationic and neutral liposomes, provoked platelet aggregation *in vitro* and *in vivo* after IV injection in Guinea pigs.<sup>161</sup> The effect was probably due to the interaction between anionic liposomes and FXIII/XI. Moreover, Constantinescu *et al.* suggested that the interaction of liposomes with platelets was independent of opsonisation but dependent on the liposome concentration.<sup>162</sup> The discrepancies between studies might be attributed to not only the surface charge but also the composition of the lipid-based nanoparticles.

Overall, all lipid-based nanoparticles (without or with PEG coating) had no effect or inhibited thrombotic effect, except for those reported in Reinish *et al.* and Zbinden *et al.* studies as discussed above.<sup>160,161</sup>

**Polystyrene nanoparticles.** Polystyrene nanoparticles can affect platelets, RBCs, and plasma factors in an approach that might possibly shift the haemostatic balance to a procoagulant state. As reported by Smyth *et al.*, unmodified, carboxyl-modified, and amine-modified polystyrene latex nanoparticles from 50 to 100 nm caused aggregation of platelets in a dose-dependent manner (15–60 µg mL<sup>-1</sup>), except for the 50 nm amine-modified ones *in vitro*.<sup>163</sup> This aggregation was mediated by secondary agonists released from platelet granules and induced GpIIb/IIIa expression depending on Ca<sup>2+</sup> influx and protein kinase C (PKC) signalling pathways. The author also described that these effects were associated with both size and surface modification. In another study, carboxyl-modified polystyrene nanoparticles (~80 nm, 260 µg mL<sup>-1</sup>) induced platelet aggregation by disrupting platelet membranes and upregulating platelet-activating markers P-selectin and PAC-1, respectively.<sup>164</sup> In contrast, another study reported that polystyrene nanobeads (PBs) (20 and 200 nm) had no effect on platelets.<sup>72</sup>

Pan *et al.* demonstrated that the absorption of polystyrene nanoparticles (PSNPs) on murine RBCs significantly reduced

Table 3 A summary of the effects of common organic nanoparticles on haemostatic balance *in vitro* and *in vivo*

Nanoparticle	Shape	Size	Charge	Coating/stabiliser	Concentration tested	Main finding	Ref.
PAMAM dendrimer (G4, G7)	Not specified	3.4 ± 0.22 nm (G4) 8.1 ± 0.42 nm (G7) (DLS)	Positive	None	Dose >10 mg kg <sup>-1</sup> of mice (IV route)	Caused disseminated intravascular coagulation-like manifestation <i>in vivo</i>	153
PAPAM dendrimer (G3–G6)	Globular	~3–8 nm (DLS)	Positive, negative, or neutral	Succinamic acid, amidoethanol, or amine surface functionalization	1.563–100 µg mL <sup>-1</sup>	Induced platelet aggregation by large and cationic PAMAM dendrimer <i>in vitro</i>	154
PAMAM dendrimer (G7) (amine-modified)	Not specified	8.1 ± 0.42 nm (DLS)	Positive	None	100 µg mL <sup>-1</sup>	Changed platelet shape, induced platelet activation and aggregation <i>in vitro</i>	155
Triazine dendrimer (amine-modified)	Not specified	3.7–13.7 nm	Positive	None	0.01–1 µM	No appreciable effect on platelet by low generation triazine dendrimer but promoted platelet aggregation with larger generation <i>in vitro</i>	157
Liposome	Spherical	109 and 139 nm (DLS)	Negative	PEG	12.5–400 µg mL <sup>-1</sup>	No effect on HUVECs <i>in vitro</i>	276
Liposome (phosphatidylglycerol, egg phosphatidylcholine, cholesterol)	Spherical	Not specified	Negative	None	2.5 mg kg <sup>-1</sup> of rat (IV route)	Induced platelet aggregation (reduced platelet number) after the first 5 min of injection. The platelet count was recovered after 60 min post-injection <i>in vivo</i>	160
Liposome (phosphatidylcholine, phosphatidic acid)	Spherical	Not specified	Negative	None	0.1–0.4 mL of stock suspension/2 × 10 <sup>5</sup> platelet <i>in vitro</i> 2 mL kg <sup>-1</sup> of Guinea pig per h for 1 h <i>in vivo</i>	Provoked platelet aggregation <i>in vitro</i> and <i>in vivo</i>	161
Liposome (photopolymerizable phosphatidylcholine derivative)	Spherical	Not specified	Positive, negative, or neutral	None	100–360 µg per 0.5 mL platelet	Inhibited platelet activation and aggregation <i>in vitro</i> by positive and negatively charged liposomes	159
Cetyl alcohol/polysorbate	Not specified	Bare NPs: 67.0 ± 17.5 nm (DLS) PEGylated NPs: 67.0 ± 11.7 nm (DLS)	Negative	None or PEG	1–1000 µg mL <sup>-1</sup>	Inhibited agonist-induced platelet activation and aggregation Prolonged whole blood clotting time at the concentration >500 µg mL <sup>-1</sup> of bare NPs <i>in vitro</i>	158
Polystyrene latex (pristine, amine- and carboxyl-modified)	Spherical	50–100 nm (TEM)	Positive, negative, or neutral	None	15–60 µg mL <sup>-1</sup>	Caused platelet aggregation except for the 50 nm amine-modified NPs <i>in vitro</i>	163
Polystyrene (unmodified, aminated-modified, carboxyl-modified)	Spherical	~60–80 nm in buffer containing 0.35% plasma (DLS)	Negative	None	260 µg mL <sup>-1</sup>	Induced platelet aggregation by both carboxyl-modified and aminated-modified polystyrene nanoparticles but not by the unmodified one <i>in vitro</i>	164
Polystyrene	Not specified	171.1 ± 3.0 nm (DLS)	Negative	None	NPs : RBCs ratio = 200 : 1 and 1000 : 1	Reduced RBC deformability and increased PS exposure <i>in vitro</i>	165
Polystyrene (amine- and carboxyl-modified)	Spherical	57.1 and 284 nm (DLS) Carboxyl- polystyrene: 27.8 or 223.9 nm (DLS)	Positive or negative	None	0.5 mg mL <sup>-1</sup>	Amine-modified polystyrene NPs bound to FVII, FIX and inhibited thrombin formation Carboxyl-modified polystyrene NPs triggered intrinsic pathway <i>in vitro</i>	166

Table 3 (Contd.)

Nanoparticle	Shape	Size	Charge	Coating/stabiliser	Concentration tested	Main finding	Ref.
Polystyrene	Sphere	Outer diameter: 20 and 200 nm	Not specified	None	100 $\mu\text{g mL}^{-1}$	No effect on platelets <i>in vitro</i>	72
Lysozyme-dextran	Not specified	268.2 $\pm$ 9.6 nm (DLS)	Negative	None	NPs : RBCs ratio = 1000 : 1	No effect on RBC <i>in vitro</i>	165
mPEG-PLA	Not specified	~20 nm (DLS)	Not specified	PEG	12.5–200 $\mu\text{g mL}^{-1}$	No effect on HUVECs <i>in vitro</i>	167
PLA	Spherical	77.1 $\pm$ 4.6 nm to 105.6 $\pm$ 3.1 nm (DLS)	Varied	DSPE-PEG (2000) methoxy-terminated, carboxylic acid-terminated, and amino-terminated	350, 700, and 1400 $\mu\text{g mL}^{-1}$	Inhibited P-selectin expression and platelet aggregation <i>in vitro</i>	277
PLGA	Spherical	~420 nm (DLS)	Positive (PEI coating) and negative (BSA coating)	PEI or BSA (bovine serum albumin)	10–150 $\mu\text{g mL}^{-1}$	Impeded on adhesion by NPs with PEI coating but not vWF secretion of endothelial cells <i>in vitro</i>	278
PLGA	Spherical	100–500 nm (DLS)	Negative and positive	None	0.1–500 $\mu\text{g mL}^{-1}$	No effect on platelet <i>in vitro</i>	168
PLGA-macrogol	Spherical	~350–800 nm (DLS)	Negative and positive	None	0.01–100 $\mu\text{g mL}^{-1}$	Slightly inhibited platelet aggregation <i>in vitro</i>	169
Chitosan-PLGA	Spherical	~20–100 nm (DLS)	Varied	Bare or functionalized with G2SN dendron or 8D3 antibody	0.75–3 mg $\text{mL}^{-1}$	PLGA NPs functionalized with G2SN led to aggregation between fibrinogen and the nanoparticles which led to anticoagulant effect at high concentration (3 mg $\text{mL}^{-1}$ )	170
PLGA	Not specified	113, 321, and 585 nm (DLS)	Not specified	PEG	0–2.2 mg $\text{mL}^{-1}$	No effect on coagulation cascade at 1 mg $\text{mL}^{-1}$ <i>in vitro</i>	279
Chitosan-fucoïdan	Spherical	~200 nm (DLS)	Positive	None	0–30 $\mu\text{g mL}^{-1}$ <i>in vitro</i> 50 mg $\text{kg}^{-1}$ of rat <i>in vivo</i> (oral administration)	Reduced platelet aggregation by large nanoparticles (321 and 585 nm) at $\geq 0.25$ mg $\text{mL}^{-1}$ <i>in vitro</i>	280
Chitosan-fucoïdan	Spherical or oval	198.00 $\pm$ 38.84 to 341.70 $\pm$ 200.00 nm (DLS)	Positive	None	0.53–13.3 $\mu\text{g mL}^{-1}$	Nanoparticles with 1% glutaraldehyde crosslink inhibited highest clot formation <i>in vitro</i> and antithrombotic effect <i>in vivo</i>	281
Chitosan-acetylsalicylic acid (ASA)	Almost spherical	~79.3 $\pm$ 24.6 nm (DLS)	Positive	None	0.25–1 g $\text{kg}^{-1}$ of rat (gastrointestinal perfusion)	Interfered with the intrinsic pathway and exhibited anticoagulant effect <i>in vitro</i>	282
Polyurethane ionomer	Spherical	234 nm (DLS)	Slightly negative	None	0–25 mg $\text{mL}^{-1}$	Delayed occlusion time in carotid artery thrombosis model <i>in vivo</i>	171
Polyester	Spherical	5 and 50 nm (TEM)	Negative	Sulfonic acid	0.1, 1, 10, 20 mg $\text{mL}^{-1}$	Possessed anticoagulant activity <i>in vitro</i>	283



RBC deformability as a function of elongation index (EI) value at both sizes (200 nm and 300 nm), as well as both low and high nanoparticle:RBC ratios (200:1 and 1000:1).<sup>165</sup> Moreover, PSNPs exerted mechanical, oxidative, and osmotic stresses on murine RBCs.<sup>165</sup> As a result, the proportion of RBCs expressing PS increased up to 87% and 92% for low and high nanoparticles:RBCs loading ratios, respectively, in comparison with only 0.1% of RBCs and 0.3% of lysozyme-dextran nanogels loading for the control.

Oslakovic *et al.* reported that amine-modified polystyrene nanoparticles (57.1 and 284 nm in size, 0.5 mg mL<sup>-1</sup>) bound to FVII and IX inhibited thrombin formation due to the depletion of these coagulation factors in solution.<sup>166</sup> Meanwhile, carboxyl-modified polystyrene nanoparticles (27.8 or 223.9 nm in size, 0.5 mg mL<sup>-1</sup>) act as an active surface to trigger intrinsic pathways.

Inclusively, most examined polystyrene showed procoagulant effects except for the following: 50 nm amine-modified,<sup>163</sup> 57 and 284 nm amine-modified,<sup>166</sup> 20 and 200 nm unmodified,<sup>72</sup> and ~73 nm unmodified<sup>164</sup> polystyrene nanoparticles (Table 3). There was no physicochemical characteristic that was more important than others in dictating polystyrene nanoparticles' effect on the haemostatic balance. Their effects could be associated with all parameters along with treatment dose and time.

**Other polymeric nanoparticles.** Polymeric nanoparticles, in general, have little toxicity to components involved in haemostatic balance. For instance, Liu *et al.* demonstrated that exposure of HUVECs to mPEG-PLA (methoxy-poly(ethylene glycol)-poly(D,L-lactide)) nanoparticles (around 20 nm) showed no significant effect on the cell viability at a concentration of up to 200 µg mL<sup>-1</sup>.<sup>167</sup> Ramtoola *et al.*<sup>168</sup> and Li *et al.*<sup>169</sup> found that chitosan (CS), poly(lactic-co-glycolic acid) (PLGA), PLGA-macrogol, and PLGA-CS nanoparticles did not exert any substantial effect on platelet activation in the concentration range of 0.1–500 µg mL<sup>-1</sup>. Lysozyme-dextran nanogels did not affect deformability of RBCs even at the nanoparticle:RBC ratio of 1000:1<sup>165</sup> and PLGA nanoparticles (bare or functionalized with G2SN dendron or 8D3 antibody) had no effect on coagulation cascade even at 1 mg mL<sup>-1</sup> *in vitro*.<sup>170</sup>

Besides polymeric nanoparticles having no effect on haemostatic balance and polystyrene nanoparticles that had been specifically discussed above, most of the reported polymeric nanoparticles shift the haemostatic balance to the tendency that reduces procoagulant effects or causes anticoagulant effect (Table 3). For example, PLGA, CS, and PLGA-CS nanoparticles (0.01–100 µg mL<sup>-1</sup>) had slight inhibitory effects toward platelet aggregation induced by collagen.<sup>169</sup> This could be due to the reduced platelet–platelet interaction and/or reduced adsorption of platelets onto collagen fibers. In a study by Mao *et al.*, polyurethane ionomer nanoparticles showed antithrombotic activity, which could be attributed to its ionomer structure.<sup>171</sup> Nevertheless, it is important to note that a wide variety of polymeric nanoparticles have not yet been comprehensively investigated.

## 4. Effects of nanoparticles on innate immune system in correlation with haemostatic balance

In addition to blood components of the haemostatic networks, nanoparticles in the bloodstream also encounter and affect the immune system, specifically the innate immunity, which could potentially interfere with the haemostatic balance.

### 4.1 Immunothrombosis – effect of innate immunity on haemostatic balance

Recently, influences of innate immunity on the haemostasis balance have been increasingly evidenced.<sup>172,173</sup> This relationship was formalised as immunothrombosis, whereby the innate immune system attributes to thrombosis and *vice versa*, the coagulation activation supports the function of the immunity.<sup>174</sup> As far as our knowledge is concerned, the innate immunity regulates haemostasis through the action of leukocytes and complement system.<sup>172,173,175</sup>

Under normal physiological conditions, quiescent leukocytes, namely monocytes, endorse the haemostasis balance by expressing anticoagulant mediators and proteins such as EPCR, TFPI, and TM.<sup>172</sup> However, activated leukocytes in apoptotic or proinflammatory conditions (*e.g.* exposure to foreign agents) will provoke blood coagulation through 3 mechanisms. (1) The first mechanism is expressing or secreting procoagulant factors. For instance, TFs expressed by activated monocytes<sup>176,177</sup> and neutrophils<sup>178–180</sup> could mediate thrombin generation. MMP, elastase, and cathepsin G secreted by stimulated neutrophils and monocytes trigger the activation of FV, FVIII, and FX<sup>181–183</sup> and degrade anticoagulant factors like AT, heparin cofactor II, and TFPI.<sup>184–188</sup> Nuclear damage-associated molecular patterns (DAMPs) (*i.e.* cell-free DNA, high mobility group box 1 (HMGB1), and extracellular histone) secreted by activated/apoptotic leukocytes activate FXI and FXII, mediate thrombin generation, and impair the protein C pathway.<sup>189–193</sup> Moreover, neutrophil extracellular traps (NETs) released by neutrophils, monocytes/macrophages, and mast cells can concentrate procoagulant factors (*i.e.* vWF, TF, fibrinogen, fibronectin, HMGB1, elastase, cathepsin G).<sup>179,194,195</sup> (2) The second mechanism is inducing changes in cellular components of coagulation systems (*i.e.* endothelial cells, platelets, and RBCs). For example, leukocyte-released cytokines such as TNF-α and IL-1β induce EPCR shedding<sup>196</sup> and reduce TM expression<sup>197</sup> on endothelial cells. Cytokines, histamine, granular enzymes, and DAMPs (*i.e.* histone and HMGB1) promote endothelium TF activity<sup>193,198,199</sup> and exocytosis of Weibel-Palade bodies, thus enhancing the release of P-selectin and/or vWF.<sup>200–202</sup> For platelets, it was reported that leukocyte-released cytokines and neutrophil generated oxidants (*e.g.* HOCl) increased circulating ultra-large vWF multimers,<sup>201,203</sup> while NETs facilitated the capture of plate-

lets by vWF.<sup>200</sup> Elastase, cathepsin G, extracellular histone, and PAF released by stimulated leukocytes act as platelet activators which induce platelet activation and aggregation.<sup>204–208</sup> Extracellular histone also can induce the PS exposure on RBCs.<sup>209</sup> (3) The last mechanism is obstructing microcirculation. Activated platelets can interact with leukocytes forming heterotypic leukocyte–platelet aggregates.<sup>208,210,211</sup> Platelet activation by extracellular histone provokes the leukocyte–platelet aggregation formation as well.<sup>208,211</sup> Besides, platelet-rich microthrombi can be built up by extracellular histone *in vivo*.<sup>207</sup> In addition to regulating coagulation induction, leukocytes also mediate fibrinolysis, thrombus resolution, and coagulation factor clearance.<sup>172</sup>

A complement system, which is genetically developed from a serine protease reaction cascade evolved from the same ancestor gene as coagulation factors, plays a significant role in haemostasis.<sup>173,175</sup> Regardless of activation path, C5b-9 as a membrane attach complex (MAC) or terminal complement complex (TCC) causes platelet activation through the induction of platelet transient membrane depolarisation, PS expression, granule secretion, and thrombin generation.<sup>212–215</sup> The combination of MAC and C3 triggers serotonin secretion and thrombin-mediated platelet aggregation.<sup>216,217</sup> C3 itself also affects platelet activation.<sup>218,219</sup> Anaphylatoxin C3a promotes the activation and aggregation of platelets,<sup>220</sup> while anaphylatoxin C5a provokes TF expression on leukocytes<sup>221</sup> and promotes procoagulant effects on mast cells.<sup>222,223</sup> C5a and MAC prompt neutrophils and endothelial cells for the activation and TF expression, activating the extrinsic pathway of the coagulation cascade.<sup>224,225</sup> Activated mannose-binding protein-associated serine protease 2 (MASP-2) is involved in thrombin activation and fibrin generation, whilst MASP-1 boosts fibrin-cross-linking and the cleavage of fibrinogen,<sup>226</sup> FXIII, and thrombin activatable fibrinolysis inhibitor (TAFI).<sup>227,228</sup> Platelet rolling and platelet activation was caused when C1q interacts with vWF and binds to gC1qR or gC1qR/p33 on platelets, respectively, which could eventually lead to platelet aggregation.<sup>229–232</sup> C1 inhibitor inhibits the activity of FXIIa, FXIa, and kallikrein of the coagulation system.<sup>233–235</sup> C4b binding protein interferes with protein S of the anticoagulant system.<sup>236</sup>

#### 4.2 Effect of nanoparticles on innate immunity potentially linked to haemostasis

To the best of our knowledge, the effect of nanoparticles on innate immune systems that directly mediate the haemostatic balance has not been investigated yet. Nevertheless, there were several studies demonstrating the effect of nanoparticles on the immunity, which could potentially interfere with the haemostatic balance, concerning the intrinsic link between the innate immunity and haemostasis. For instance, long needle-like carbon nanotube (trade name: Mitsui MWCNT-7, outer diameter >50 nm, length ~13  $\mu\text{m}$ ) induced the release of IL-1R and activated the release of IL-1 $\beta$  from bacterial lipopolysaccharide (LPS)-primed human monocyte-derived macrophages at the tested concentration of 100  $\mu\text{g mL}^{-1}$ .<sup>237</sup> MWCNTs (dia-

meter: 20–30 nm, length: 10–30 nm) dispersed in serum bovine albumin caused vigorous IL-1 $\beta$  secretion from THP-1 cells *in vitro* (tested concentrations of 10, 25, 50, and 100  $\mu\text{g mL}^{-1}$ ) and *in vivo* (12.5–100  $\mu\text{g}$  per mice).<sup>238</sup> Chowdhury *et al.* reported that dextran-coated graphene nanoplatelets (60–100 nm) at concentration  $\geq 7 \text{ mg mL}^{-1}$  caused 12–20% increments in complement protein levels.<sup>239</sup> However, the level of TNF- $\alpha$  was retained in the normal range and the nanoplatelets did not induce platelet activation. In another study, the secretion of IL-1 $\beta$  and TNF- $\alpha$  by THP-1 cells was induced in a bell-shaped distribution manner after being treated with silica nanoparticles (12.5–200  $\mu\text{g mL}^{-1}$ ) of different sizes (10–1000 nm), where the maximum effect was recorded for the 50 nm-nanoparticles and the lesser effect was for those with larger or smaller sizes.<sup>240</sup> It was presented that mannan-binding lectin bound to the dextran coating of dextran-coated superparamagnetic iron oxide nanoparticles (Dex-SPIONs) (50 nm, 200  $\mu\text{g}$  per 300  $\mu\text{L}$  mouse plasma).<sup>241</sup> Histidine-rich glycoprotein and kininogen tended to bind to the exposed iron oxide part while complement lectin and clotting factors (kininogen, kallikrein, FXI, and FXII) were the secondary binders. Although the bound clotting factors could potentially activate the coagulation intrinsic pathway, the systemic administration of SPIONs was not adequate to promote the clotting in another study examined by the same group.<sup>242</sup> Only SPIONs coated with carboxymethyl-dextran (ferucarbotran, Resosvist®) and dextran (ferumoxtran-10, Sinerem®) significantly activated the complement system, while those with a citric acid (FluidMAG-CT), phosphatidylcholine (FluidMAG-Lipid), starch (FluidMAG-D), and chitosan (FluidMAG-Chitosan) coating did not when incubating nanoparticles with serum at volume ratio of 1:4.<sup>243</sup> Moreover, coating of SPION with human serum albumin or dextran decreased the NETs formation by neutrophils compared with pristine and unstable lauric acid-coated SPIONs (55.8–127.9 nm), both *in vitro* (200  $\mu\text{g mL}^{-1}$ ) and *in vivo* (500  $\mu\text{g}$  nanoparticles per rabbit).<sup>244</sup> Gold nanoparticles (10–100 nm at doses of 2.5–10  $\mu\text{g mL}^{-1}$ ) synergised with LPS also induced the release of NETs from human neutrophils.<sup>245</sup> For liposomes, those ~100 nm in size (5–40  $\text{mg mL}^{-1}$ ) did not interfere with the complement system, while the micro-multilamellar liposomes did.<sup>246</sup> Among liposomes with ~100 nm, negatively charged liposomes containing phosphatidylglycerol, phosphatidic acid, cardiolipin, phosphatidylinositol, or phosphatidylserine activated classical complement pathways whilst positively charged liposomes containing 1,2-bis(oleoyloxy)-3-(trimethylammonio)propane or stearylamine activated alternative complement pathways, which was in contrast to neutral liposomes.<sup>247</sup> C9 and C3b were associated with these liposomes. The C3 opsonization on nanoparticles not only raises the potential risk of haemostatic imbalance but also targets the nanoparticles for reticuloendothelial system (RES) uptake, triggers toxin release, and may likely foul the targeting agents conjugated on nanoparticles.<sup>248</sup> Coating the nanoparticles with PEG can reduce C3b-nanoparticle adduct formation. Another approach is infusing complement inhibitors with nanoparticles.<sup>242,249</sup>

## 5. Physicochemical characteristics affecting interactions between nanoparticles and haemostatic balance

It is important to note that not every nanoparticle is exactly the same. Changes in any nanoparticle's physicochemical characteristics, such as size, shape, surface charge, and coating materials, might correlate with different ways of interaction and lead to alternative effects on haemostatic balance.

### 5.1 Effect of size

The size of a nanoparticle is a critical aspect that significantly affects its biodistribution, circulation and clearance in the body.<sup>250</sup> Additionally, size can also impact their interfacial area for blood–nanoparticle and cell–nanoparticle communication.<sup>251</sup> Generally, small nanoparticles exhibit larger surface area to volume ratio, hence larger interfacial area to cells and blood components compared with large nanoparticles.<sup>251</sup> Intrinsically, smaller sized silica nanoparticles demonstrated a more substantial effect on the haemostatic balance, specifically the coagulation system.<sup>48,88,139,252,253</sup> Nanoparticles with the largest size resulted in the release of Weibel-Palade bodies and vWF from endothelial cells among silica nanoparticles with size ranging from 16 to 304 nm after 24 h of incubation, whereas this effect only takes a few hours with smaller sized nanoparticles.<sup>252</sup> Previous reported studies have established that silica nanoparticles with a diameter of 10 nm generated greater platelet activation in comparison with nanoparticles larger than 50 nm.<sup>139</sup> Correspondingly, due to the increased specific surface area exposed to the coagulation system, smaller sized silica nanoparticles between 30 to 70 nm resulted in enhanced procoagulant activity in comparison with nanoparticles bigger than 100 nm.<sup>48,88,253</sup> Nonetheless, another study demonstrated a more significant haemostasis *in vivo* in larger sized silica nanoparticles (200 nm),<sup>153</sup> and interestingly ultrasmall silica nanoparticles (4–7 nm) did not exhibit coagulation activity owing to their higher surface curvatures.<sup>133</sup>

Likewise, AuNPs ( $\leq 50$  nm) were easily internalised and accumulated in platelets, stimulating platelet activation in comparison with larger size (60 nm) nanoparticles which were inert.<sup>111,118</sup> Paradoxically, there were other studies that established that small AuNPs (5–30 nm) had no effect on platelets, while 60 nm-ones blocked platelet aggregation.<sup>119</sup> A concentration of 5–40  $\mu\text{M}$  of Au in PRP was employed, which corresponds to 0.94–7.5  $\mu\text{g mL}^{-1}$  blood in the abovementioned studies. A size-dependent trend was observed with AuNPs within the size range of 12–85 nm, in which 45 and 85 nm-AuNPs induced quicker pro-thrombotic response and 28 nm-ones exhibited the greatest decrement in clot strength.<sup>116</sup>

The effect of particle size was also verified for silver nanoparticles,<sup>87,94</sup> carbon-based nanoparticles,<sup>71,254</sup> and iron oxide nanoparticles.<sup>130</sup> For instance, longer MWCNTs (both carboxylated and aminated) had a more significant effect on

platelet activation than the shorter ones.<sup>254</sup> Among those, long carboxylated MWCNTs soften the clot while long aminated MWCNTs increased clot hardness. Interestingly, 30 nm-PVP-AgNPs reduced RBC deformability to a higher degree in comparison with 100 nm-PVP-AgNPs *in vitro*.<sup>94</sup> Small AgNPs (10–15 nm) repressed platelet activation *in vitro*.<sup>87</sup> Size-dependent effects on RBCs were observed with PAA-IONPs where the larger size corresponded to the higher RBCs morphology alteration.<sup>130</sup> Furthermore, 5 nm-nanoparticles delayed blood clotting time relative to the 10 and 30 nm-ones.

The discrepancies in the size-dependent effects of nanoparticles on coagulation need to be carefully taken into account because the characterisation of nanoparticle size might not be carried out using similar media and techniques (e.g. water vs. buffer solution or TEM/SEM vs. dynamic light scattering). Additionally, the degree of influence of a particular nanoparticle on the coagulation system may also be associated with other factors, such as the concentration and surface charge of nanoparticles.

### 5.2 Effect of shape

The shape of a nanoparticle has been presented in previously reported studies as a crucial parameter that has a significant impact on the interaction with haemostatic balance.<sup>94,109,117,255,256</sup> Regarding silver nanomaterials coated with PVP, 30 nm spherical AgNPs reduced RBC deformability the most in comparison with 100 nm spherical AgNPs and silver nanowires (40 nm in diameter and 1–2  $\mu\text{m}$  in length).<sup>94</sup> Silver nanowires reduced RBC aggregation at 50  $\mu\text{g mL}^{-1}$  while 30 nm spherical AgNPs did not. Meher *et al.* reported that heparin coated AgNPs with hexagonal shape displayed the longest delayed coagulation time amongst other shapes in this order: hexagonal > truncated triangular > triangular > spherical.<sup>109</sup> Whilst these studies established a correlation of shape to haemostatic balance, there were also conflicting results from studies demonstrating that carbon-based nanoparticles can cause thrombus formation regardless of their shape.<sup>256</sup> Also, the shape of AuNPs (spherical, hollow sphere, or rod shape) had no significant effect on endothelial cells.<sup>117</sup>

### 5.3 Effect of surface charge

A key factor influencing the interaction of nanoparticles with haemostatic balance is their surface charge. Positively charged groups on nanoparticle surfaces can facilitate platelet–platelet interaction and aggregation *via* neutralizing and forming cross-bridges with negatively charged ionisable sialic acid groups on the platelets' surface.<sup>29,257</sup> Besides, positively charged nanoparticles can induce the changes in the size and number of platelet aggregates by altering platelet morphology<sup>156</sup> and disrupting platelet membrane integrity.<sup>154</sup> Large and cationic PAMAM ( $\geq\text{G4}$ ) and triazine dendrimers (G5 and G7) provoked platelet aggregation, in which the degree of aggregation was proportional to the number of amine groups on the nanoparticles' surface.<sup>154</sup>

Negatively charged nanoparticle surfaces can initiate the coagulation cascade which eventually disrupts haemostatic

balance.<sup>62–65</sup> For instance, the upregulation of activation markers (P-selectin or PAC-1) of platelets was triggered by anionic polystyrene (carboxyl-modification) whilst the interruption of the platelet membrane was initiated by cationic polystyrene (amine-modification).<sup>164</sup> Positively and negatively charged polystyrene nanoparticles<sup>164</sup> can eventually lead to thrombotic events, except for the 50 nm amine-modified nanoparticles reported by Smyth *et al.*<sup>163</sup> and the 57 and 284 nm amine-modified ones reported by Oslakovic *et al.*<sup>166</sup> This is in contradiction with liposomes where both anionic and cationic nanoparticles inhibited platelet activation and aggregation.<sup>159</sup> Nevertheless, there are still contradictory studies that reported evoked platelet aggregation effects of anionic liposomes,<sup>160,161</sup> or the independence of the surface charge of polystyrene nanoparticles towards platelet activation.<sup>163</sup>

In conclusion, it is apparent that the charge-dependent effect of nanoparticles on the haemostatic balance is unpredictable. The influence of nanoparticle charge is even more difficult to clarify in physiological conditions due to the absorption of plasma proteins on the surface of nanoparticles.

#### 5.4 Effect of surface functionality

Reactivity of a nanoparticle to the haemostatic balance can be altered by a layer of coating material on its surface. Among all, polyethylene glycol (PEG) is the most commonly used polymeric material. As reported in previous studies, the presence of PEG on the nanoparticles surface reduced their interference with endothelial cells and platelets, probably due to the capability to prevent protein binding.<sup>90,142,158,258–260</sup> Therefore, unattended haemostasis is reduced and the compatibility of nanoparticles is improved. However, PEGylation of nanoparticles is not successful for all nanoparticles.<sup>74</sup> In addition to PEG, other polymers, namely dextran,<sup>261</sup> albumin,<sup>84</sup> and starch,<sup>125</sup> did not cause any effect on endothelial cells and platelets, or reduced platelet aggregation. Citrate coating either had no effect<sup>92,96,111,112,119</sup> or was one factor contributing to antiplatelet activity of the nanoparticles.<sup>87,125,127,150</sup> Nevertheless, citrate coating/stabilising also synergises with other factors such as size and dose, indicating the influences of nanoparticles on the haemostatic balance, which is the reason for the procoagulant effects of some citrate coated nanoparticles.<sup>85,111,116,120</sup> It was reported that PAA conjugated on the surface of gold nanoparticles binds to fibrinogen and promotes changes in its conformation (unfolding).<sup>115</sup> However, gold nanoparticles coated with PEI and PVP induced platelet aggregation.<sup>118</sup> Interestingly, superparamagnetic iron oxide nanoparticles at the same size of 5–6 nm functionalized with either hyaluronic acid or chitosan showed less effect on platelets, RBCs, and coagulation than those with PAA coating (tested concentration of 4–1000  $\mu\text{g mL}^{-1}$ ).<sup>130</sup> All the findings above have demonstrated that specific coating material is worth investigating for these commonly used nanoparticles during their interactions with the haemostatic balance.

#### 5.5 Effect of other characteristics

The concentration of nanoparticle metal cores (such as gold) had an impact on haemostasis. Hsu *et al.* revealed that a lower gold concentration (43.5 ppm) incorporated with polyurethane (PU) nanocomposites resulted in less platelet adhesion and activation compared with a higher amount of gold incorporated (174 ppm).<sup>262</sup>

Because of the binding of plasma proteins or simply pH value, the surface charges of the nanoparticle can be altered in the physiological fluids, which could come along with the change in nanoparticle's hydrophobicity.<sup>24,31</sup> A study clarifying the influence of latex polystyrene nanoparticles' hydrophobicity on the blood haemostatic balance was carried out by Miyamoto *et al.*<sup>263</sup> The results revealed that hydrophobic latex nanoparticles provoked platelet aggregation to a higher extent than the hydrophilic ones. This could be due to their ability to interact more closely with the cell membrane and activate the platelets.<sup>264</sup> In another study, TiO<sub>2</sub> nanotubes with a superhydrophobic surface had a tendency to prevent platelet adhesion.<sup>265</sup> Not only were very few adhered platelets detected on their surface, but also these adhered platelets were not activated, which was opposite to bare TiO<sub>2</sub> nanotubes and superhydrophilic TiO<sub>2</sub> nanotubes. However, further investigation relating to the relationship between hydrophobicity of nanoparticles and the haemostatic balance is rarely found.

## 6. Challenges and future directions

According to ISO 10993-4 guidelines, thrombosis, haematology (hemolysis and leukocyte count), and complement activation are blood incompatibilities that should be considered for *in vivo* study, while coagulation, platelet activation, platelet aggregation, haematology, and complement activation are blood incompatibilities considered for *in vitro* study, acquired prior to clinical translation of blood-contacting biomaterials.<sup>266,267</sup> As systematically reviewed by Urbán *et al.* in 2019, thrombosis, haematology, and complement activation are the main blood toxicities triggered by inorganic, lipid-based, and polymeric nanoparticles.<sup>267</sup> Thrombosis, as a consequence of the haemostatic imbalance, accounts for 61% of the total reported cases of *in vivo* blood toxicities in nanomedicine. It is therefore the most common blood incompatibility caused by nanomedicine. Anticoagulant and antifibrinolytic effects, as other consequences of haemostatic imbalance, also imply hidden risk of haemorrhage triggered by nanoparticles.

There are several things that should be taken into consideration when it comes to the nanoparticle-haemostatic balance:

(1) There is still room for more studies in the future as not all commonly examined nanoparticles are comprehensively investigated and fully understood regarding the underlying mechanisms. Establishing an approach for the systemic investigation of nanoparticle effects on the haemostatic balance, especially with the focus on clinically and preclinically used nanoparticles, is tremendously encouraged.

(2) Further research investigating the effects of nanoparticles on RBCs and specific plasma factors of the haemostatic balance will be of high interest as most of the current studies focus more on their interactions with platelets and endothelial cells. Regarding their interactions with RBCs, a haemolysis assay is usually utilised to demonstrate hemocompatibility but cannot be used independently to evaluate the influences of nanoparticles on haemostatic balance. RBC aggregation, deformability, and PS exposure should also be taken into account.

(3) Alterable interferences with the haemostatic balance in correlation to changes in nanoparticle physicochemical parameters have been examined in many studies but not in a systematic way. The discrepancies in results need to be treated with caution since the characterisation techniques adopted might not be comparable in terms of methods, setting, and media. More importantly, the effects of a specific nanoparticle on haemostasis could be associated with a myriad of synergistic physicochemical characteristics.

(4) As discussed, coating material is an important factor that can alter nanoparticle reactivity to the haemostatic balance. Nevertheless, there is a limited variety of investigated polymeric materials. The effect of metal coating of core-shell nanoparticles, regarding types of metal, thickness of metal coating, and coating method, on the haemostasis balance has not been explored yet. Therefore, more studies are needed to elucidate the effects of coating materials on haemostatic balance. It is worth examining specific coating materials for commonly used nanoparticles.

(5) The interface between the haemostatic balance and other characteristics of nanoparticles, such as hydrophobicity, porosity, lipid composition of lipid-based nanoparticles, and surface topography, may attract much interest in the future.

(6) Apparently, *in vivo* studies are encouraged since the behaviour of nanoparticles is not always predictable in physiological conditions due to the absorption of plasma proteins on their surface. Moreover, the discrepancies in administration routes (*i.e.* inhalation, instillation, or IV) must be taken into account when interpreting *in vivo* results.

(7) Along with the physicochemical characteristics of nanoparticles that were discussed, the dose multiplied by the duration of exposure is one of the most crucial factors in deciding nanoparticle effects on the haemostatic balance.

(8) Different types of nanoparticles will affect the haemostatic balance in different ways. Slight changes in one or more parameters of a specific type of nanoparticle, even the well-established ones, could significantly alter their behaviour to an extent that we can no longer predict.

(9) There are many degradable nanoparticles intentionally designed to stay at the target site for a long time for therapeutic treatment. Hence, we also need to take extreme care to evaluate the influence of their degradation products on the haemostatic balance over time.

(10) Nanoparticles can encounter and affect the innate immune system (*i.e.* leukocytes and complement system), which could potentially interfere with the haemostatic balance

concerning the intrinsic link between the innate immunity and haemostasis. There were several studies demonstrating the effect of nanoparticles on immunity. However, the effect of nanoparticles on innate immune systems that directly mediate the haemostatic balance has not been examined yet to the best of our knowledge, encouraging more studies in the future.

## 7. Conclusion

Nanoparticles in the bloodstream always interfere with the haemostatic balance through interactions with one or more components of the blood coagulation, anticoagulation, and fibrinolytic system. Our review presents a thorough outline of the haemostatic balance and possible interference of various inorganic and organic nanoparticles by focusing on the underlying mechanisms and factors that could have some effects. The effect of nanoparticles on the innate immune system that could potentially link to haemostasis is discussed as well. This collated information is valuable for the establishment of nanoparticles that can either avoid unintended interferences with the haemostatic balance or purposely downregulate/upregulate their components under a controlled manner, thus speeding up their successful translation to the clinic and market.

## Abbreviations

ADP	Adenosine diphosphate
AFM	Atomic force microscopy
AgNPs	Silver nanoparticles
APC	Activated protein C
AT	Antithrombin III
AuNPs	Gold nanoparticles
DLS	Dynamic light scattering
DAMPs	Nuclear damage-associated molecular patterns
EPCR	Endothelial protein C receptor
GpIIb/IIIa	Glycoprotein IIb/IIIa
GSH	Reduced glutathione
HMWK	High-molecular-weight kininogen
HUVECs	Human umbilical vein endothelial cells
HMGB1	High mobility group box 1
IONPs	Iron oxide nanoparticles
IV	Intravenous injection
LPS	Bacterial lipopolysaccharide
MMP	Matrix metalloproteinase
MWCNT	Multiple wall carbon nanotubes
MAC	Membrane attach complex
MASP	Mannose-binding protein-associated serine protease
NO	Nitric oxide
NOS	Nitric oxide synthase
NETs	Neutrophil extracellular traps
PAA	Poly(acrylic acid)
PAF	Platelet-activating factor
PAI-1	Plasminogen activator inhibitor-1

PAMAM	Poly(amidoamine)
PAR	Protease-activated receptor
PECAM-1	Platelet endothelial cell adhesion molecule-1
PEG	Polyethylene glycol
PEI	Polyethylenimine
PGI2	Prostacyclin
PK	Prekallikrein
PLA	Poly(D,L-lactide)
PLGA	Poly(lactic-co-glycolic acid)
PRP	Platelet rich plasma
PS	Phosphatidylserine
PVA	Polyvinyl alcohol
PVP	Polyvinylpyrrolidone
PZ	Protein Z
RBCs	Red blood cells
SAED	Selected area (electron) diffraction
SOCE	Store-operated Ca <sup>2+</sup> entry
SWCNT	Single wall carbon nanotubes
TEM	Transmission electron microscopy
TF	Tissue factor
TFPI	Tissue factor pathway inhibitor
TiO <sub>2</sub>	Rutile titanium
TM	Thrombomodulin
t-PA	Tissue-type plasminogen activator
TXA2	Thromboxane A2
TCC	Terminal complement complex
TAFI	Thrombin activatable fibrinolysis inhibitor
u-PA	Urokinase-type plasminogen activator
vWF	Von Willebrand factor
XRD	X-ray powder diffraction
ZnO NPs	Zinc oxide nanoparticles
ZPI	Z-Dependent protease inhibitor

## Conflicts of interest

There are no conflicts to declare.

## Acknowledgements

This work is funded by National Health and Medical Research Council (HTT: APP1037310, APP1182347, APP2002827) and Heart Foundation (HTT: 102761).

## References

- J. Jeevanandam, A. Barhoum, Y. S. Chan, A. Dufresne and M. K. Danquah, Review on nanoparticles and nanostructured materials: history, sources, toxicity and regulations, *Beilstein J. Nanotechnol.*, 2018, **9**, 1050–1074.
- K. M. de la Harpe, P. P. Kondiah, Y. E. Choonara, T. Marimuthu, L. C. du Toit and V. Pillay, The hemocompatibility of nanoparticles: a review of cell–nanoparticle interactions and hemostasis, *Cells*, 2019, **8**, 1209.
- M. F. Matus, C. Vilos, B. A. Cisterna, E. Fuentes and I. Palomo, Nanotechnology and primary hemostasis: Differential effects of nanoparticles on platelet responses, *Vasc. Pharmacol.*, 2018, **101**, 1–8.
- T. T. H. Thi, D. H. T. Nguyen, D. T. D. Nguyen, D. H. Nguyen and M.-D. Truong, Decellularized Porcine Epiphyseal Plate-Derived Extracellular Matrix Powder: Synthesis and Characterization, *Cells Tissues Organs*, 2020, **209**, 1–9.
- H. D. Tran, K. D. Park, Y. C. Ching, C. Huynh and D. H. Nguyen, A comprehensive review on polymeric hydrogel and its composite: Matrices of choice for bone and cartilage tissue engineering, *J. Ind. Eng. Chem.*, 2020, **89**, 58–82.
- E. Reimhult, *Nanoparticle interactions with blood proteins and what it means: a tutorial review*, 2019.
- N. Arndt, H. D. Tran, R. Zhang, Z. P. Xu and H. T. Ta, Different approaches to develop nanosensors for diagnosis of diseases, *Adv. Sci.*, 2020, **7**, 2001476.
- H. Adelnia, H. D. Tran, P. J. Little, I. Blakey and H. T. Ta, Poly (aspartic acid) in Biomedical Applications: From Polymerization, Modification, Properties, Degradation, and Biocompatibility to Applications, *ACS Biomater. Sci. Eng.*, 2021, **7**, 2083–2105.
- T. N. T. Nguyen, D.-H. Nguyen-Tran, L. G. Bach, T. H. Du Truong, N. T. T. Le and D. H. Nguyen, Surface PEGylation of hollow mesoporous silica nanoparticles via aminated intermediate, *Prog. Nat. Sci.: Mater. Int.*, 2019, **29**, 612–616.
- D. H. Nguyen, L. G. Bach, D.-H. Nguyen Tran, V. D. Cao, T. N. Q. Nguyen, T. T. H. Le, T. T. Tran and T. T. H. Thi, Partial surface modification of low generation polyamidoamine dendrimers: Gaining insight into their potential for improved carboplatin delivery, *Biomolecules*, 2019, **9**, 214.
- D. H. N. Tran, T. H. Nguyen, T. N. N. Vo, L. P. T. Pham, D. M. H. Vo, C. K. Nguyen, L. G. Bach and D. H. Nguyen, Self-assembled poly (ethylene glycol) methyl ether-grafted gelatin nanogels for efficient delivery of curcumin in cancer treatment, *J. Appl. Polym. Sci.*, 2019, **136**, 47544.
- T. T. Hoang Thi, D.-H. Nguyen Tran, L. G. Bach, H. Vu-Quang, D. C. Nguyen, K. D. Park and D. H. Nguyen, Functional magnetic core-shell system-based iron oxide nanoparticle coated with biocompatible copolymer for anticancer drug delivery, *Pharmaceutics*, 2019, **11**, 120.
- V. M. H. Do, L. G. Bach, D.-H. N. Tran, T. N. Q. Nguyen, D. T. Hoang, D. H. Nguyen and T. T. H. Thi, Effective Elimination of Charge-associated Toxicity of Low Generation Polyamidoamine Dendrimer Eases Drug Delivery of Oxaliplatin, *Biotechnol. Bioprocess Eng.*, 2020, 1–11.
- B. Q. Bao, N. H. Le, D. H. T. Nguyen, T. V. Tran, L. P. T. Pham, L. G. Bach, H. M. Ho, T. H. Nguyen and D. H. Nguyen, Evolution and present scenario of multifunctionalized mesoporous nanosilica platform: A mini review, *Mater. Sci. Eng., C*, 2018, **91**, 912–928.

- 15 Y. Wu, R. Zhang, H. D. Tran, N. D. Kurniawan, S. S. Moonshi, A. K. Whittaker and H. T. Ta, Chitosan Nanococktails Containing Both Ceria and Superparamagnetic Iron Oxide Nanoparticles for Reactive Oxygen Species-Related Theranostics, *ACS Appl. Nano Mater.*, 2021, **4**, 3604–3618.
- 16 A. U. Rehman, Y. Wu, H. D. Tran, K. Vazquez-Prada, Y. Liu, H. Adelnia, N. D. Kurniawan, M. N. Anjum, S. S. Moonshi and H. T. Ta, Silver/Iron Oxide Nanopopcorns for Imaging and Therapy, *ACS Appl. Nano Mater.*, 2021, **4**(10), 10136–10147.
- 17 N. N. M. Yusof, A. McCann, P. J. Little and H. T. Ta, Non-invasive imaging techniques for the differentiation of acute and chronic thrombosis, *Thromb. Res.*, 2019, **177**, 161–171.
- 18 A. Zia, Y. Wu, T. Nguyen, X. Wang, K. Peter and H. T. Ta, The choice of targets and ligands for site-specific delivery of nanomedicine to atherosclerosis, *Cardiovasc. Res.*, 2020, **116**, 2055–2068.
- 19 Y. Liu, Y. Wu, R. Zhang, J. Lam, J. C. Ng, Z. P. Xu, L. Li and H. T. Ta, Investigating the use of layered double hydroxide nanoparticles as carriers of metal oxides for theranostics of ROS-related diseases, *ACS Appl. Bio Mater.*, 2019, **2**, 5930–5940.
- 20 K. X. Vazquez-Prada, J. Lam, D. Kamato, Z. P. Xu, P. J. Little and H. T. Ta, Targeted Molecular Imaging of Cardiovascular Diseases by Iron Oxide Nanoparticles, *Arterioscler., Thromb., Vasc. Biol.*, 2021, **41**, 601–613.
- 21 H. T. Ta, Z. Li, C. Hagemeyer, Y. Wu, H. J. Lim, W. Wang, J. Wei, G. Cowin, A. Whittaker and K. Peter, Novel bionanotechnological solutions based on metal oxide and metal to preserve and assess organs for transplantation, *Cryobiology*, 2018, **81**, 233.
- 22 Y. Wu, K. X. Vazquez-Prada, Y. Liu, A. K. Whittaker, R. Zhang and H. T. Ta, Recent Advances in the Development of Theranostic Nanoparticles for Cardiovascular Diseases, *Nanotheranostics*, 2021, **5**, 499.
- 23 Y. Wu and H. T. Ta, Different approaches to synthesise cerium oxide nanoparticles and their corresponding physical characteristics, ROS scavenging and anti-inflammatory capabilities, *J. Mater. Chem. B*, 2021, **9**, 7291–7301.
- 24 M. I. Setyawati, C. Y. Tay, D. Docter, R. H. Stauber and D. T. Leong, Understanding and exploiting nanoparticles' intimacy with the blood vessel and blood, *Chem. Soc. Rev.*, 2015, **44**, 8174–8199.
- 25 H. D. Tran, F. Akther, Z. P. Xu and H. T. Ta, Effects of nanoparticles on the blood coagulation system (nanoparticle interface with the blood coagulation system), in *Nanotechnology for Hematology, Blood Transfusion, and Artificial Blood*, Elsevier, 2022, pp. 113–140.
- 26 G. Blanco and A. Blanco, *Medical biochemistry*, Academic Press, 2017.
- 27 T. Astrup, The Haemostatic Balance, *Thromb. Haemostasis*, 1958, **2**, 347–357.
- 28 P. J. Gaffney, T. A. Edgell and C. M. Whitton, The haemostatic balance—Astrup revisited, *Pathophysiol. Haemostasis Thromb.*, 1999, **29**, 58–71.
- 29 N. K. Hante, C. Medina and M. J. Santos-Martinez, Effect on Platelet Function of Metal-Based Nanoparticles Developed for Medical Applications, *Front. Cardiovasc. Med.*, 2019, **6**, 139.
- 30 H. Rasche, Haemostasis and thrombosis: an overview, *Eur. Heart J. Suppl.*, 2001, **3**, Q3–Q7.
- 31 E. Fröhlich, Action of nanoparticles on platelet activation and plasmatic coagulation, *Curr. Med. Chem.*, 2016, **23**, 408–430.
- 32 D. Sobot, S. Mura, P. Couvreur, S. Kobayashi and K. Müllen, Nanoparticles: blood components interactions, in *Encyclopedia of polymeric nanomaterials*, Springer Berlin Heidelberg, Berlin, Heidelberg, 2014, pp. 1–10.
- 33 A. N. Ilinskaya and M. A. Dobrovolskaia, Nanoparticles and the blood coagulation system, in *Handbook of immunological properties of engineered nanomaterials: Volume 2: Haematocompatibility of Engineered Nanomaterials*, World Scientific, 2016, pp. 261–302.
- 34 M. Franchini and P. M. Mannucci, The hemostatic balance revisited through the lessons of mankind evolution, *Intern. Emerg. Med.*, 2008, **3**, 3–8.
- 35 K. Martin, A. D. Ma and N. S. Key, Molecular basis of hemostatic and thrombotic diseases, in *Molecular Pathology*, Elsevier, 2018, pp. 277–297.
- 36 A. N. Ilinskaya and M. A. Dobrovolskaia, Nanoparticles and the blood coagulation system. Part I: benefits of nanotechnology, *Nanomedicine*, 2013, **8**, 773–784.
- 37 R. E. Rumbaut and P. Thiagarajan, Platelet-vessel wall interactions in hemostasis and thrombosis, in *Synthesis Lectures on Integrated Systems Physiology: From Molecule to Function*, 2010, vol. 2, pp. 1–75.
- 38 E. Gaston, J. F. Fraser, Z. P. Xu and H. T. Ta, Nano-and micro-materials in the treatment of internal bleeding and uncontrolled hemorrhage, *Nanomedicine*, 2018, **14**, 507–519.
- 39 J. A. Ezihe-Ejiofor and N. Hutchinson, Anticlotting mechanisms 1: physiology and pathology, *Anaesth. Crit. Care Pain Med.*, 2013, **13**, 87–92.
- 40 S. Reitsma, D. W. Slaaf, H. Vink, M. A. Van Zandvoort and M. G. oude Egbrink, The endothelial glycocalyx: composition, functions, and visualization, *Pflügers Arch.*, 2007, **454**, 345–359.
- 41 P. Hangege, J. Stone, H. Albadawi, Y. S. Zhang, A. Khademhosseini and R. Oklu, Hemostasis and nanotechnology, *Cardiovasc. Diagn. Ther.*, 2017, **7**, S267.
- 42 K. N. Ekdahl, K. Fromell, C. Mohlin, Y. Teramura and B. Nilsson, A human whole-blood model to study the activation of innate immunity system triggered by nanoparticles as a demonstrator for toxicity, *Sci. Technol. Adv. Mater.*, 2019, **20**, 688–698.
- 43 J. W. Yau, H. Teoh and S. Verma, Endothelial cell control of thrombosis, *BMC Cardiovasc. Disord.*, 2015, **15**, 1–11.

- 44 S. Palta, R. Saroa and A. Palta, Overview of the coagulation system, *Indian J. Anaesth.*, 2014, **58**, 515.
- 45 K. Broos, H. B. Feys, S. F. De Meyer, K. Vanhoorelbeke and H. Deckmyn, Platelets at work in primary hemostasis, *Blood Rev.*, 2011, **25**, 155–167.
- 46 E. Demir, D. Burgucu, F. Turna, S. Aksakal and B. Kaya, Determination of TiO<sub>2</sub>, ZrO<sub>2</sub>, and Al<sub>2</sub>O<sub>3</sub> nanoparticles on genotoxic responses in human peripheral blood lymphocytes and cultured embryonic kidney cells, *J. Toxicol. Environ. Health, Part A*, 2013, **76**, 990–1002.
- 47 G. G. De La Cruz, P. Rodríguez-Fragoso, J. Reyes-Esparza, A. Rodríguez-López, R. Gómez-Cansino and L. Rodríguez-Fragoso, Interaction of nanoparticles with blood components and associated pathophysiological effects, in *Unraveling the Safety Profile of Nanoscale Particles and Materials-From Biomedical to Environmental Applications*, 2018.
- 48 H. Nabeshi, T. Yoshikawa, K. Matsuyama, Y. Nakazato, A. Arimori, M. Isobe, S. Tochigi, S. Kondoh, T. Hirai and T. Akase, Amorphous nanosilicas induce consumptive coagulopathy after systemic exposure, *Nanotechnology*, 2012, **23**, 045101.
- 49 P. J. Sims, M. Ginsberg, E. Plow and S. Shattil, Effect of platelet activation on the conformation of the plasma membrane glycoprotein IIb-IIIa complex, *J. Biol. Chem.*, 1991, **266**, 7345–7352.
- 50 A. Matzdorff and R. Voss, Upregulation of GP IIb/IIIa receptors during platelet activation: Influence on efficacy of receptor blockade, *Thromb. Res.*, 2006, **117**, 307–314.
- 51 N. S. Kleiman, A. E. Raizner, R. Jordan, A. L. Wang, D. Norton, K. F. Mace, A. Joshi, B. S. Collier and H. F. Weisman, Differential inhibition of platelet aggregation induced by adenosine diphosphate or a thrombin receptor-activating peptide in patients treated with bolus chimeric 7E3 Fab: implications for inhibition of the internal pool of GPIIb/IIIa receptors, *J. Am. Coll. Cardiol.*, 1995, **26**, 1665–1671.
- 52 J. Weisel and R. Litvinov, Red blood cells: the forgotten player in hemostasis and thrombosis, *J. Thromb. Haemostasis*, 2019, **17**, 271–282.
- 53 V. X. Du, D. Huskens, C. Maas, R. Al Dieri, P. G. de Groot and B. de Laat, New insights into the role of erythrocytes in thrombus formation, in *Seminars in thrombosis and hemostasis*, Thieme Medical Publishers, 2014, pp. 072–080.
- 54 R. Mehri, C. Mavriplis and M. Fenech, Red blood cell aggregates and their effect on non-Newtonian blood viscosity at low hematocrit in a two-fluid low shear rate microfluidic system, *PLoS One*, 2018, **13**, e0199911.
- 55 K. Sriram, M. Intaglietta and D. M. Tartakovsky, Non-Newtonian flow of blood in arterioles: consequences for wall shear stress measurements, *Microcirculation*, 2014, **21**, 628–639.
- 56 B. L. Walton, M. Lehmann, T. Skorczewski, L. A. Holle, J. D. Beckman, J. A. Cribb, M. J. Mooberry, A. R. Wufsus, B. C. Cooley and J. W. Homeister, Elevated hematocrit enhances platelet accumulation following vascular injury, *Blood*, 2017, **129**, 2537–2546.
- 57 Y.-F. Wu, P.-S. Hsu, C.-S. Tsai, P.-C. Pan and Y.-L. Chen, Significantly increased low shear rate viscosity, blood elastic modulus, and RBC aggregation in adults following cardiac surgery, *Sci. Rep.*, 2018, **8**, 1–10.
- 58 S. Yedgar, A. Koshkaryev and G. Barshtein, The red blood cell in vascular occlusion, *Pathophysiol. Haemostasis Thromb.*, 2002, **32**, 263–268.
- 59 H. C. Kwaan and M. Samama, *Clinical thrombosis*, CRC Press, 2019.
- 60 L. Guo, D. Tong, M. Yu, Y. Zhang, T. Li, C. Wang, P. Zhou, J. Jin, B. Li and Y. Liu, Phosphatidylserine-exposing cells contribute to the hypercoagulable state in patients with multiple myeloma, *Int. J. Oncol.*, 2018, **52**, 1981–1990.
- 61 S. A. Smith, R. J. Travers and J. H. Morrissey, How it all starts: Initiation of the clotting cascade, *Crit. Rev. Biochem. Mol. Biol.*, 2015, **50**, 326–336.
- 62 J. Simak and S. De Paoli, The effects of nanomaterials on blood coagulation in hemostasis and thrombosis, *Wiley Interdiscip. Rev.: Nanomed. Nanobiotechnol.*, 2017, **9**, e1448.
- 63 R. C. Wiggins and C. C. Cochrane, The autoactivation of rabbit Hageman factor, *J. Exp. Med.*, 1979, **150**, 1122–1133.
- 64 F. van der Graaf, F. Keus, R. Vlooswijk and B. N. Bouma, *The contact activation mechanism in human plasma: activation induced by dextran sulfate*, 1982.
- 65 D. L. Tankersley, B. M. Alving and J. Finlayson, *Activation of factor XII by dextran sulfate: the basis for an assay of factor XII*, 1983.
- 66 P. K. Bendapudi, K. Deceunynck, S. Koseoglu, R. H. Bekendam, S. D. Mason, J. Kenniston and R. C. Flaumenhaft, *Stimulated platelets but not endothelium generate thrombin via a factor XIIa-dependent mechanism requiring phosphatidylserine exposure*, American Society of Hematology Washington, DC, 2016.
- 67 Y. Buyue, T. M. Misenheimer and J. P. Sheehan, Low molecular weight heparin inhibits plasma thrombin generation via direct targeting of factor IXa: contribution of the serpin-independent mechanism, *J. Thromb. Haemostasis*, 2012, **10**, 2086–2098.
- 68 J. C. Chapin and K. A. Hajjar, Fibrinolysis and the control of blood coagulation, *Blood Rev.*, 2015, **29**, 17–24.
- 69 H. Sun, L. Lv, Y. Bai, H. Yang, H. Zhou, C. Li and L. Yang, Nanotechnology-enabled materials for hemostatic and anti-infection treatments in orthopedic surgery, *Int. J. Nanomed.*, 2018, **13**, 8325.
- 70 K. D. Patel, R. K. Singh and H.-W. Kim, Carbon-based nanomaterials as an emerging platform for theranostics, *Mater. Horiz.*, 2019, **6**, 434–469.
- 71 A. Radomski, P. Jurasz, D. Alonso-Escolano, M. Drews, M. Morandi, T. Malinski and M. W. Radomski, Nanoparticle-induced platelet aggregation and vascular thrombosis, *Br. J. Pharmacol.*, 2005, **146**, 882–893.



- 72 J. Semberova, S. H. De Paoli Lacerda, O. Simakova, K. Holada, M. P. Gelderman and J. Simak, Carbon nanotubes activate blood platelets by inducing extracellular Ca<sup>2+</sup> influx sensitive to calcium entry inhibitors, *Nano Lett.*, 2009, **9**, 3312–3317.
- 73 S. H. De Paoli Lacerda, J. Semberova, K. Holada, O. Simakova, S. D. Hudson and J. Simak, Carbon nanotubes activate store-operated calcium entry in human blood platelets, *ACS Nano*, 2011, **5**, 5808–5813.
- 74 A. R. Burke, R. N. Singh, D. L. Carroll, J. D. Owen, N. D. Kock, R. D'Agostino Jr., F. M. Torti and S. V. Torti, Determinants of the thrombogenic potential of multi-walled carbon nanotubes, *Biomaterials*, 2011, **32**, 5970–5978.
- 75 K. Luyts, S. Smulders, D. Napierska, K. Poels, H. Scheers, B. Hemmerlyckx, B. Nemery, M. F. Hoylaerts and P. H. Hoet, Pulmonary and hemostatic toxicity of multi-walled carbon nanotubes and zinc oxide nanoparticles after pulmonary exposure in Bmal1 knockout mice, *Part. Fibre Toxicol.*, 2014, **11**, 1–15.
- 76 J. Luo, M. Zhang, J. Cheng, S. Wu, W. Xiong, H. Kong, Y. Zhao and H. Qu, Hemostatic effect of novel carbon dots derived from *Cirsium setosum* Carbonisata, *RSC Adv.*, 2018, **8**, 37707–37714.
- 77 T.-Y. Lee, T. Jayakumar, P. Thanasekaran, K.-C. Lin, H.-M. Chen, P. Veerakumar and J.-R. Sheu, Carbon dot nanoparticles exert inhibitory effects on human platelets and reduce mortality in mice with acute pulmonary thromboembolism, *Nanomaterials*, 2020, **10**, 1254.
- 78 S. Kumari, M. K. Singh, S. K. Singh, J. J. Grácio and D. Dash, Nanodiamonds activate blood platelets and induce thromboembolism, *Nanomedicine*, 2014, **9**, 427–440.
- 79 T. Avsievich, A. Popov, A. Bykov and I. Meglinski, Mutual interaction of red blood cells influenced by nanoparticles, *Sci. Rep.*, 2019, **9**, 1–6.
- 80 M. P. Gelderman, O. Simakova, J. D. Clogston, A. K. Patri, S. F. Siddiqui, A. C. Vostal and J. Simak, Adverse effects of fullerenes on endothelial cells: Fullerenol C60 (OH) 24 induced tissue factor and ICAM-1 membrane expression and apoptosis in vitro, *Int. J. Nanomed.*, 2008, **3**, 59.
- 81 S. Xia, J. Li, M. Zu, J. Li, J. Liu, X. Bai, Y. Chang, K. Chen, W. Gu and L. Zeng, Small size fullerenol nanoparticles inhibit thrombosis and blood coagulation through inhibiting activities of thrombin and FXa, *Nanomedicine*, 2018, **14**, 929–939.
- 82 S. K. Singh, M. K. Singh, M. K. Nayak, S. Kumari, S. Shrivastava, J. J. Grácio and D. Dash, Thrombus inducing property of atomically thin graphene oxide sheets, *ACS Nano*, 2011, **5**, 4987–4996.
- 83 S. K. Singh, M. K. Singh, P. P. Kulkarni, V. K. Sonkar, J. J. Grácio and D. Dash, Amine-modified graphene: thrombo-protective safer alternative to graphene oxide for biomedical applications, *ACS Nano*, 2012, **6**, 2731–2740.
- 84 T. V. Vakhrusheva, A. A. Gusev, S. A. Gusev and I. I. Vlasova, Albumin reduces thrombogenic potential of single-walled carbon nanotubes, *Toxicol. Lett.*, 2013, **221**, 137–145.
- 85 X. Sun, J. Shi, X. Zou, C. Wang, Y. Yang and H. Zhang, Silver nanoparticles interact with the cell membrane and increase endothelial permeability by promoting VE-cadherin internalization, *J. Hazard. Mater.*, 2016, **317**, 570–578.
- 86 P. H. Danielsen, Y. Cao, M. Roursgaard, P. Møller and S. Loft, Endothelial cell activation, oxidative stress and inflammation induced by a panel of metal-based nanomaterials, *Nanotoxicology*, 2015, **9**, 813–824.
- 87 S. Shrivastava, T. Bera, S. K. Singh, G. Singh, P. Ramachandrarao and D. Dash, Characterization of anti-platelet properties of silver nanoparticles, *ACS Nano*, 2009, **3**, 1357–1364.
- 88 E.-A. Jun, K.-M. Lim, K. Kim, O.-N. Bae, J.-Y. Noh, K.-H. Chung and J.-H. Chung, Silver nanoparticles enhance thrombus formation through increased platelet aggregation and procoagulant activity, *Nanotoxicology*, 2011, **5**, 157–167.
- 89 S. Krajewski, R. Prucek, A. Panacek, M. Avci-Adali, A. Nolte, A. Straub, R. Zboril, H. P. Wendel and L. Kvitek, Hemocompatibility evaluation of different silver nanoparticle concentrations employing a modified Chandler-loop in vitro assay on human blood, *Acta Biomater.*, 2013, **9**, 7460–7468.
- 90 V. Ragaseema, S. Unnikrishnan, V. K. Krishnan and L. K. Krishnan, The antithrombotic and antimicrobial properties of PEG-protected silver nanoparticle coated surfaces, *Biomaterials*, 2012, **33**, 3083–3092.
- 91 J. Laloy, V. Minet, L. Alpan, F. Mullier, S. Beken, O. Toussaint, S. Lucas and J.-M. Dogné, Impact of silver nanoparticles on haemolysis, platelet function and coagulation, *Nanobiomedicine*, 2014, **1**, 4.
- 92 H. Huang, W. Lai, M. Cui, L. Liang, Y. Lin, Q. Fang, Y. Liu and L. Xie, An evaluation of blood compatibility of silver nanoparticles, *Sci. Rep.*, 2016, **6**, 1–15.
- 93 M. Marulasiddeshwara, S. Dakshayani, M. S. Kumar, R. Chethana, P. R. Kumar and S. Devaraja, Facile-one pot-green synthesis, antibacterial, antifungal, antioxidant and antiplatelet activities of lignin capped silver nanoparticles: A promising therapeutic agent, *Mater. Sci. Eng., C*, 2017, **81**, 182–190.
- 94 M. J. Kim and S. Shin, Toxic effects of silver nanoparticles and nanowires on erythrocyte rheology, *Food Chem. Toxicol.*, 2014, **67**, 80–86.
- 95 D. Bandyopadhyay, H. Baruah, B. Gupta and S. Sharma, Silver nano particles prevent platelet adhesion on immobilized fibrinogen, *Indian J. Clin. Biochem.*, 2012, **27**, 164–170.
- 96 J. H. Lee, M. Gulumian, E. M. Faustman, T. Workman, K. Jeon and I. J. Yu, Blood biochemical and hematological study after subacute intravenous injection of gold and silver nanoparticles and coadministered gold and silver nanoparticles of similar sizes, *BioMed Res. Int.*, 2018, **2018**, 8460910.

- 97 J. Hajtuch, N. Hante, E. Tomczyk, M. Wojcik, M. W. Radomski, M. J. Santos-Martinez and I. Inkielewicz-Stepniak, Effects of functionalized silver nanoparticles on aggregation of human blood platelets, *Int. J. Nanomed.*, 2019, **14**, 7399.
- 98 V. Trivedi, A. Boire, B. Tchernychev, N. C. Kaneider, A. J. Leger, K. O'Callaghan, L. Covic and A. Kuliopulos, Platelet matrix metalloprotease-1 mediates thrombogenesis by activating PAR1 at a cryptic ligand site, *Cell*, 2009, **137**, 332–343.
- 99 S. Shrivastava, S. K. Singh, A. Mukhopadhyay, A. S. Sinha, R. K. Mandal and D. Dash, Negative regulation of fibrin polymerization and clot formation by nanoparticles of silver, *Colloids Surf., B*, 2011, **82**, 241–246.
- 100 K. Heise, M. Hobisch, L. Sacarescu, U. Maver, J. Hobisch, T. Reichelt, M. Sega, S. Fischer and S. Spirk, Low-molecular-weight sulfonated chitosan as template for anticoagulant nanoparticles, *Int. J. Nanomed.*, 2018, **13**, 4881.
- 101 R. N. Krishnaraj and S. Berchmans, In vitro antiplatelet activity of silver nanoparticles synthesized using the microorganism *Gluconobacter roseus*: an AFM-based study, *RSC Adv.*, 2013, **3**, 8953–8959.
- 102 M. Jeyaraj, S. Varadan, K. J. P. Anthony, M. Murugan, A. Raja and S. Gurunathan, Antimicrobial and anticoagulation activity of silver nanoparticles synthesized from the culture supernatant of *Pseudomonas aeruginosa*, *J. Ind. Eng. Chem.*, 2013, **19**, 1299–1303.
- 103 K. Roy, A. K. Srivastwa and C. K. Ghosh, Anticoagulant, thrombolytic and antibacterial activities of *Euphorbia acruensis* latex-mediated bioengineered silver nanoparticles, *Green Process. Synth.*, 2019, **8**, 590–599.
- 104 A. Lateef, B. I. Folarin, S. M. Oladejo, P. O. Akinola, L. S. Beukes and E. B. Gueguim-Kana, Characterization, antimicrobial, antioxidant, and anticoagulant activities of silver nanoparticles synthesized from *Petiveria alliacea* L. leaf extract, *Prep. Biochem. Biotechnol.*, 2018, **48**, 646–652.
- 105 A. Lateef, S. A. Ojo, J. A. Elegbede, M. A. Azeez, T. A. Yekeen and A. Akinboro, Evaluation of some bio-synthesized silver nanoparticles for biomedical applications: hydrogen peroxide scavenging, anticoagulant and thrombolytic activities, *J. Cluster Sci.*, 2017, **28**, 1379–1392.
- 106 A. Lateef, M. A. Akande, S. A. Ojo, B. I. Folarin, E. B. Gueguim-Kana and L. S. Beukes, Paper wasp nest-mediated biosynthesis of silver nanoparticles for antimicrobial, catalytic, anticoagulant, and thrombolytic applications, *3 Biotech*, 2016, **6**, 1–10.
- 107 A. Lateef, M. A. Akande, M. A. Azeez, S. A. Ojo, B. I. Folarin, E. B. Gueguim-Kana and L. S. Beukes, Phytosynthesis of silver nanoparticles (AgNPs) using miracle fruit plant (*Synsepalum dulcificum*) for antimicrobial, catalytic, anticoagulant, and thrombolytic applications, *Nanotechnol. Rev.*, 2016, **5**, 507–520.
- 108 B. Harish, K. B. Uppuluri and V. Anbazhagan, Synthesis of fibrinolytic active silver nanoparticle using wheat bran xylan as a reducing and stabilizing agent, *Carbohydr. Polym.*, 2015, **132**, 104–110.
- 109 M. K. Meher and K. M. Poluri, Anticoagulation and antibacterial properties of heparinized nanosilver with different morphologies, *Carbohydr. Polym.*, 2021, **266**, 118124.
- 110 J. Berry, B. Arnoux, G. Stanislas, P. Galle and J. Chretien, A microanalytic study of particles transport across the alveoli: role of blood platelets, *Biomedicine*, 1977, **27**, 354–357.
- 111 S. Deb, H. K. Patra, P. Lahiri, A. K. Dasgupta, K. Chakrabarti and U. Chaudhuri, Multistability in platelets and their response to gold nanoparticles, *Nanomedicine*, 2011, **7**, 376–384.
- 112 S. A. Love, J. W. Thompson and C. L. Haynes, Development of screening assays for nanoparticle toxicity assessment in human blood: preliminary studies with charged Au nanoparticles, *Nanomedicine*, 2012, **7**, 1355–1364.
- 113 G. Chen, N. Ni, J. Zhou, Y.-J. Chuang, B. Wang, Z. Pan and B. Xu, Fibrinogen clot induced by gold-nanoparticle in vitro, *J. Nanosci. Nanotechnol.*, 2011, **11**, 74–81.
- 114 M. A. Dobrovolskaia, A. K. Patri, J. Zheng, J. D. Clogston, N. Ayub, P. Aggarwal, B. W. Neun, J. B. Hall and S. E. McNeil, Interaction of colloidal gold nanoparticles with human blood: effects on particle size and analysis of plasma protein binding profiles, *Nanomedicine*, 2009, **5**, 106–117.
- 115 Z. J. Deng, M. Liang, M. Monteiro, I. Toth and R. F. Minchin, Nanoparticle-induced unfolding of fibrinogen promotes Mac-1 receptor activation and inflammation, *Nat. Nanotechnol.*, 2011, **6**, 39–44.
- 116 N. Ajdari, C. Vyas, S. L. Bogan, B. A. Lwaleed and B. G. Cousins, Gold nanoparticle interactions in human blood: a model evaluation, *Nanomedicine*, 2017, **13**, 1531–1542.
- 117 D. Bartczak, O. L. Muskens, S. Nitti, T. Sanchez-Elsner, T. M. Millar and A. G. Kanaras, Interactions of human endothelial cells with gold nanoparticles of different morphologies, *Small*, 2012, **8**, 122–130.
- 118 M. Hecold, R. Buczkowska, A. Mucha, J. Grzesiak, O. Rac-Rumijowska, H. Teterycz and K. Marycz, The effect of PEI and PVP-stabilized gold nanoparticles on equine platelets activation: potential application in equine regenerative medicine, *J. Nanomater.*, 2017, **2017**, 8706921.
- 119 A. Aseychev, O. Azizova, E. Beckman, L. Dudnik and V. Sergienko, Effect of gold nanoparticles coated with plasma components on ADP-induced platelet aggregation, *Bull. Exp. Biol. Med.*, 2013, **155**, 685–688.
- 120 M. J. Santos-Martinez, I. Inkielewicz-Stepniak, C. Medina, K. Rahme, D. M. D'Arcy, D. Fox, J. D. Holmes, H. Zhang and M. W. Radomski, The use of quartz crystal microbalance with dissipation (QCM-D) for studying nanoparticle-induced platelet aggregation, *Int. J. Nanomed.*, 2012, **7**, 243.
- 121 L. Bircher, O. M. Theusinger, S. Locher, P. Eugster, B. Roth-Z'graggen, C. M. Schumacher, J.-D. Studt, W. J. Stark, B. Beck-Schimmer and I. K. Herrmann,

- Characterization of carbon-coated magnetic nanoparticles using clinical blood coagulation assays: effect of PEG-functionalization and comparison to silica nanoparticles, *J. Mater. Chem. B*, 2014, 2, 3753–3758.
- 122 Q. Ran, Y. Xiang, Y. Liu, L. Xiang, F. Li, X. Deng, Y. Xiao, L. Chen, L. Chen and Z. Li, Eryptosis indices as a novel predictive parameter for biocompatibility of Fe<sub>3</sub>O<sub>4</sub> magnetic nanoparticles on erythrocytes, *Sci. Rep.*, 2015, 5, 16209.
- 123 C. Achilli, S. Grandi, G. Guidetti, A. Ciana, C. Tomasi, D. Capsoni and G. Minetti, Fe<sub>3</sub>O<sub>4</sub>@SiO<sub>2</sub> core-shell nanoparticles for biomedical purposes: adverse effects on blood cells, *Biomater. Sci.*, 2016, 4, 1417–1421.
- 124 M. G. Villegas, M. T. Ceballos, J. Urquijo, E. Y. Torres, B. L. Ortiz-Reyes, O. L. Arnache-Olmos and M. R. López, Poly (acrylic acid)-Coated Iron Oxide Nanoparticles interact with mononuclear phagocytes and decrease platelet aggregation, *Cell. Immunol.*, 2019, 338, 51–62.
- 125 S. Deb, S. Raja, A. K. Dasgupta, R. Sarkar, A. P. Chattopadhyay, U. Chaudhuri, P. Guha and P. Sardar, Surface tunability of nanoparticles in modulating platelet functions, *Blood Cells, Mol., Dis.*, 2012, 48, 36–44.
- 126 R. K. Kottana, L. Maurizi, B. Schnoor, K. Morris, J. A. Webb, M. A. Massiah, N. Millot and A. I. Papa, Anti-Platelet Effect Induced by Iron Oxide Nanoparticles: Correlation with Conformational Change in Fibrinogen, *Small*, 2021, 17, 2004945.
- 127 D. Cabrera, K. Walker, S. Moise, N. D. Telling and A. G. Harper, Controlling human platelet activation with calcium-binding nanoparticles, *Nano Res.*, 2020, 13, 2697–2705.
- 128 C. Li, M. Zhang, X. Liu, W. Zhao and C. Zhao, Immobilization of heparin-mimetic biomacromolecules on Fe<sub>3</sub>O<sub>4</sub> nanoparticles as magnetic anticoagulant via mussel-inspired coating, *Mater. Sci. Eng., C*, 2020, 109, 110516.
- 129 S. L. Easo and P. Mohanan, In vitro hematological and in vivo immunotoxicity assessment of dextran stabilized iron oxide nanoparticles, *Colloids Surf., B*, 2015, 134, 122–130.
- 130 T. Liu, R. Bai, H. Zhou, R. Wang, J. Liu, Y. Zhao and C. Chen, The effect of size and surface ligands of iron oxide nanoparticles on blood compatibility, *RSC Adv.*, 2020, 10, 7559–7569.
- 131 S. E. Baker, A. M. Sawvel, J. Fan, Q. Shi, N. Strandwitz and G. D. Stucky, Blood clot initiation by mesocellular foams: dependence on nanopore size and enzyme immobilization, *Langmuir*, 2008, 24, 14254–14260.
- 132 T. Yoshida, Y. Yoshioka, S. Tochigi, T. Hirai, M. Uji, K.-I. Ichihashi, K. Nagano, Y. Abe, H. Kamada and S.-I. Tsunoda, Intranasal exposure to amorphous nanosilica particles could activate intrinsic coagulation cascade and platelets in mice, *Part. Fibre Toxicol.*, 2013, 10, 1–12.
- 133 T. Kushida, K. Saha, C. Subramani, V. Nandwana and V. M. Rotello, Effect of nano-scale curvature on the intrinsic blood coagulation system, *Nanoscale*, 2014, 6, 14484–14487.
- 134 L. Feng, X. Yang, S. Liang, Q. Xu, M. R. Miller, J. Duan and Z. Sun, Silica nanoparticles trigger the vascular endothelial dysfunction and prethrombotic state via miR-451 directly regulating the IL6R signaling pathway, *Part. Fibre Toxicol.*, 2019, 16, 1–13.
- 135 D. Kudela, S. A. Smith, A. May-Masnou, G. B. Braun, A. Pallaoro, C. K. Nguyen, T. T. Chuong, S. Nownes, R. Allen and N. R. Parker, Clotting activity of polyphosphate-functionalized silica nanoparticles, *Angew. Chem.*, 2015, 127, 4090–4094.
- 136 X. Liu and J. Sun, Time-course effects of intravenously administrated silica nanoparticles on blood coagulation and endothelial function in rats, *J. Nanosci. Nanotechnol.*, 2013, 13, 222–228.
- 137 C. Guo, Y. Xia, P. Niu, L. Jiang, J. Duan, Y. Yu, X. Zhou, Y. Li and Z. Sun, Silica nanoparticles induce oxidative stress, inflammation, and endothelial dysfunction in vitro via activation of the MAPK/Nrf2 pathway and nuclear factor- $\kappa$ B signaling, *Int. J. Nanomed.*, 2015, 10, 1463.
- 138 L. Jiang, Y. Li, Y. Li, C. Guo, Y. Yu, Y. Zou, Y. Yang, Y. Yu, J. Duan and W. Geng, Silica nanoparticles induced the pre-thrombotic state in rats via activation of coagulation factor XII and the JNK-NF- $\kappa$ B/AP-1 pathway, *Toxicol. Res.*, 2015, 4, 1453–1464.
- 139 J. J. Corbalan, C. Medina, A. Jacoby, T. Malinski and M. W. Radomski, Amorphous silica nanoparticles aggregate human platelets: potential implications for vascular homeostasis, *Int. J. Nanomed.*, 2012, 7, 631.
- 140 J. Saikia, R. Mohammadpour, M. Yazdimamaghani, H. Northrup, V. Hlady and H. Ghandehari, Silica Nanoparticle-Endothelial Interaction: Uptake and Effect on Platelet Adhesion under Flow Conditions, *ACS Appl. Bio Mater.*, 2018, 1, 1620–1627.
- 141 D. Kim, S. Finkenstaedt-Quinn, K. R. Hurley, J. T. Buchman and C. L. Haynes, On-chip evaluation of platelet adhesion and aggregation upon exposure to mesoporous silica nanoparticles, *Analyst*, 2014, 139, 906–913.
- 142 R. Tavano, D. Segat, E. Reddi, J. Kos, M. Rojnik, P. Kocbek, S. Iratni, D. Scheglmann, M. Colucci and I. M. R. Echevarria, Procoagulant properties of bare and highly PEGylated vinyl-modified silica nanoparticles, *Nanomedicine*, 2010, 5, 881–896.
- 143 A. Yildirim, E. Ozgur and M. Bayindir, Impact of mesoporous silica nanoparticle surface functionality on hemolytic activity, thrombogenicity and non-specific protein adsorption, *J. Mater. Chem. B*, 2013, 1, 1909–1920.
- 144 A. Nemmar, K. Melghit and B. H. Ali, The acute proinflammatory and prothrombotic effects of pulmonary exposure to rutile TiO<sub>2</sub> nanorods in rats, *Exp. Biol. Med.*, 2008, 233, 610–619.
- 145 N. Haberl, S. Hirn, M. Holzer, G. Zuchtriegel, M. Rehberg and F. Krombach, Effects of acute systemic administration of TiO<sub>2</sub>, ZnO, SiO<sub>2</sub>, and Ag nanoparticles on hemody-

- namics, hemostasis and leukocyte recruitment, *Nanotoxicology*, 2015, **9**, 963–971.
- 146 P. Bihari, M. Holzer, M. Praetner, J. Fent, M. Lerchenberger, C. A. Reichel, M. Rehberg, S. Lakatos and F. Krombach, Single-walled carbon nanotubes activate platelets and accelerate thrombus formation in the microcirculation, *Toxicology*, 2010, **269**, 148–154.
- 147 P. Akinola, A. Lateef, T. Asafa, L. Beukes, A. Hakeem and H. Irshad, Multifunctional titanium dioxide nanoparticles biofabricated via photosynthetic route using extracts of *Cola nitida*: antimicrobial, dye degradation, antioxidant and anticoagulant activities, *Heliyon*, 2020, **6**, e04610.
- 148 K. Lingaraju, R. Basavaraj, K. Jayanna, S. Bhavana, S. Devaraja, H. K. Swamy, G. Nagaraju, H. Nagabhushana and H. R. Naika, Biocompatible fabrication of TiO<sub>2</sub> nanoparticles: Antimicrobial, anticoagulant, antiplatelet, direct hemolytic and cytotoxicity properties, *Inorg. Chem. Commun.*, 2021, **127**, 108505.
- 149 M. Šimundić, B. Drašler, V. Šuštar, J. Zupanc, R. Štukelj, D. Makovec, D. Erdogmus, H. Hägerstrand, D. Drobne and V. Kralj-Iglič, Effect of engineered TiO<sub>2</sub> and ZnO nanoparticles on erythrocytes, platelet-rich plasma and giant unilamellar phospholipid vesicles, *BMC Vet. Res.*, 2013, **9**, 7.
- 150 J.-Y. Yang, J. Bae, A. Jung, S. Park, S. Chung, J. Seok, H. Roh, Y. Han, J.-M. Oh and S. Sohn, Surface functionalization-specific binding of coagulation factors by zinc oxide nanoparticles delays coagulation time and reduces thrombin generation potential in vitro, *PLoS One*, 2017, **12**, e0181634.
- 151 Z. Gu, S. Yan, S. Cheong, Z. Cao, H. Zuo, A. C. Thomas, B. E. Rolfe and Z. P. Xu, Layered double hydroxide nanoparticles: Impact on vascular cells, blood cells and the complement system, *J. Colloid Interface Sci.*, 2018, **512**, 404–410.
- 152 M. J. Akhtar, M. Ahamed and H. Alhadlaq, Gadolinium oxide nanoparticles induce toxicity in human endothelial HUVECs via lipid peroxidation, mitochondrial dysfunction and autophagy modulation, *Nanomaterials*, 2020, **10**, 1675.
- 153 K. Greish, G. Thiagarajan, H. Herd, R. Price, H. Bauer, D. Hubbard, A. Burckle, S. Sadekar, T. Yu and A. Anwar, Size and surface charge significantly influence the toxicity of silica and dendritic nanoparticles, *Nanotoxicology*, 2012, **6**, 713–723.
- 154 M. A. Dobrovolskaia, A. K. Patri, J. Simak, J. B. Hall, J. Semberova, S. H. De Paoli Lacerda and S. E. McNeil, Nanoparticle size and surface charge determine effects of PAMAM dendrimers on human platelets in vitro, *Mol. Pharm.*, 2012, **9**, 382–393.
- 155 S. J. Marrink, A. H. De Vries and A. E. Mark, Coarse grained model for semiquantitative lipid simulations, *J. Phys. Chem. B*, 2004, **108**, 750–760.
- 156 C. F. Jones, R. A. Campbell, Z. Franks, C. C. Gibson, G. Thiagarajan, A. Vieira-de-Abreu, S. Sukavaneshvar, S. F. Mohammad, D. Y. Li and H. Ghandehari, Cationic PAMAM dendrimers disrupt key platelet functions, *Mol. Pharm.*, 2012, **9**, 1599–1611.
- 157 A. E. Enciso, B. Neun, J. Rodriguez, A. P. Ranjan, M. A. Dobrovolskaia and E. E. Simanek, Nanoparticle effects on human platelets in vitro: A comparison between PAMAM and triazine dendrimers, *Molecules*, 2016, **21**, 428.
- 158 J. Koziara, J. Oh, W. Akers, S. Ferraris and R. Mumper, Blood compatibility of cetyl alcohol/polysorbate-based nanoparticles, *Pharm. Res.*, 2005, **22**, 1821–1828.
- 159 R. Juliano, M. Hsu, D. Peterson, S. Regen and A. Singh, Interactions of conventional or photopolymerized liposomes with platelets in vitro, *Exp. Cell Res.*, 1983, **146**, 422–427.
- 160 L. Reinish, M. Bally, H. Loughrey and P. Cullis, Interactions of liposomes and platelets, *Thromb. Haemostasis*, 1988, **59**, 518–523.
- 161 G. Zbinden, H. Wunderli-Allenspach and L. Grimm, Assessment of thrombogenic potential of liposomes, *Toxicology*, 1989, **54**, 273–280.
- 162 I. Constantinescu, E. Levin and M. Gyongyossy-Issa, Liposomes and blood cells: a flow cytometric study, *Artif. Cells, Blood Substitutes, Biotechnol.*, 2003, **31**, 395–424.
- 163 E. Smyth, A. Solomon, A. Vydyanath, P. K. Luther, S. Pitchford, T. D. Tetley and M. Emerson, Induction and enhancement of platelet aggregation in vitro and in vivo by model polystyrene nanoparticles, *Nanotoxicology*, 2015, **9**, 356–364.
- 164 C. McGuinness, R. Duffin, S. Brown, N. L. Mills, I. L. Megson, W. MacNee, S. Johnston, S. L. Lu, L. Tran and R. Li, Surface derivatization state of polystyrene latex nanoparticles determines both their potency and their mechanism of causing human platelet aggregation in vitro, *Toxicol. Sci.*, 2011, **119**, 359–368.
- 165 D. C. Pan, J. W. Myerson, J. S. Brenner, P. N. Patel, A. C. Anselmo, S. Mitragotri and V. Muzykantov, Nanoparticle properties modulate their attachment and effect on carrier red blood cells, *Sci. Rep.*, 2018, **8**, 1–12.
- 166 C. Oslakovic, T. Cedervall, S. Linse and B. Dahlbäck, Polystyrene nanoparticles affecting blood coagulation, *Nanomedicine*, 2012, **8**, 981–986.
- 167 F. Liu, H. Huang, Y. Gong, J. Li, X. Zhang and Y. Cao, Evaluation of in vitro toxicity of polymeric micelles to human endothelial cells under different conditions, *Chem.-Biol. Interact.*, 2017, **263**, 46–54.
- 168 Z. Ramtoola, P. Lyons, K. Keohane, S. W. Kerrigan, B. P. Kirby and J. G. Kelly, Investigation of the interaction of biodegradable micro- and nanoparticulate drug delivery systems with platelets, *J. Pharm. Pharmacol.*, 2011, **63**, 26–32.
- 169 X. Li, A. Radomski, O. I. Corrigan, L. Tajber, F. De Sousa Menezes, S. Endter, C. Medina and M. W. Radomski, Platelet compatibility of PLGA, chitosan and PLGA-chitosan nanoparticles, *Nanomedicine*, 2009, **4**, 735–746.
- 170 C. Fornaguera, G. Calderó, M. Mitjans, M. P. Vinardell, C. Solans and C. Vauthier, Interactions of PLGA nano-

- particles with blood components: protein adsorption, coagulation, activation of the complement system and hemolysis studies, *Nanoscale*, 2015, **7**, 6045–6058.
- 171 C. Mao, L.-C. Jiang, W.-P. Luo, H.-K. Liu and J.-C. Bao, Novel blood-compatible polyurethane ionomer nanoparticles, *Macromolecules*, 2009, **42**, 9366–9368.
- 172 L. L. Swystun and P. C. Liaw, The role of leukocytes in thrombosis, *Blood*, 2016, **128**, 753–762.
- 173 S. Luo, D. Hu, M. Wang, P. F. Zipfel and Y. Hu, Complement in hemolysis-and thrombosis-related diseases, *Front. Immunol.*, 2020, **11**, 1212.
- 174 B. Engelmann and S. Massberg, Thrombosis as an intravascular effector of innate immunity, *Nat. Rev. Immunol.*, 2013, **13**, 34–45.
- 175 V. Afshar-Kharghan, Complement and clot, *Blood*, 2017, **129**, 2214–2215.
- 176 M. M. Aleman, C. Gardiner, P. Harrison and A. S. Wolberg, Differential contributions of monocyte- and platelet-derived microparticles towards thrombin generation and fibrin formation and stability, *J. Thromb. Haemostasis*, 2011, **9**, 2251–2261.
- 177 A. Angelillo-Scherrer, Leukocyte-derived microparticles in vascular homeostasis, *Circ. Res.*, 2012, **110**, 356–369.
- 178 N. Maugeri, M. Brambilla, M. Camera, A. Carbone, E. Tremoli, M. Donati, G. De Gaetano and C. Cerletti, Human polymorphonuclear leukocytes produce and express functional tissue factor upon stimulation 1, *J. Thromb. Haemostasis*, 2006, **4**, 1323–1330.
- 179 M.-L. von Brühl, K. Stark, A. Steinhart, S. Chandraratne, I. Konrad, M. Lorenz, A. Khandoga, A. Tirniceriu, R. Coletti and M. Köllnberger, Monocytes, neutrophils, and platelets cooperate to initiate and propagate venous thrombosis in mice in vivo, *J. Exp. Med.*, 2012, **209**, 819–835.
- 180 R. Darbousset, G. M. Thomas, S. Mezouar, C. Frere, R. Bonier, N. Mackman, T. Renné, F. Dignat-George, C. Dubois and L. Panicot-Dubois, Tissue factor-positive neutrophils bind to injured endothelial wall and initiate thrombus formation, *Blood*, 2012, **120**, 2133–2143.
- 181 D. H. Allen and P. B. Tracy, Human Coagulation Factor V Is Activated to the Functional Cofactor by Elastase and Cathepsin G Expressed at the Monocyte Surface (\*), *J. Biol. Chem.*, 1995, **270**, 1408–1415.
- 182 A. J. Gale and D. Rozenshteyn, Cathepsin G, a leukocyte protease, activates coagulation factor VIII, *Thromb. Haemostasis*, 2008, **99**, 44–51.
- 183 J. Plescia and D. C. Altieri, Activation of Mac-1 (CD11b/CD18)-bound factor X by released cathepsin G defines an alternative pathway of leukocyte initiation of coagulation, *Biochem. J.*, 1996, **319**, 873–879.
- 184 M. Jochum, S. Lander, N. Heimbürger and H. Fritz, *Effect of human granulocytic elastase on isolated human antithrombin III*, 1981.
- 185 C. W. Pratt, R. B. Tobin and F. C. Church, Interaction of heparin cofactor II with neutrophil elastase and cathepsin G, *J. Biol. Chem.*, 1990, **265**, 6092–6097.
- 186 S. Massberg, L. Grahl, M.-L. von Bruehl, D. Manukyan, S. Pfeiler, C. Goosmann, V. Brinkmann, M. Lorenz, K. Bidzhekov and A. B. Khandagale, Reciprocal coupling of coagulation and innate immunity via neutrophil serine proteases, *Nat. Med.*, 2010, **16**, 887–896.
- 187 A. azzaq Belaaouaj, A. Li, T.-C. Wun, H. G. Welgus and S. D. Shapiro, Matrix metalloproteinases cleave tissue factor pathway inhibitor: effects on coagulation, *J. Biol. Chem.*, 2000, **275**, 27123–27128.
- 188 D. A. Higuchi, T.-C. Wun, K. M. Likert and G. J. Broze, *The effect of leukocyte elastase on tissue factor pathway inhibitor*, 1992.
- 189 L. L. Swystun, S. Mukherjee and P. C. Liaw, Breast cancer chemotherapy induces the release of cell-free DNA, a novel procoagulant stimulus, *J. Thromb. Haemostasis*, 2011, **9**, 2313–2321.
- 190 T. J. Gould, T. T. Vu, L. L. Swystun, D. J. Dwivedi, S. H. Mai, J. I. Weitz and P. C. Liaw, Neutrophil extracellular traps promote thrombin generation through platelet-dependent and platelet-independent mechanisms, *Arterioscler., Thromb., Vasc. Biol.*, 2014, **34**, 1977–1984.
- 191 S. Barranco-Medina, N. Pozzi, A. D. Vogt and E. Di Cera, Histone H4 promotes prothrombin autoactivation, *J. Biol. Chem.*, 2013, **288**, 35749–35757.
- 192 C. T. Ammollo, F. Semeraro, J. Xu, N. Esmon and C. Esmon, Extracellular histones increase plasma thrombin generation by impairing thrombomodulin-dependent protein C activation, *J. Thromb. Haemostasis*, 2011, **9**, 1795–1803.
- 193 T. Ito, K. Kawahara, T. Nakamura, S. Yamada, T. Nakamura, K. Abeyama, T. Hashiguchi and I. Maruyama, High-mobility group box 1 protein promotes development of microvascular thrombosis in rats, *J. Thromb. Haemostasis*, 2007, **5**, 109–116.
- 194 T. A. Fuchs, A. Brill and D. D. Wagner, Neutrophil extracellular trap (NET) impact on deep vein thrombosis, *Arterioscler., Thromb., Vasc. Biol.*, 2012, **32**, 1777–1783.
- 195 I. Mitroulis, K. Kambas, A. Chrysanthopoulou, P. Skendros, E. Apostolidou, I. Kourtzelis, G. I. Drosos, D. T. Boumpas and K. Ritis, Neutrophil extracellular trap formation is associated with IL-1 $\beta$  and autophagy-related signaling in gout, *PLoS One*, 2011, **6**, e29318.
- 196 M. Menschikowski, A. Hagelgans, G. Eisenhofer and G. Siegert, Regulation of endothelial protein C receptor shedding by cytokines is mediated through differential activation of MAP kinase signaling pathways, *Exp. Cell Res.*, 2009, **315**, 2673–2682.
- 197 B. Nan, P. Lin, A. B. Lumsden, Q. Yao and C. Chen, Effects of TNF- $\alpha$  and curcumin on the expression of thrombomodulin and endothelial protein C receptor in human endothelial cells, *Thromb. Res.*, 2005, **115**, 417–426.
- 198 X. Yang, L. Li, J. Liu, B. Lv and F. Chen, Extracellular histones induce tissue factor expression in vascular endothelial cells via TLR and activation of NF- $\kappa$ B and AP-1, *Thromb. Res.*, 2016, **137**, 211–218.

- 199 J. Herbert, P. Savi, M. Laplace and A. Lale, IL-4 inhibits LPS-, IL-1 $\beta$ - and TNF $\alpha$ -induced expression of tissue factor in endothelial cells and monocytes, *FEBS Lett.*, 1992, **310**, 31–33.
- 200 A. Michels, L. L. Swystun, S. Albáñez, J. Mewburn, K. Sponagle and D. Lillcrap, *Histones induce endothelial von Willebrand factor release and subsequent platelet capture in in vitro and in vivo models*, American Society of Hematology Washington, DC, 2014.
- 201 A. Bernardo, C. Ball, L. Nolasco, J. F. Moake and J.-F. Dong, Effects of inflammatory cytokines on the release and cleavage of the endothelial cell-derived ultra-large von Willebrand factor multimers under flow, *Blood*, 2004, **104**, 100–106.
- 202 K. K. Hamilton and P. J. Sims, Changes in cytosolic Ca<sup>2+</sup> associated with von Willebrand factor release in human endothelial cells exposed to histamine. Study of microcarrier cell monolayers using the fluorescent probe indo-1, *J. Clin. Invest.*, 1987, **79**, 600–608.
- 203 J. Chen, X. Fu, Y. Wang, M. Ling, B. McMullen, J. Kulman, D. W. Chung and J. A. López, Oxidative modification of von Willebrand factor by neutrophil oxidants inhibits its cleavage by ADAMTS13, *Blood*, 2010, **115**, 706–712.
- 204 P. Renesto and M. Chignard, *Enhancement of cathepsin G-induced platelet activation by leukocyte elastase: consequence for the neutrophil-mediated platelet activation*, 1993.
- 205 C. A. LaRosa, M. J. Rohrer, S. E. Benoit, L. J. Rodino, M. R. Barnard and A. D. Michelson, Human neutrophil cathepsin G is a potent platelet activator, *J. Vasc. Surg.*, 1994, **19**, 306–320.
- 206 P. Seth, R. Kumari, M. Dikshit and R. Srimal, Effect of platelet activating factor antagonists in different models of thrombosis, *Thromb. Res.*, 1994, **76**, 503–512.
- 207 T. A. Fuchs, A. A. Bhandari and D. D. Wagner, Histones induce rapid and profound thrombocytopenia in mice, *Blood*, 2011, **118**, 3708–3714.
- 208 F. Semeraro, C. T. Ammollo, J. H. Morrissey, G. L. Dale, P. Friese, N. L. Esmon and C. T. Esmon, Extracellular histones promote thrombin generation through platelet-dependent mechanisms: involvement of platelet TLR2 and TLR4, *Blood*, 2011, **118**, 1952–1961.
- 209 F. Semeraro, C. Ammollo, N. Esmon and C. Esmon, Histones induce phosphatidylserine exposure and a procoagulant phenotype in human red blood cells, *J. Thromb. Haemostasis*, 2014, **12**, 1697–1702.
- 210 S. R. Clark, A. C. Ma, S. A. Tavener, B. McDonald, Z. Goodarzi, M. M. Kelly, K. D. Patel, S. Chakrabarti, E. McAvoy and G. D. Sinclair, Platelet TLR4 activates neutrophil extracellular traps to ensnare bacteria in septic blood, *Nat. Med.*, 2007, **13**, 463–469.
- 211 A. Carestia, L. Rivadeneyra, M. A. Romaniuk, C. Fondevila, S. Negrotto and M. Schattner, Functional responses and molecular mechanisms involved in histone-mediated platelet activation, *Thromb. Haemostasis*, 2013, **110**, 1035–1045.
- 212 P. J. Sims and T. Wiedmer, The response of human platelets to activated components of the complement system, *Immunol. Today*, 1991, **12**, 338–342.
- 213 B. Ando, T. Wiedmer, K. Hamilton and P. Sims, Complement proteins C5b-9 initiate secretion of platelet storage granules without increased binding of fibrinogen or von Willebrand factor to newly expressed cell surface GPIIb-IIIa, *J. Biol. Chem.*, 1988, **263**, 11907–11914.
- 214 M. J. Polley and R. L. Nachman, Human complement in thrombin-mediated platelet function: uptake of the C5b-9 complex, *J. Exp. Med.*, 1979, **150**, 633–645.
- 215 P. J. Sims, E. Faioni, T. Wiedmer and S. Shattil, Complement proteins C5b-9 cause release of membrane vesicles from the platelet surface that are enriched in the membrane receptor for coagulation factor Va and express prothrombinase activity, *J. Biol. Chem.*, 1988, **263**, 18205–18212.
- 216 T. Wiedmer, C. T. Esmon and P. J. Sims, *Complement proteins C5b-9 stimulate procoagulant activity through platelet prothrombinase*, 1986.
- 217 M. J. Polley and R. Nachman, The human complement system in thrombin-mediated platelet function, *J. Exp. Med.*, 1978, **147**, 1713–1726.
- 218 S. Subramaniam, K. Jurk, L. Hobohm, S. Jäckel, M. Saffarzadeh, K. Schwierczek, P. Wenzel, F. Langer, C. Reinhardt and W. Ruf, Distinct contributions of complement factors to platelet activation and fibrin formation in venous thrombus development, *Blood*, 2017, **129**, 2291–2302.
- 219 E. Peerschke and B. Ghebrehiwet, C1q augments platelet activation in response to aggregated Ig, *J. Immunol.*, 1997, **159**, 5594–5598.
- 220 T. Wiedmer, S. Hall, T. Ortel, W. Kane, W. Rosse and P. Sims, *Complement-induced vesiculation and exposure of membrane prothrombinase sites in platelets of paroxysmal nocturnal hemoglobinuria*, 1993.
- 221 P. F. Zipfel and C. Skerka, Complement regulators and inhibitory proteins, *Nat. Rev. Immunol.*, 2009, **9**, 729–740.
- 222 J. Wojta, C. Kaun, G. Zorn, M. Ghannadan, A. W. Hauswirth, W. R. Sperr, G. Fritsch, D. Printz, B. R. Binder and G. Schatzl, C5a stimulates production of plasminogen activator inhibitor-1 in human mast cells and basophils, *Blood*, 2002, **100**, 517–523.
- 223 J. Wojta, K. Huber and P. Valent, New aspects in thrombotic research: complement induced switch in mast cells from a profibrinolytic to a prothrombotic phenotype, *Pathophysiol. Haemostasis Thromb.*, 2003, **33**, 438–441.
- 224 K. Ikeda, K. Nagasawa, T. Horiuchi, T. Tsuru, H. Nishizaka and Y. Niho, C5a induces tissue factor activity on endothelial cells, *Thromb. Haemostasis*, 1997, **77**, 394–398.
- 225 K. Ritis, M. Doumas, D. Mastellos, A. Micheli, S. Giaglis, P. Magotti, S. Rafail, G. Kartalis, P. Sideras and J. D. Lambris, A novel C5a receptor-tissue factor cross-talk in neutrophils links innate immunity to coagulation pathways, *J. Immunol.*, 2006, **177**, 4794–4802.

- 226 K. C. Gulla, K. Gupta, A. Krarup, P. Gal, W. J. Schwaeble, R. B. Sim, C. D. O'Connor and K. Hajela, Activation of mannan-binding lectin-associated serine proteases leads to generation of a fibrin clot, *Immunology*, 2010, **129**, 482–495.
- 227 K. Hess, R. Ajjan, F. Phoenix, J. Dobó, P. Gál and V. Schroeder, Effects of MASP-1 of the complement system on activation of coagulation factors and plasma clot formation, *PLoS One*, 2012, **7**, e35690.
- 228 H. Kozarcanin, C. Lood, L. Munthe-Fog, K. Sandholm, O. A. Hamad, A. A. Bengtsson, M. O. Skjoedt, M. Huber-Lang, P. Garred and K. N. Ekdahl, The lectin complement pathway serine proteases (MASPs) represent a possible crossroad between the coagulation and complement systems in thromboinflammation, *J. Thromb. Haemostasis*, 2016, **14**, 531–545.
- 229 R. Kölm, M. Schaller, L. T. Roumenina, I. Niemiec, J. A. K. Hovinga, E. Khanicheh, B. A. Kaufmann, H. Hopfer and M. Trendelenburg, Von Willebrand factor interacts with surface-bound C1q and induces platelet rolling, *J. Immunol.*, 2016, **197**, 3669–3679.
- 230 E. I. Peerschke, T. K. Murphy and B. Ghebrehiwet, Activation-dependent surface expression of gC1qR/p33 on human blood platelets, *Thromb. Haemostasis*, 2003, **89**, 331–339.
- 231 K. N. Ekdahl and B. Nilsson, Alterations in C3 activation and binding caused by phosphorylation by a casein kinase released from activated human platelets, *J. Immunol.*, 1999, **162**, 7426–7433.
- 232 P. J. Sims and T. Wiedmer, *Repolarization of the membrane potential of blood platelets after complement damage: evidence for a Ca<sup>++</sup>-dependent exocytotic elimination of C5b-9 pores*, 1986.
- 233 A. E. Davis III, P. Mejia and F. Lu, Biological activities of C1 inhibitor, *Mol. Immunol.*, 2008, **45**, 4057–4063.
- 234 E. Conway, Reincarnation of ancient links between coagulation and complement, *J. Thromb. Haemostasis*, 2015, **13**, S121–S132.
- 235 B. Ghebrehiwet, A. P. Kaplan, K. Joseph and E. I. Peerschke, The complement and contact activation systems: partnership in pathogenesis beyond angioedema, *Immunol. Rev.*, 2016, **274**, 281–289.
- 236 D. Ermert and A. M. Blom, C4b-binding protein: the good, the bad and the deadly. Novel functions of an old friend, *Immunol. Lett.*, 2016, **169**, 82–92.
- 237 J. Palomaki, E. Valimaki, J. Sund, M. Vippola, P. A. Clausen, K. A. Jensen, K. Savolainen, S. Matikainen and H. Alenius, Long, needle-like carbon nanotubes and asbestos activate the NLRP3 inflammasome through a similar mechanism, *ACS Nano*, 2011, **5**, 6861–6870.
- 238 X. Wang, T. Xia, S. Addo Ntim, Z. Ji, S. Lin, H. Meng, C.-H. Chung, S. George, H. Zhang and M. Wang, Dispersal state of multiwalled carbon nanotubes elicits profibrogenic cellular responses that correlate with fibrogenesis biomarkers and fibrosis in the murine lung, *ACS Nano*, 2011, **5**, 9772–9787.
- 239 S. M. Chowdhury, S. Kanakia, J. D. Toussaint, M. D. Frame, A. M. Dewar, K. R. Shroyer, W. Moore and B. Sitharaman, In vitro hematological and in vivo vasoactivity assessment of dextran functionalized graphene, *Sci. Rep.*, 2013, **3**, 1–10.
- 240 N. Nishijima, T. Hirai, K. Misato, M. Aoyama, E. Kuroda, K. J. Ishii, K. Higashisaka, Y. Yoshioka and Y. Tsutsumi, Human scavenger receptor A1-mediated inflammatory response to silica particle exposure is size specific, *Front. Immunol.*, 2017, **8**, 379.
- 241 D. Simberg, J.-H. Park, P. P. Karmali, W.-M. Zhang, S. Merkulov, K. McCrae, S. N. Bhatia, M. Sailor and E. Ruoslahti, Differential proteomics analysis of the surface heterogeneity of dextran iron oxide nanoparticles and the implications for their in vivo clearance, *Biomaterials*, 2009, **30**, 3926–3933.
- 242 H. Gaikwad, Y. Li, G. Gifford, E. Groman, N. K. Banda, L. Saba, R. Scheinman, G. Wang and D. Simberg, Complement Inhibitors Block Complement C3 Opsonization and Improve Targeting Selectivity of Nanoparticles in Blood, *Bioconjugate Chem.*, 2020, **31**, 1844–1856.
- 243 T. Fülöp, R. Nemes, T. Mészáros, R. Urbanics, R. J. Kok, J. A. Jackman, N.-J. Cho, G. Storm and J. Szebeni, Complement activation in vitro and reactogenicity of low-molecular weight dextran-coated SPIONs in the pig CARPA model: Correlation with physicochemical features and clinical information, *J. Controlled Release*, 2018, **270**, 268–274.
- 244 R. Bilyy, H. Unterweger, B. Weigel, T. Dumych, S. Paryzhak, V. Vovk, Z. Liao, C. Alexiou, M. Herrmann and C. Janko, Inert coats of magnetic nanoparticles prevent formation of occlusive intravascular co-aggregates with neutrophil extracellular traps, *Front. Immunol.*, 2018, **9**, 2266.
- 245 Y. Yang, N. Wang, Y. Zhu, Y. Lu, Q. Chen, S. Fan, Q. Huang, X. Chen, L. Xia and Y. Wei, Gold nanoparticles synergize with bacterial lipopolysaccharide to enhance class A scavenger receptor dependent particle uptake in neutrophils and augment neutrophil extracellular traps formation, *Ecotoxicol. Environ. Saf.*, 2021, **211**, 111900.
- 246 J. Szebeni, L. Baranyi, S. Savay, M. Bodo, D. S. Morse, M. Basta, G. L. Stahl, R. Bünger and C. R. Alving, Liposome-induced pulmonary hypertension: properties and mechanism of a complement-mediated pseudoallergic reaction, *Am. J. Physiol.: Heart Circ. Physiol.*, 2000, **279**, H1319–H1328.
- 247 A. Chonn, P. Cullis and D. Devine, The role of surface charge in the activation of the classical and alternative pathways of complement by liposomes, *J. Immunol.*, 1991, **146**, 4234–4241.
- 248 Z. Wang and J. S. Brenner, The Nano-War Against Complement Proteins, *AAPS J.*, 2021, **23**, 1–8.
- 249 G. Gifford, V. P. Vu, N. K. Banda, V. M. Holers, G. Wang, E. V. Groman, D. Backos, R. Scheinman, S. M. Moghimi and D. Simberg, Complement therapeutics meets nano-

- medicine: overcoming human complement activation and leukocyte uptake of nanomedicines with soluble domains of CD55, *J. Controlled Release*, 2019, **302**, 181–189.
- 250 F. Alexis, E. Pridgen, L. K. Molnar and O. C. Farokhzad, Factors affecting the clearance and biodistribution of polymeric nanoparticles, *Mol. Pharm.*, 2008, **5**, 505–515.
- 251 M. A. Ashraf, W. Peng, Y. Zare and K. Y. Rhee, Effects of size and aggregation/agglomeration of nanoparticles on the interfacial/interphase properties and tensile strength of polymer nanocomposites, *Nanoscale Res. Lett.*, 2018, **13**, 1–7.
- 252 A. T. Bauer, E. A. Strozyk, C. Gorzelanny, C. Westerhausen, A. Desch, M. F. Schneider and S. W. Schneider, Cytotoxicity of silica nanoparticles through exocytosis of von Willebrand factor and necrotic cell death in primary human endothelial cells, *Biomaterials*, 2011, **32**, 8385–8393.
- 253 A. Nemmar, S. Albarwani, S. Beegam, P. Yuvaraju, J. Yasin, S. Attoub and B. H. Ali, Amorphous silica nanoparticles impair vascular homeostasis and induce systemic inflammation, *Int. J. Nanomed.*, 2014, **9**, 2779.
- 254 J. Meng, X. Cheng, J. Liu, W. Zhang, X. Li, H. Kong and H. Xu, Effects of long and short carboxylated or aminated multiwalled carbon nanotubes on blood coagulation, *PLoS One*, 2012, **7**, e38995.
- 255 Y. He, J. Xu, X. Sun, X. Ren, A. Maharjan, P. York, Y. Su, H. Li and J. Zhang, Cuboidal tethered cyclodextrin frameworks tailored for hemostasis and injured vessel targeting, *Theranostics*, 2019, **9**, 2489.
- 256 M. Holzer, P. Bihari, M. Praetner, B. Uhl, C. Reichel, J. Fent, M. Vippola, S. Lakatos and F. Krombach, Carbon-based nanomaterials accelerate arteriolar thrombus formation in the murine microcirculation independently of their shape, *J. Appl. Toxicol.*, 2014, **34**, 1167–1176.
- 257 O. L. Gobbo, K. Sjaastad, M. W. Radomski, Y. Volkov and A. Prina-Mello, Magnetic nanoparticles in cancer theranostics, *Theranostics*, 2015, **5**, 1249.
- 258 Y. Su, L. Zhao, F. Meng, Q. Wang, Y. Yao and J. Luo, Silver nanoparticles decorated lipase-sensitive polyurethane micelles for on-demand release of silver nanoparticles, *Colloids Surf., B*, 2017, **152**, 238–244.
- 259 M. Yu, S. Huang, K. J. Yu and A. M. Clyne, Dextran and polymer polyethylene glycol (PEG) coating reduce both 5 and 30 nm iron oxide nanoparticle cytotoxicity in 2D and 3D cell culture, *Int. J. Mol. Sci.*, 2012, **13**, 5554–5570.
- 260 M. J. Santos-Martinez, K. Rahme, J. J. Corbalan, C. Faulkner, J. D. Holmes, L. Tajber, C. Medina and M. W. Radomski, Pegylation increases platelet biocompatibility of gold nanoparticles, *J. Biomed. Nanotechnol.*, 2014, **10**, 1004–1015.
- 261 S. M. Chowdhury, S. Kanakia, J. D. Toussaint, M. D. Frame, A. M. Dewar, K. R. Shroyer, W. Moore and B. Sitharaman, In vitro hematological and in vivo vasoactivity assessment of dextran functionalized graphene, *Sci. Rep.*, 2013, **3**, 2584.
- 262 S. H. Hsu, C. M. Tang and H. J. Tseng, Biocompatibility of poly (ether) urethane–gold nanocomposites, *J. Biomed. Mater. Res., Part A*, 2006, **79**, 759–770.
- 263 M. Miyamoto, S. Sasakawa, T. Ozawa, H. Kawaguchi and Y. Ohtsuka, Mechanisms of blood coagulation induced by latex particles and the roles of blood cells, *Biomaterials*, 1990, **11**, 385–388.
- 264 L. Kou, J. Sun, Y. Zhai and Z. He, The endocytosis and intracellular fate of nanomedicines: Implication for rational design, *Asian J. Pharm. Sci.*, 2013, **8**, 1–10.
- 265 Y. Yang, Y. Lai, Q. Zhang, K. Wu, L. Zhang, C. Lin and P. Tang, A novel electrochemical strategy for improving blood compatibility of titanium-based biomaterials, *Colloids Surf., B*, 2010, **79**, 309–313.
- 266 I. Standard, *ISO 10993-4: Biological Evaluation of Medical Devices Part 4—Selection of Tests for Interactions with Blood*, International Organization for Standardization, Geneva, Switzerland, 2017.
- 267 P. Urbán, N. J. Liptrott and S. Bremer, Overview of the blood compatibility of nanomedicines: A trend analysis of in vitro and in vivo studies, *Wiley Interdiscip. Rev.: Nanomed. Nanobiotechnol.*, 2019, **11**, e1546.
- 268 H. K. Kim, M.-J. Choi, S.-H. Cha, Y. K. Koo, S. H. Jun, S. Cho and Y. Park, Earthworm extracts utilized in the green synthesis of gold nanoparticles capable of reinforcing the anticoagulant activities of heparin, *Nanoscale Res. Lett.*, 2013, **8**, 1–7.
- 269 V. Gryshchuk and N. Galagan, Silica nanoparticles effects on blood coagulation proteins and platelets, *Biochem. Res. Int.*, 2016, **2016**, 2959414.
- 270 A. Guildford, T. Poletti, L. Osbourne, A. Di Cerbo, A. Gatti and M. Santin, Nanoparticles of a different source induce different patterns of activation in key biochemical and cellular components of the host response, *J. R. Soc., Interface*, 2009, **6**, 1213–1221.
- 271 C. Santos, S. Turiel, P. S. Gomes, E. Costa, A. Santos-Silva, P. Quadros, J. Duarte, S. Battistuzzo and M. H. Fernandes, Vascular biosafety of commercial hydroxyapatite particles: discrepancy between blood compatibility assays and endothelial cell behavior, *J. Nanobiotechnol.*, 2018, **16**, 1–15.
- 272 A. K. Sharma, A. K. Swami, M. Saran and M. Mathur, Synthesis of tungsten nanoparticles for their biomedical application, *Int. J. Pharm. Sci. Res.*, 2020, **11**, 4070–4077.
- 273 H. Derakhshankhah, M. J. Hajipour, E. Barzegari, A. Lotfabadi, M. Ferdousi, A. A. Saboury, E. P. Ng, M. Raoufi, H. Awala and S. Mintova, Zeolite nanoparticles inhibit A $\beta$ –fibrinogen interaction and formation of a consequent abnormal structural clot, *ACS Appl. Mater. Interfaces*, 2016, **8**, 30768–30779.
- 274 H. Li, X. Zhang, X. Lin, S. Zhuang, Y. Wu, Z. Liu, J. Rong and J. Zhao, CaCO<sub>3</sub> nanoparticles pH-sensitively induce blood coagulation as a potential strategy for starving tumor therapy, *J. Mater. Chem. B*, 2020, **8**, 1223–1234.
- 275 S. Del Turco, G. Ciofani, V. Cappello, P. Parlanti, M. Gemmi, C. Caselli, R. Ragusa, A. Papa, D. Battaglia and L. Sabatino, Effects of cerium oxide nanoparticles on



- hemostasis: Coagulation, platelets, and vascular endothelial cells, *J. Biomed. Mater. Res., Part A*, 2019, **107**, 1551–1562.
- 276 J. Matuszak, J. Baumgartner, J. Zaloga, M. Juenet, A. E. Da Silva, D. Franke, G. Almer, I. Texier, D. Faivre and J. M. Metselaar, Nanoparticles for intravascular applications: physicochemical characterization and cytotoxicity testing, *Nanomedicine*, 2016, **11**, 597–616.
- 277 E. Fuentes, B. Yameen, S.-J. Bong, C. Salvador-Morales, I. Palomo and C. Vilos, Antiplatelet effect of differentially charged PEGylated lipid-polymer nanoparticles, *Nanomedicine*, 2017, **13**, 1089–1094.
- 278 D. Yu, Y. Zhang, X. Zhou, Z. Mao and C. Gao, Influence of surface coating of PLGA particles on the internalization and functions of human endothelial cells, *Biomacromolecules*, 2012, **13**, 3272–3282.
- 279 R. Bakhaidar, S. O'Neill and Z. Ramtoola, PLGA-PEG Nanoparticles Show Minimal Risks of Interference with Platelet Function of Human Platelet-Rich Plasma, *Int. J. Mol. Sci.*, 2020, **21**, 9716.
- 280 L. C. R. P. da Silva, V. Todaro, F. A. do Carmo, F. S. Frattani, V. P. de Sousa, C. R. Rodrigues, P. C. Sathler and L. M. Cabral, A promising oral fucoidan-based antithrombotic nanosystem: development, activity and safety, *Nanotechnology*, 2018, **29**, 165102.
- 281 L. C. da Silva, T. Garcia, M. Mori, G. Sandri, M. C. Bonferoni, P. V. Finotelli, L. P. Cinelli, C. Caramella and L. M. Cabral, Preparation and characterization of polysaccharide-based nanoparticles with anticoagulant activity, *Int. J. Nanomed.*, 2012, **7**, 2975.
- 282 S. Luo, H. Man, X. Jia, Y. Li, A. Pan, X. Zhang and Y. Song, Preparation and characterization of acetylsalicylic acid/chitosan nanoparticles and its antithrombotic effects, *Des. Monomers Polym.*, 2018, **21**, 172–181.
- 283 Q. Han, X. Chen, Y. Niu, B. Zhao, B. Wang, C. Mao, L. Chen and J. Shen, Preparation of water-soluble hyperbranched polyester nanoparticles with sulfonic acid functional groups and their micelles behavior, anticoagulant effect and cytotoxicity, *Langmuir*, 2013, **29**, 8402–8409.